DESIGNING DATA CENTER NETWORKS FOR HIGH THROUGHPUT

BY

ANKIT SINGLA

DISSERTATION

Submitted in partial fulfillment of the requirements
for the degree of Doctor of Philosophy in Computer Science
in the Graduate College of the
University of Illinois at Urbana-Champaign, 2015

Urbana, Illinois

Doctoral Committee:

Associate Professor P. Brighten Godfrey, Chair and Director of Research
Associate Professor Indranil Gupta
Professor Klara Nahrstedt
Professor Scott Shenker, University of California at Berkeley, ICSI Berkeley

Abstract

Data centers with tens of thousands of servers now support popular Internet services, scientific research, as well as industrial applications. The network is the foundation of such facilities, giving the large server pool the ability to work together on these applications. The network needs to provide high throughput between servers to ensure that computations are not slowed down by network bottlenecks, with servers waiting on data from other servers. This work address two broad, related questions about high-throughput data center network design: (a) how do we measure and benchmark various network designs for throughput? and (b) how do we design such networks for near-optimal throughput?

The problem of designing high-throughput networks has received a lot of attention, with multiple interesting architectures being proposed every year. However, there is no clarity on how one should benchmark these networks and how they compare to each other. In fact, this work shows that commonly used measurement approaches, in particular, cut-metrics like bisection bandwidth, do not predict throughput accurately. In contrast, we directly evaluate the throughput of networks on both uniform and (heretofore unknown) *nearly-worst-case* traffic matrices, and include here a comparison of 10 networks using this approach.

Further, prior work has not addressed a fundamental question: *how far are we from throughput-optimal design?* In this work, we propose the first upper bound on network throughput for *any* topology with identical switches. Although designing optimal topologies is infeasible, we demonstrate that random graphs achieve throughput surprisingly close to this bound – within a few percent at the scale of a few thousand servers for uniform traffic.

Our approach also addresses important practical concerns in the design of data center networks, such as incremental expansion and heterogeneous design – as more and varied equipment is added to a data center over the years in response to evolving needs, how do we best accommodate such equipment? Our networks can achieve the same incremental growth at 40% of the expense such growth would incur with past techniques for Clos networks. Further, our approach to designing heterogeneous topologies (*i.e.,* where all

the network switches are not identical) achieves 43% higher throughput than a comparable VL2 topology, a heterogeneous network already deployed in Microsoft's data centers.

We acknowledge that the use of random graphs also poses challenges, particularly with regards to efficient routing and physical cabling. We thus present here high-efficiency routing and cabling schemes for such networks as well.

To my family and friends

Acknowledgments

I owe a great debt to my adviser, P. Brighten Godfrey. His mentorship has been invaluable throughout my graduate studies. He has given me guidance, but also great freedom, and I have *always* looked forward to our meetings and discussions. He has served as a role model not only in terms of research success, but also as a wonderful person. At research conferences, innumerable folks have extended a certain warmth to me on learning that he is my adviser, and that has always struck me as impressive.

My research collaborators have, of course, been instrumental in my work, and I have learnt a lot from them. George Candea, Admela Jukan, and Ashwin Gumaste witnessed and supported my first, uncertain steps into research. I was less committed than desirable, and I thank them for their patience. The first published research output I produced came from work with Katerina Argyraki and Petros Maniatis. I greatly enjoyed my work as Katerina's intern, and continue to enjoy following her work. Over my PhD, I got the opportunity to work with a large number of smart and wonderful people at UIUC, Intel Labs, NEC Labs, ICSI Berkeley, IBM Research Austin, Duke University, as well as collaborators I came into contact with through these first-degree connections. A special thanks is owed to Brighten Godfrey, Chi-Yao Hong, Sangeetha Abdu Jyothi, Alexandra Kolla, and Lucian Popa, collaborations with whom produced the results included in this thesis. Participating in the creative process that is research with these people will, I hope, form enduring connections. Scott Shenker and Bruce Maggs have also been great mentors for me. In spite of being so accomplished, they have graciously tolerated my humor, sometimes at their expense; I have great regard for both of them. All of these people have contributed to my success, and in moulding me as a researcher and person. Katerina Argyraki, John Carter, Brighten Godfrey, Bruce Maggs, and Scott Shenker also helped make my academic job search a success, for which I'm immensely grateful. I also wish to thank my dissertation committee members, Brighten Godfrey, Indranil Gupta, Klara Nahrstedt, and Scott Shenker, for their useful feedback and their encouragement.

Besides being a great collaborator, Chi-Yao Hong has also been a great friend, and I have missed him

since his graduation and departure from Illinois; we undertook several fun adventures together, and I remember these often[1]. Support from fellow students and colleagues has been crucial to my progress and happiness over the years. This includes not only the network-systems grads and faculty at Illinois, but many others at Illinois and other places. They have asked probing questions, and made useful suggestions.

I am also thankful to the NSF, Cisco, and Google, for funding my work.

I have been extremely fortunate in being able to make friends across a variety of academic departments and pursuits, and you are too many to list. I have shared housing with some of you, countless meals and movies, road trips and adventures, dancing, music and singing, and lots of hilarity. Some of you became my friends starting with our multiple chance encounters on public transport! Nevertheless, I feel compelled to mention Nick Easter and Darienne Ciuro, friendships with whom have spanned the entirety of my stay here. Also, Itxaso Rodriguez, who fed me lots of her delicious food[2]. I greatly enjoy her brutally honest, yet somehow comical, approach to life.

A lot of my good friends from before graduate school have maintained contact all these years, and I look forward to the same in the future. Support from Aditya Parameswaran and Prasang Upadhyaya over my job search was particularly valuable.

I have, of course, missed my family here. My parents and my brother have provided a nurturing and loving environment throughout my life, and have led me where I stand today. With the completion of this endeavor, I *finally* join all of them in having post-graduate degrees!

[1] At Yellowstone National Park, I comment on our sighting of a bison: "Such an impressive, odd, large animal.", to which Chi-Yao responds: "Looks delicious; it'd make so many burgers!!"

[2] Itxaso: "I am bored; if you tell me what you want, I'll cook it for you."

TABLE OF CONTENTS

CHAPTER 1

Introduction

The combination of two inexorable trends—increasing parallelism and increasing "big data" analytics—means computing systems urgently need efficient high-capacity network interconnects. Modern warehouse-scale data centers, operated by large Internet services like Google, Amazon, Facebook, and many others, require networks connecting tens of thousands of servers. High throughput is useful in these networks to support data intensive applications such as Map-Reduce and scientific simulations. In cloud computing, a high capacity network gives operators the freedom to place virtual machines on any physical host, without needing to worry about capacity constraints between hosts [46]. This freedom translates into higher server utilization, lower management overhead, and thus lower operating costs. In turn, such networks, under unilateral control, and unencumbered by legacy concerns, present unique opportunities for network design, and the industry is actively exploring novel architectures.

How do we build high throughput networks? The topology of the network is critical in obtaining high throughput. At data center scales, with thousands of network switches connecting tens of thousands of servers, it is simply infeasible to have all network switches connect to each other in a full mesh. Instead, each switch has a few network ports which it uses to connect to servers or other switches. How much traffic the network can carry between the servers depends on the network topology, *i.e.,* on how the servers are distributed across the switches, and how the switches are connected to each other using their limited connectivity. However, designing a topology that provides the highest possible throughput within a given equipment budget is hard in general, because of the combinatorial explosion of the number of possible networks with size. Data center network designers have thus focused either on adapting known graph structures such as Clos networks [59] and hypercubes [47], or suggesting new ones based on intuitions about structure and symmetry (for instance, DCell [43] and BCube [42]). However, while numerous data

center network architectures have recently been proposed [83, 36, 87, 42, 43, 41, 73, 59, 79, 52, 6] to achieve high throughput, this work has left unresolved the question of how far we may be from *optimal* topology design, even in the homogeneous case, where all the network switches are identical.

Topology design is made even more challenging by practical concerns like flexibility and heterogeneity, which traditional, *structured* topologies fail to address. For instance, hypercubes [47] may only be built at power-of-2 sizes, such that one may build a hypercube network with 1024 switches or with 2048 switches, with no size options in between. There is also no evident way of adding equipment incrementally in response to changes in applications and users. Fat-trees [7] and other existing network designs are similarly restrictive. Further, how do we incorporate in these structured, homogeneous network designs switches with different port-counts and line-speeds? Such heterogeneous network equipment is, in fact, the common case in the typical data center: servers connect to top-of-rack (ToR) switches, which connect to aggregation switches, which connect to core switches, with each type of switch possibly having a different number of ports as well some variations in line-speed. Further, as the network expands over the years and new, more powerful equipment is added to the data center, one can expect more heterogeneity — each year the number of ports supported by non-blocking commodity Ethernet switches increases. In spite of heterogeneity being commonplace in data center networks, very little is known about heterogeneous network design. For instance, there is no clarity on whether the traditional ToR-aggregation-core organization is superior to a "flatter" network without such a switch hierarchy; or on whether powerful core switches should be connected densely together, or spread more evenly throughout the network.

This work approaches network design with a simple idea: if *structure* is the enemy of flexibility and heterogeneity, why not look beyond structure? After all, random graphs, being good *expanders* [19], have been known in theory to have high resilience and short path lengths. They are also naturally flexible — you can build a random graph at any size, and adding more nodes just requires a few edge swaps. These attributes could be of enough practical value to warrant a compromise on throughput, but surprisingly, our Jellyfish architecture, based on random graphs, beats state-of-the-art topologies on throughput as well — a Jellyfish network built with the same equipment as a fat-tree achieves throughput higher by 25% at sizes of a few thousand servers, with the gap increasing with size! The flexibility advantage is also quantifiable: Jellyfish is much cheaper to expand than prior work, achieving the same network expansion at 40% cost. But these results are a starting point, and raise several interesting questions, which this work also addresses:

(a) How far are we from throughput-optimal topology design? With Jellyfish, we achieve a large throughput improvement over state-of-the-art fat-tree topologies; how much farther can we improve? Towards addressing this question, we formulated the first non-trivial upper bound on the throughput achievable by *any* topology built with a given set of identical switches, and showed that topologies such as fat-trees achieve throughput much lower than the bound—often by as much as 40%, while Jellyfish achieves high throughput and short path lengths, both within a few percent of optimal. This result is valuable both in providing near-optimal topologies, and in suggesting that the community should focus its research effort on other aspects of the problem. (Chapter 4.)

(b) How do we network heterogeneous equipment, ***i.e.,*** **with switches with different port-counts and line-speeds?** We proposed the use of random graphs as building blocks for heterogeneous network design by first optimizing the volume of connectivity between groups of nodes, and then forming connections randomly within the volume constraints. Built using this approach, our heterogeneous topologies achieve 43% higher throughput than a same-equipment VL2 topology, a heterogeneous network already deployed in Microsoft's data centers. (Chapter 5.)

(c) Structure simplifies routing; how do we route efficiently over our unstructured topologies? We found that existing routing techniques such as ECMP were indeed inefficient for Jellyfish. Instead, we designed a new multi-path routing mechanism that achieves throughput within 86-90% of optimal routing, and is deployable over commodity hardware. The 25% throughput advantage we report over fat-trees already accounts for these minor routing inefficiencies. (Chapter 6.)

(d) Is cabling a random topology a nightmare? Cabling a random topology requires a new approach. We proposed an organization based on dividing the network into multiple clusters, with a significantly smaller volume of cables running across clusters than would be dictated by uniform randomness. We showed, using both graph theory and experiments, that such a scheme has minimal impact on throughput while greatly cutting cabling costs, making cabling our topologies cheaper than fat-trees. Our cabling scheme also allows cable consolidation, *i.e.,* running cables in bundles across clusters. (Chapter 6.)

(e) How do we benchmark network topologies on throughput? While network topology proposals have proliferated as data centers have advanced, a clear throughput comparison of these proposals has been missing. In fact, our work revealed that commonly used metrics such as bisection bandwidth do not accurately represent network throughput. (Note however, that Jellyfish handily beats fat-trees on bisection bandwidth as

well.) In contrast, our work allows direct polynomial-time flow-based throughput benchmarking of networks across both uniform and (heretofore unknown) *nearly worst-case traffic matrices*. We have made available a throughput benchmark for topologies [5], with the objectives of facilitating open and reproducible research, and easing head-to-head comparisons of the large number of past and future proposed network topologies. (Chapter 3.)

Outline

In Chapter 2, we discuss relevant background on network topology design and measurement. Chapter 3 details our methods of benchmarking and comparing networks, and uses these methods to compare 10 data center network designs. Chapter 4 addresses the problem of homogeneous network design, where all the network switches have the same port-count and line-speed. We show that our random graph based design achieves nearly optimal throughput performance, while accommodating incremental addition of equipment to the data center. Chapter 5 discusses heterogeneous network design, where some switches may have larger port-counts or different line-speeds. Chapter 6 addresses systems challenges that arise from the lack of structure in out proposed networks — efficient routing and physical cabling. Chapter 7 concludes by pointing to some open problems and directions for future work.

Note on collaborative work

This thesis includes results from multiple collaborations with P. Brighten Godfrey, Chi-Yao Hong, Sangeetha Abdu Jyothi, Alexandra Kolla, and Lucian Popa. These results have been previously published as follows:

1. *Jellyfish: Networking Data Centers Randomly*. Ankit Singla, Chi-Yao Hong, Lucian Popa, P. Brighten Godfrey. USENIX NSDI, 2012.

2. *High Throughput Data Center Topology Design*. Ankit Singla, P. Brighten Godfrey, and Alexandra Kolla. USENIX NSDI, 2014.

3. *Measuring and Understanding Throughput of Network Topologies*. Sangeetha Abdu Jyothi, Ankit Singla, P. Brighten Godfrey, and Alexandra Kolla. Manuscript, arXiv:1402.2531, 2015.

Chapter 3 includes results from (3) above; Chapters 4 and 5 include results from (1) and (2); and Chapter 6 includes results from (1).

CHAPTER 2

Background and related work

We discuss here prior work related to both the broad questions we are tackling in this work: (a) high throughput network topology design; and (b) throughput measurement and comparison of networks.

2.1 Network topology design

High capacity has been a core goal of electronic communication networks since their inception. How that goal manifests in network topology, however, has changed with systems considerations. More than 150 years ago, the first electronic communication networks connected the wide area and were driven by geographic considerations such as the location of cities and railroads.[1] Decades later, to interconnect telephone lines at a single site such as a telephone exchange, *nonblocking* switches were developed which could match inputs to any permutation of outputs. Beginning with the basic crossbar switch which requires $\Theta(n^2)$ size to interconnect n inputs and outputs, these designs were optimized to scale to larger size, culminating with the Clos network developed at Bell Labs in 1953 [27] which constructs a nonblocking interconnect out of $\Theta(n \log n)$ constant-size crossbars.

In the 1980s, supercomputer systems began to reach a scale of parallelism for which the topology connecting compute nodes was critical. Since a packet in a supercomputer is often a low-latency memory reference (unlike, say, a heavyweight TCP connection establishment) traversing nodes with tiny forwarding tables, these systems were constrained by the need for very simple, loss-free and deadlock-free routing. As a result the series of designs developed through the 1990s have simple and very regular structure, some based on non-blocking Clos networks and others turning to the fat-tree, butterfly, hypercube, 3D torus, 2D mesh,

[1] "It is anticipated that the whole of the populous parts of the United States will, within two or three years, be covered with net-work like a spider's web." —*The London Anecdotes*, 1848, writing of the spread of the electric telegraph.

and other designs [56].

In commodity compute clusters, increasing parallelism, bandwidth-intensive big data applications and cloud computing have driven a surge in data center network architecture research. An influential 2008 paper of Al-Fares, Loukissas and Vahdat [59] proposed moving from a traditional hierarchical data center design utilizing expensive core switches, to a network built of small components which nevertheless achieved high throughput — a folded Clos or "fat tree" network (Fig. 2.1). This work was followed by several related designs including Portland [73] and VL2 [41], designs utilizing servers for forwarding [42, 43, 87], and designs incorporating optical circuit switches [36, 83].

Despite making progress towards building high throughput networks, this literature does not address what in hindsight is a natural question to ask: *How far are we from throughput-optimal network design?*. Even if topology designers are continuously designing topologies better than the previous state-of-the-art, it is crucial to know what the finish line to this race is! This is the first work to propose an upper bound on the throughput of *any* topology built with given set of (identical) switches. We further show that our random graph based approach achieves throughput within a few percent of this upper bound.

Further, none of the past architectures address the issue of *incremental expansion* of the network. For some (the fat-tree, for instance), adding servers while preserving the structural properties would require replacing a large number of network elements and extensive rewiring. MDCube [87] allows expansion at a very coarse rate (several thousand servers). DCell and BCube [43, 42] allow expansion to an *a priori* known target size, but require servers with free ports reserved for planned future expansion.

LEGUP [29] directly attacks the problem of expansion by attempting to find the optimal upgrades for a Clos network. However, such an approach is fundamentally limited by having to start from a rigid structure, and adhering to it during the upgrade process. Unless free ports are preserved for such expansion (which is part of LEGUP's approach), this can cause significant overhauls of the topology even when adding just a few new servers. We show that Jellyfish provides a simple method to expand the network to almost any desirable scale. Further, our comparison with LEGUP over a sequence of network expansions illustrates that Jellyfish provides significant cost-efficiency gains in incremental expansion.

Curtis et al. proposed REWIRE [30], a heuristic optimization-based method to find high capacity topologies with a given cost budget, taking into account length-varying cable cost. While [30] compares with random graphs, their experiments are very restricted (in both the assumptions made, and the scenarios eval-

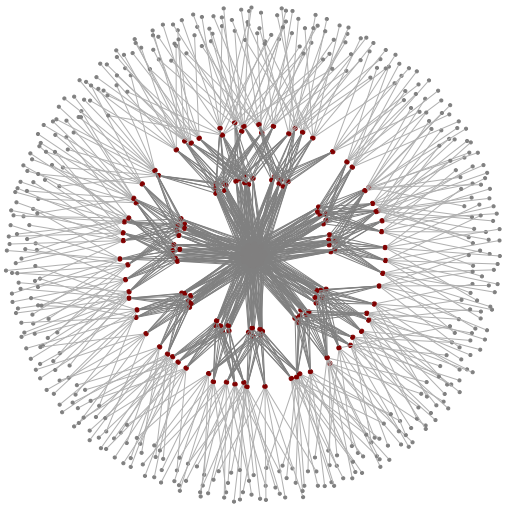

Figure 2.1 ***A fat-tree network of 432 servers and 180 12-port switches.***

uated), and their results comparing REWIRE with random graphs are inconclusive. Results in [30] show, in some cases, fat-trees obtaining more than an order of magnitude worse bisection bandwidth than random graphs, which in turn are more than an order of magnitude worse than REWIRE topologies — all at equal cost. In other cases, [30] shows random graphs that are disconnected. These significant discrepancies could arise from: (a) [30] assuming linear physical placement of all racks, so cable costs for distant servers scale as $\Theta(n)$ rather than $\Theta(\sqrt{n})$ in a more typical two-dimensional layout; (b) evaluating very low bisection bandwidths (**0.04** to 0.37) – at the highest bisection bandwidth evaluated, [30] indicates the random graph, in fact, has 23% *higher* throughput than REWIRE's topologies; and (c) separating network port costs from cable costs, resulting in the random graph ending up with too many ports and too few cables to connect them. REWIREs code is not available, so a comparison has not been possible. But more fundamentally, all of the above approaches are either point designs or heuristics which by their blackbox nature, provide neither an understanding of the solution space, nor any evidence of near-optimality.

Random graphs have been previously examined in the context of theoretical models of communication networks [65]. Prior to our work, however, the efficiency gains (in throughput) that such graphs bring over traditional data center topologies had not been characterized. Moreover, random networks had not been made practically implementable; in this work, by addressing the problems of efficient routing and physical cabling, we make it feasible to build data center networks randomly.

Two recent proposals, Scafida [45] and Small-World Datacenters (SWDC) [79] incorporate randomness into the design, but these topologies have substantial correlation (i.e., structure) among edges. Such structure can cause problems with incremental expansion because it makes it unclear whether the topology retains its characteristics on expansion; neither proposal investigates this issue. Further, in SWDC, the use of a regular lattice underlying the topology creates familiar problems with incremental expansion.[2] Scafida also does not improve on throughput and has marginally worse diameter than a fat-tree. Similarly, as we show later, SWDC topologies have lower throughput than our Jellyfish design built using the same equipment.

Two proposals that merit special attention are ones that achieve throughput performance very similar to our Jellyfish proposal, although we note that the Jellyfish work pre-dates both of these. These are SlimFly [14] and Long Hop Networks [82]. While their throughput performance is indeed nearly the same as Jellyfish networks (and in the case of SlimFly, a bit worse under near-worst-case traffic), neither addresses the problem of heterogeneity. Long Hop networks may also be difficult to expand, while SlimFly proposes either leaving ports free for future expansion, or wiring them up with random links in the manner of Jellyfish.

2.2 Evaluation of network topologies

While the literature on network topology design is large and growing quickly, with a number of designs having been proposed in the past few years [7, 41, 42, 73, 43, 83, 36, 80, 29, 30], each of these research proposals only makes a comparison with one or two other past proposals, with no standard benchmarks for the comparison. There has been no rigorous evaluation of a large number of topologies.

The most significant work in the space is from Popa et. al. [76]. They assess 4 topologies to determine the one that incurs least expense while achieving a target level of performance under a specific workload (all-to-all traffic). Their attempts to equalize performance required careful calibration, and approximations still had to be made. Accounting for the different costs of building different topologies is also an inexact process. We sidestep that issue by using the random graph as a normalizer: instead of attempting to match performance, for each topology, we build a random graph with *identical* equipment, and then compare throughput performance of the topology with that of the random graph. Each topology is compared to the random graph and thus the problem of massaging structured designs into roughly equivalent configurations

[2] For instance, using a $2D$-Torus as the lattice implies that to maintain the network structure when expanding an n node network, one must add $2\sqrt{n} - 1$ new nodes. The higher the dimensionality of the lattice, the more complicated expansion becomes.

is alleviated. This also makes it easy for others to use our tools, and to test arbitrary workloads. Apart from comparing topologies, our work also argues the superiority of flow-metrics to cuts.

Other work on comparing topologies is more focused on reliability and cuts in the topology [55].

Several researchers have used bisection bandwidth and sparsest cut as proxies for throughput performance. Further, the usage of these two terms is not consistent across the literature. For instance, REWIRE [30] explicitly optimizes its topology designs for high sparsest cut, although it refers to the standard sparsest cut metric as bisection bandwidth. Tomic [82] builds topologies with the objective of maximizing bisection bandwidth (in a particular class of graphs). Webb et. al [85] use bisection bandwidth to pick virtual topologies over the physical topology. An interesting point of note is that they consider all-to-all traffic "a worst-case communication scenario", while our results (Figure 3.4) show that other traffic patterns can be significantly worse. PAST [81] tests 3 data center network proposals with the same sparsest cut (while referring to it as bisection bandwidth). Although it is not stated, the authors presumably used approximate methods because even approximating sparsest cut is believed to be NP-Hard [21]. While that does not imply that it could not be efficiently computed for these particular graphs, to the best of our knowledge, no sparsest-cut computation procedures are known for any of the networks tested in PAST. Further, PAST finds that the throughput performance of topologies with the same sparsest cut is different in packet-level simulations, raising questions about the usefulness of such a comparison; one must either build topologies of the same cost and compare them on throughput (as we do), or build topologies with the same performance and compare cost (as Popa et. al [76] do). These observations underscore the community's lack of clarity on the relationship between bisection bandwidth, sparsest cut, and throughput. A significant component of our work tackles this subject.

CHAPTER 3

How do we evaluate topologies?

Throughput is a fundamental property of communication networks: how much data can be carried across the network between desired end-points per unit time? Particularly in the application areas of data centers and high performance computing (HPC), an increase in throughput demand among compute elements has reinvigorated research on the subject, and a large number of network topologies have been proposed in the past few years to achieve high capacity at low cost [7, 41, 42, 73, 43, 83, 36, 80, 29, 30].

However, there is little order to this large and ever-growing set of network topologies. We lack a broad comparison of topologies, and there is no open, public framework available for testing and comparing topology designs. The absence of a well specified benchmark complicates research on network design, making it difficult to evaluate a new design against the numerous past proposals, and difficult for industry to know which threads of research are most promising to adopt.

In fact, not only are we lacking throughput comparisons across a spectrum of topologies, we argue that the situation is worse: the community has, in many cases, been using the wrong metrics for measuring throughput. Cut-based metrics such as bisection bandwidth and sparsest cut are commonly used to estimate throughput, because minimum cuts are assumed to measure worst-case throughput [75]. However, while this is true for the case where the network carries only one flow, it does not hold for the common case of general traffic matrices. In the latter case, the cut is only an upper bound on throughput. The resulting gap between the cut-metric and the throughput leaves open the possibility that in a comparison of two topologies, the cut-metric could be larger in one topology, while the throughput could be greater in the other. Later in this chapter, we shall demonstrate that this discrepancy indeed occurs in practice.

This chapter includes previously published results from *Measuring and Understanding Throughput of Network Topologies*. Sangeetha Abdu Jyothi, Ankit Singla, P. Brighten Godfrey, and Alexandra Kolla. Manuscript, arXiv:1402.2531, 2015. This work was led by Sangeetha Abdu Jyothi.

Our goal is to build a framework for accurate and consistent measurement of the throughput of network topologies, and use this framework to benchmark proposed topologies. We make the following contributions towards this goal:

(1) Bisection bandwidth is the wrong metric. We show that the commonly used cut-based metrics, bisection bandwidth and sparsest cut, are flawed predictors of performance: topology A can have a higher cut-metric than topology B while topology B has asymptotically higher throughput, even for worst-case traffic. In addition, these cut metrics are NP-complete to compute. We implement a suite of heuristics to find sparse cuts, and show that the resulting sparse cuts do in fact differ from throughput for a number of proposed topologies.[1]

(2) Towards a throughput metric. Since cuts are the wrong metric, one can instead measure throughput directly. But throughput depends on the traffic workload presented. Therefore it is useful to test networks with worst-case traffic matrices (TMs). We develop an efficient heuristic for generating a near-worst-case TM for any given topology, and show that these near-worst-case TMs approach a theoretical lower bound of throughput in practice. One can therefore benchmark topologies using this TM, along with other workloads of interest. Finally, to make fair comparisons across proposals with differing equipment (e.g. different numbers of switches or distribution of links), we compare each topology against a random graph constructed with the same equipment, and use the throughput relative to the random graph as a consistent measure of the topology's throughput.

(3) Benchmarking proposed topologies. We evaluate a set of 10 topologies proposed for data centers and high performance computing. We find that:

- Throughput differs depending on TM, with some topologies dropping substantially in performance for near-worst-case TMs.
- The bulk of proposals, for all TMs, perform worse than Jellyfish (our own design based on random graphs, detailed in Chapter 4), with the latter's advantage increasing with scale.
- Proposals for networks based on expander graphs, including Jellyfish's random topology, Long Hop [82], and Slim Fly [14], have nearly identical performance for uniform traffic (e.g. all-to-all). This contrasts

[1] While some studies use better metrics [41], many do evaluate or optimize based on bisection bandwidth, e.g. [30, 82, 85, 81, 6]. Furthermore, to the best of our knowledge, our work is the first to quantitatively evaluate the error of bisection bandwidth compared to worst-case throughput.

with conclusions of [82, 14]; note that [14] analyzed bisection bandwidth rather than throughput.

To the best of our knowledge, this work is the most expansive comparison of network topology throughput to date, and the only one to use an accurate and consistent method of comparison. Our evaluation framework and the set of topologies tested are freely available [5]. We hope these tools will facilitate future work on rigorously designing and evaluating networks, and replication of research results.

3.1 Metrics for throughput

In this section, we investigate the metrics currently used for estimating throughput, identify their shortcomings and propose a new metric which is more efficient and more accurate.

3.1.1 Throughput defined

This chapter focuses on network throughput treating the network as a graph, ignoring systems-level design issues like routing and congestion control[2]. Therefore, the metric of interest is end-to-end throughput supported by a network in a fluid-flow model with optimal routing. We next define this more precisely.

A **network** is a graph $G = (V, E)$ with capacities $c(u, v)$ for every edge $(u, v) \in E_G$. Among the nodes V are **servers**, which send and receive traffic flows, connected through non-terminal nodes called **switches**. Each server is connected to one switch, and each switch is connected to zero or more servers, and other switches. Unless otherwise specified, for switch-to-switch edges (u, v), we set $c(u, v) = 1$, while server-to-switch links have infinite capacity. This allows us to stress-test the network topology itself, rather than the servers.

A **traffic matrix (TM)** T defines the traffic demand: for any two servers v and w, $T(v, w)$ is an amount of requested flow from v to w. We assume without loss of generality that the traffic matrix is normalized so that it conforms to the "hose model": each server sends at most 1 unit of traffic and receives at most 1 unit of traffic ($\forall v$, $\sum_w T(v, w) \leq 1$ and $\sum_w T(w, v) \leq 1$).

The **throughput** of a network G with TM T is defined as the maximum value t for which $T \cdot t$ is feasible in G. That is, we seek the maximum t for which there exists a feasible multicommodity flow that routes flow $T(v, w) \cdot t$ through the network from each v to each w, subject to the link capacity and the usual flow

[2]We do consider other aspects of our specific network topology proposal in later chapters, where we also show that at least for our proposal, Jellyfish, routing and congestion control can be made very efficient, thus making raw throughput analysis valuable.

conservation constraints. This can be formulated in a standard way as a linear program (which we omit for brevity) and is thus computable in polynomial time. If the nonzero traffic demands $T(v, w)$ have equal weight, as they will throughout this chapter, this is equivalent to the *maximum concurrent flow* [78] problem: maximizing the minimum throughput of any requested end-to-end flow.

Note that we could alternately maximize the *total* throughput of all flows. We avoid this because it would allow the network to pick and choose among the TM's flows, giving high bandwidth only to the "easy" ones (e.g., short flows that do not cross a bottleneck). The formulation above ensures that *all* flows in the given TM can be satisfied at the desired rates specified by the TM, all scaled by a constant factor.

We now have a precise definition of throughput, but it depends on the choice of TM. How can we evaluate a *topology* independent of assumptions about the traffic?

3.1.2 Bisection bandwidth defined

Bisection bandwidth is by far the most commonly-used attempt to provide an evaluation of a topology's performance independent of a specific TM. Since any cut in the graph upper-bounds the flow across the cut, if we find the minimum cut then we can bound the worst-case performance. The intuition is that this corresponds to the unfortunate case that all communicating pairs are located on opposite sides of this cut. Now, of course, the smallest cuts might just slice off a single node, while we are interested in larger-scale bottlenecks; so the bisection bandwidth requires splitting the nodes into two equal-sized groups. Bisection bandwidth of a graph G is typically (see [75], p. 974) defined as

$$BB(G) = \min_{S \subseteq V, |S| = \frac{n}{2}} c(S, \bar{S}),$$

where $\bar{S}$ is the complement of S and $c(S, \bar{S})$ is the total capacity of edges crossing the bisection $(S, \bar{S})$.

3.1.3 Bisection bandwidth is the wrong metric

Bisection bandwidth does give some insight into the capacity of a network. It provides an upper-bound on worst-case network performance, is simple to state, and can sometimes be "eyeballed" for simple networks.

However, it has several limitations. First, it is NP-complete to compute [40]; the , where we also show that at least for our proposal, Jellyfish, routing and congestion control can be made very efficient, thus making raw throughput analysis valuable.best approximation algorithm has a polylogarithmic approximation

factor [37]. Even if one could use specialized algorithms to calculate it for structured topologies, no such methods are known for unstructured networks (such as our own Jellyfish proposal which we discuss later, as well as several others proposed recently [30, 38]). This makes comparisons across networks difficult.

Second, the insistence on splitting the network in half means that bisection bandwidth may not uncover the true bottleneck. For example, consider a graph G where the bottleneck is a single edge that divides $\frac{1}{4}n$ of the nodes (node set A) from the rest of the network (node set B) where A and B are themselves cliques. Within each set, nodes have $\Theta(n)$ neighbors, and hence $BB(G) = \Theta(n^2)$ while the graph actually has a bottleneck consisting of a single link.

This is, of course, a rather trivial problem. It may not arise in practice for highly symmetric networks typically encountered in the HPC community where bisection bandwidth has historically been used. However, it is worth mentioning here since (1) the above definition of bisection bandwidth has been used extensively, (2) the above issue means bisection bandwidth is not a sufficiently robust metric to handle general irregular and heterogeneous networks including those we shall consider in later chapters. We also note that recently-proposed data center networks are both heterogeneous [41] and irregularly structured [79, 30, 38], so bisection bandwidth may be unsuitable for them.

Next, we will see how this particular problem with bisection bandwidth can be fixed, but how cut-based metrics (including bisection bandwidth) are subject to a more fundamental problem.

3.1.4 Sparsest cut defined

There are several ways to fix bisection bandwidth's overly rigid requirement of exact bisection, such as balanced partitioning [12] and sparsest cut. Our overall conclusions are not sensitive to the distinction; we use sparsest cut here.

The **uniform sparsest cut** weights the cut by the number of separated vertex pairs. That is, the uniform sparsity of a cut $S \subseteq V$ is

$$\phi(S) = \frac{c(S, \bar{S})}{|S| \cdot |\bar{S}|},$$

where $c(S, \bar{S})$ is the total capacity of edges crossing the cut. The uniform sparsest cut is the cut of sparsity $min_{S \subseteq V} \phi(S)$. To motivate this definition, it helps to generalize it. The (nonuniform) sparsity of a cut weights the cut by the amount of *traffic demand* across the cut. That is, for a given TM T, the sparsity of a

cut is

$$\phi(S,T) = \frac{c(S,\bar{S})}{T(S,\bar{S})},$$

where $T(S,\bar{S})$ is the traffic demand crossing the cut, i.e., $T(S,\bar{S}) = \sum_{v\in S, w\in\bar{S}} T(v,w)$. The **nonuniform sparsest cut** for TM T is then the cut of sparsity $min_{S\subseteq V}\phi(S,T)$. Intuitively, this cut should be the one across which it's hardest to push the traffic demand T.

Observe that the uniform sparsest cut is a special case of the nonuniform sparsest cut when we take T to be the complete traffic matrix ($T(v,w) = 1\ \forall v,w$). Also observe that bisection bandwidth is equivalent to the uniform sparsest cut if it happens that the uniform sparsest cut has $\frac{n}{2}$ nodes on either side. The reader can assume sparsest cut refers to the uniform case unless otherwise specified.

3.1.5 Sparsest cut is the wrong metric

The improved cut metric will now succeed in finding the true bottleneck, unlike bisection bandwidth. But have we found the right metric for worst-case throughput? We argue that the answer is no, for three reasons.

(1) Sparsest cut and bisection bandwidth are not actually TM-independent, contrary to our original goal of evaluating a topology independent of traffic. As discussed above, bisection bandwidth and the uniform sparsest cut correspond to the worst cuts for the complete (all-to-all) TM, so they have a hidden implicit assumption of this particular TM.

(2) Even for a specific TM, computing sparsest cut is NP-hard for most TMs, and it is believed that there is no efficient constant factor approximation algorithm [21]. In contrast, throughput is computable in polynomial time for any specific TM. Sparsest cut's difficulty is both practically inconvenient and strong evidence that cut-based metrics are not computing the same physical quantity as throughput.

(3) While cuts upper-bound throughput, it is only a *loose* upper bound. This may be counterintuitive, if our intuition is guided by the well-known max-flow min-cut theorem. In a network with a single $v \to w$ traffic flow, the theorem states that the maximum $v \to w$ flow is equal to the minimum capacity over all cuts separating v and w [39, 32]. The result is also true for networks with two flows [50]. But it is not true when there are more than two flows (i.e., *multi-commodity flow*), which is of course the case of primary interest in computer networks. Specifically, in a multi-commodity flow with uniform demands, the maximum flow throughput can be an $O(\log n)$ factor lower than the sparsest cut [57]. Hence, sparse cuts do not directly

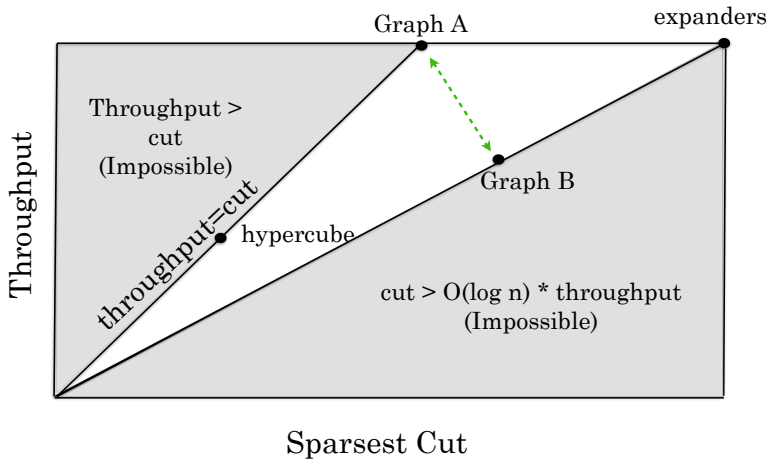

Figure 3.1 ***Sparsest cut vs. Throughput***

capture the maximum flow.

Figure 3.1 depicts the relationship between sparsest cut and throughput. The flow (throughput) in the network cannot exceed the upper bound imposed by the worst-case cut. On the other hand, the cut cannot be more than a factor $O(\log n)$ greater than the flow [57]. Thus, any graph and an associated TM can be represented by a unique point in the region bounded by these limits.

While this distinction is well-established [57], we strengthen the point by showing that *it can lead to incorrect decisions when evaluating networks*. Specifically, we will exhibit a pair of graphs A and B such that, as shown in Figure 3.1, A has higher throughput but B has higher sparsest cut. If sparsest cut is the metric used to choose a network, graph B will be wrongly assessed to have better performance than graph A, while in fact it has a factor $\Omega(\sqrt{\log n})$ worse performance!

Graph A is a clustered random graph with n nodes and degree $2d$. A is composed of two equal-sized clusters with $n/2$ nodes each. Each node in a cluster is connected by degree α to nodes inside its cluster, and degree β to nodes in the other cluster, such that $\alpha+\beta = 2d$. A is sampled uniformly at random from the space of all graphs satisfying these constraints. We can pick α and β such that $\beta = \Theta(\frac{\alpha}{\log n})$. Then, as we show in Lemma 3, the throughput of A (denoted T_A) and its sparsest cut (denoted Φ_A) are both $\Theta(\frac{1}{n \log n})$.

Let graph G be any $2d$-regular expander on $N = \frac{n}{dp}$ nodes, where d is a constant and p is a parameter we shall adjust later. **Graph B** is constructed by replacing each edge of G with a path of length p. It is easy to see that B has n nodes. We prove in Appendix A, the following theorem.

Theorem 1. $T_B = O(\frac{1}{np\log n})$ *and* $\Phi_B = \Omega(\frac{1}{np})$.

In the above, setting $p = 1$ corresponds to the 'expanders' point in Figure 3.1: both A and B have the same throughput (within constant factors), but the B's cut is larger by $O(\log n)$. Increasing p creates an asymptotic separation in both the cut and the throughput such that $\Phi_A < \Phi_B$, while $T_A > T_B$. For instance, if $p = \sqrt{\log n}$, $T_B = O(\frac{1}{n(\log n)^{3/2}})$ and $\Phi_B = \Omega(\frac{1}{n\sqrt{\log n}})$. Further, if $p = \Theta(\log n)$, we can tune the constants such that $T_A > T_B\Theta(\log n)$ even though $\Phi_A < \Phi_B$.

Intuition. The reason that throughput may be smaller than sparsest cut is that in addition to being limited by bottlenecks, the network is limited by the total volume of "work" it has to accomplish within its total link capacity. That is, if the TM has equal-weight flows,

$$Throughput\ per\ flow \leq \frac{Total\ link\ capacity}{\#\ of\ flows\ \cdot\ Average\ path\ length}$$

where the total capacity is $\sum_{(i,j)\in E} c(i,j)$ and the average path length is computed over the flows in the TM. This "volumetric" upper bound may be tighter than a cut-based bound.

3.1.6 Aside: Are cut metrics useful at all?

While throughput is the focus of this work, it is not the only graph property of interest, and cut-based metrics do capture important graph properties. One obvious example is reliability: cut-based metrics directly capture the difficulty of partitioning a network.

A less obvious example is physical network layout. Consider two networks A, B with the same throughput, but with B having greater bisection bandwidth. Suppose we desire a physical realization of these networks grouping them into two equal-sized clusters, such that shorter, cheaper cables will be used to create links within clusters and longer, more expensive cables must be used across clusters. Since A has lower bisection bandwidth, there is a way to partition it which uses fewer long cables. In other words, in this case, B's higher bisection bandwidth is actually bad — it yields no performance benefit and corresponds to greater difficulty in physical cabling! — so we actually wish to *minimize* bisection bandwidth.

3.1.7 Towards a throughput metric

Having exhausted cut-based metrics, we return to the original metric of throughput defined in §3.1.1, and suggest a simple solution: network topologies should simply be evaluated directly in terms of throughput

(via LP optimization software), for specific TMs.

The key, of course, is how to choose the TM. If we can find a worst-case TM, this would fulfill the goal of evaluating topologies independent of assumptions about traffic. However, computing a worst-case TM is an unsolved, computationally non-trivial problem [22].[3] Here, we offer practical, efficient heuristics to find a *bad-case TM* which can be used to benchmark topologies.

We begin with the complete or **all-to-all TM** T_{A2A} which for all v, w has $T_{A2A}(v, w) = \frac{1}{n}$. We observe that T_{A2A} is in fact within $2\times$ of the worst case TM. This fact is simple and known to some researchers, but at the same time, we have not seen it in the literature, so we give the statement here and the proof in Appendix B.

Theorem 2. *Let G be any graph. If T_{A2A} is feasible in G with throughput t, then any hose model traffic matrix is feasible in G with throughput $\geq t/2$.*

Can we get closer to the worst case TM? In our experience, TMs with a smaller number of "elephant" flows are more difficult to route than TMs with a large number of small flows, like T_{A2A}. This suggests a **random matching TM** in which we have only one outgoing flow and one incoming flow per server, chosen uniform-randomly among servers. We can further stress the network topology by decreasing the number of servers attached to each switch, so there are even fewer flows originating from each switch. These TMs actually lack the factor of 2 near-worst-case guarantee of T_{A2A}, but in practice we have found they consistently result in lower throughput than T_{A2A}.

Can we get *even closer* to the worst-case TM? Intuitively, the all-to-all and random matching TMs will tend to find sparse cuts, but only have average-length paths. Drawing on the intuition that throughput decreases with average flow path length, we seek to produce traffic matrices that force the use of long paths. To do this, given a network G, we compute all-pairs shortest paths and create a complete bipartite graph H, whose nodes represent all sources and destinations in G, and for which the weight of edge $v \to w$ is the length of the shortest $v \to w$ path in G. We then find the maximum weight matching in H. The resulting matching corresponds to the pairing of servers which maximizes average flow path length, assuming flow is routed on shortest paths between each pair. We call this a **longest matching TM**.

Kodialam et al. [54] proposed another heuristic to find a near-worst-case TM: maximizing the average

[3] Our problem corresponds to the separation problem of the minimum-cost robust network design in [22]. This problem is shown to be hard for single-source hose model. However, the complexity is unknown for the hose model with multiple sources which is the scenario we consider.

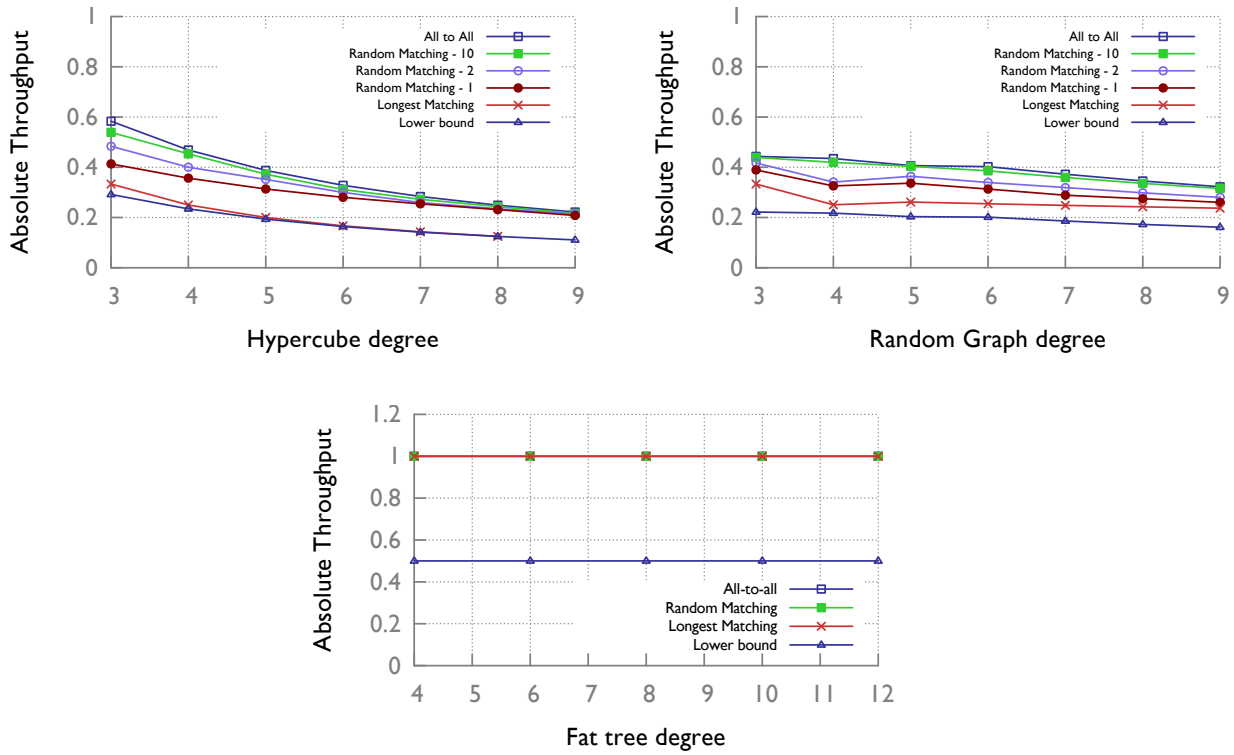

Figure 3.2 ***Throughput resulting from several different traffic matrices in three topologies***

path length of a flow. This **Kodialam TM** is similar to the longest matching but may have many flows attached to each source and destination. This TM was used in [54] to evaluate oblivious routing algorithms, but there was no evaluation of how close it is to the worst case, so our evaluation here is new.

Figure 3.2 shows the resulting throughput of these TMs in three topologies: hypercubes, random regular graphs, and fat trees [7]. In Figure 3.2, the meaningful comparison is of the various TMs within each topology. In all cases, A2A traffic has the highest throughput; throughput decreases or does not change as we move to a random matching TM with 10 servers per switch, and progressively decreases as the number of servers per switch is decreased to 1 under random matching, and finally to the longest matching TM and the Kodialam TM. We also plot the lower bound given by Theorem 2: $T_{A2A}/2$. Comparison across topologies is not relevant here since the topologies are not built with the same "equipment" (node degree, number of servers, etc.)

These three topologies were chosen to illustrate cases when our approach is most helpful, somewhat helpful, and least helpful at finding near-worst-case TMs. In the **hypercube**, the longest matching TM is extremely close to the worst-case performance. To see why, note that the longest paths have length d in a

d-dimensional hypercube, twice as long as the mean path length; and the hypercube has $n \cdot d$ uni-directional links. The total flow in the network will thus be $(\#\ flows \cdot average\ flow\ path\ length) = n \cdot d$. Thus, all links will be perfectly utilized if the flow can be routed, which empirically it is. In the **random graph**, there is less variation in end-to-end path length, but across our experiments the longest matching is always within $1.5\times$ of the provable lower bound (and may be even closer to the true lower bound, since Theorem 2 may not be tight). In the **fat tree**, which is here built as a three-level nonblocking topology, there is essentially no variation in path length since asymptotically nearly all paths go three hops up to the core switches and three hops down to the destination. Here, our TMs are no worse than all-to-all, and the simple $T_{A2A}/2$ lower bound is off by a factor of 2 from the true worst case (which is throughput of 1 as this is a nonblocking topology).

The longest matching and Kodialam TMs are identical in hypercubes and fat trees. On random graphs, they yield slightly different TMs, with differences disappearing for larger networks. However, longest matching has a significant practical advantage: it produces far fewer end-to-end flows than the Kodialam TMs. Since the memory requirements of computing throughput of a given TM (via the multicommodity flow LP) depends on the number of flows, longest matching requires less memory and compute time. For example, in random graphs on a 32 GB machine using the Gurobi optimization package, the Kodialam TM can be computed up to 128 nodes while the longest matching scales to 1,024. Hence, we choose longest matching as our representative nearly-worst-case traffic matrix.

3.1.8 Summary and implications

Cut-based metrics can be safely abandoned for the purposes of topology performance evaluation. They are not in fact independent of assumptions on the traffic matrix; they are NP-complete to compute; and they are not always an accurate measure of worst-case throughput, which as we showed can lead to incorrect performance evaluations. These facts call into question work which has optimized networks based on bisection bandwidth [82] and work which compared networks on "equal footing" by attempting to approximately equalize their bisection bandwidth [81].

Having surmounted that moment of catharsis, we actually obtain some relief: directly evaluating throughput with particular TMs using LP optimization is both more accurate and more tractable than cut-based metrics. In choosing a TM to evaluate, both "average case" and near-worst-case TMs are reasonable choices.

A2A, random permutation, and measurements from real-world applications may offer reasonable average-case benchmarks. For near-worst-case traffic, we developed a practical heuristic that often succeeds in substantially worsening the TM compared with A2A.

Note that measuring throughput directly is not in itself a novel idea: numerous papers have evaluated particular topologies on particular TMs. In contrast, our study provides a rigorous analysis of throughput vs. cut-metrics, a way to generate near-worst-case traffic for any given topology, and an experimental evaluation of both our metrics and of a large number of proposed topologies in those metrics.

3.2 Experimental evaluation

Having established a framework for evaluating throughput, in this section we evaluate the framework experimentally: Are cut-metrics indeed worse predictors of performance? When measuring throughput directly, how close do we come to worst-case traffic? Then, we employ our framework for a comparison of commonly-used and proposed data center and HPC network topologies. But first, we present our experimental methodology.

3.2.1 Methodology

3.2.1.1 Computing cut-metrics

Before we can evaluate whether cuts predict throughput, we need to deal with the fact that the cut-metrics themselves are NP-complete to compute. Bisection bandwidth considers all cuts that divide the network in half, and sparsest cut considers all possible cuts; both are exponentially large sets. We focus our evaluation on sparsest cut, since in general it finds bottlenecks better than bisection bandwidth (§3.1.4).

To deal with the computational complexity, we implemented a set of heuristics that find potentially bad cuts, apply all of them, and finally use the sparsest cut found by any heuristic. These heuristics are: (1) Brute force, which is feasible only for networks of up to around 20 nodes, after which we have the code simply output the sparsest of 100,000 considered cuts. (2) Cutting every single node and (3) every pair of nodes, to catch cases when sparse cuts are near the edge of the network. (4) Cutting expanding regions of the network, defined by nodes within distance k from each node, for each relevant value of k. (5) An eigenvector-based technique which is known to be within a constant factor of the actual sparsest cut. Details of these heuristics

are in Appendix D. We thus made every effort to use the best available means for calculating cut metrics, lest we dismiss them casually. We believe this is the most thorough empirical evaluation of cut metrics that has appeared for data center and HPC networks.

3.2.1.2 Computing throughput

Throughput is computed as a solution to a linear program whose objective is to maximize the minimum flow across all flow demands, as explained in §3.1. We use the Gurobi [44] solver to compute throughput. Throughput depends on the traffic workload provided to the network.

3.2.1.3 Traffic workload

We evaluate three traffic matrix families given in §3.1.7: all to all, random matching and our longest matching TM. In addition, we need to specify where the traffic endpoints (sources and destinations, i.e., servers) are attached. In structured networks with restrictions on server-locations (fat-tree, BCube, DCell), servers are added at the locations prescribed by the models. For example, in fat-trees, servers are attached only to the lowest layer. For all other networks, we add servers to each switch. Note that our traffic matrices effectively encode switch-to-switch traffic, so the particular *number* of servers doesn't matter.

3.2.1.4 Topologies

Our evaluation uses 10 families of computer networks, plus a collection of "natural" networks.

BCube [42], designed for modular data center networks, differs from other structured computer networks in its server-centric design. $BCube_k$ consists of $(k+1)$ levels with each level containing n^k n-port switches. Each server in $BCube_k$ has degree $(k+1)$ and is connected to one switch in each of the $(k+1)$ levels. A BCube network of $(k+1) \cdot n^k$ switches supports exactly n^{k+1} hosts. (In our framework, a BCube server is represented equivalently as a switch with an extra port connected to a server.)

DCell [43] is also designed for data center networks, and like BCube is server-centric. It is constructed as a recursive design starting with a building block where a switch is connected to a small number of servers. $DCell_0$ has n servers connected to a switch. $DCell_1$ is constructed from $n+1$ copies of $DCell_0$. The number of servers supported by $DCell_k$ is $t_k = t_{k-1} \cdot (t_{k-1}+1)$. (Similar to BCube, servers in DCell are replaced by equivalent switches during comparison.)

Dragonfly [53] combines a group of routers to form a virtual router with a higher effective radix, thereby reducing the network diameter. This topology is primarily intended for HPC environments. A Dragonfly with a routers per group, where each router has h connections to other groups and p connections to servers, can support $ap(ah + 1)$ servers.

Fat Tree [59] based designs are used in modern data centers and HPC. A three-level fat-tree constructed from degree-k switches consists of $\frac{5}{4}k^2$ switches and supports $\frac{k^3}{4}$ hosts.

Flattened butterfly [52] is used in on-chip networks. A k-ary n-fly topology consists of k^{n-1} switches.

Hypercubes [47] are used in HPC and computer architecture to interconnect processors. A d-dimensional hypercube consists of 2^d nodes and has a bisection bandwidth of 2^{d-1}.

HyperX [6] designs HPC topologies by searching through combinations of flattened butterflies and hypercubes to find the optimal configuration to support a given number of servers with desired bisection bandwidth.

Jellyfish is our own proposal based on a uniform-random degree-specified graph. We proposed it for data center networks to enable flexible design and expansion, and to achieve higher throughput than structured designs. Since Jellyfish can be constructed for any size and node degree distribution, we use it as a reference point for direct comparison with other proposals.

Long Hop networks [82] are designed for data centers with the objective of maximizing the bisection bandwidth of the topology. This is achieved by translating best-known linear error correction codes to optimal designs in a family of Cayley networks. Networks of size 2^d can be constructed with node degrees varying from d to $2^d - 1$.

Slim Fly [14] is designed for HPC environments with the objective of reducing network diameter. The average path length of Slim Fly is equal to the theoretical lower bound. However, these networks can be constructed only for a limited number of node degrees.

Natural networks. For evaluating the cut-based metrics in a wider variety of environments, we consider 66 non-computer networks – food webs, social networks, and more [5].

3.2.2 Evaluation of the metrics

In this section, we experimentally compare cut-based metrics and the new throughput metric. We show that:

Topology family	Number of networks with throughput = estimated cut	Sparsest cut estimator					Total
		Brute force	1-node	2-node	Expanding regions	Eigenvector	
BCube	2	2	0	0	3	7	7
DCell	2	2	0	0	2	3	4
Dragonfly	0	2	0	0	0	2	4
Fat tree	8	8	8	8	8	8	8
Flattened butterfly	5	6	0	1	0	5	8
Hypercube	3	3	0	0	1	6	7
HyperX	1	1	0	0	1	10	11
Jellyfish	3	0	0	0	2	349	350
LongHop	9	45	0	0	1	66	110
SlimFly	1	1	0	0	0	5	6
Natural networks	48	18	21	11	34	38	66
Total	82	88	29	20	52	499	581

Table 3.1 ***Estimated sparse cuts: do they match throughput, and which estimators produce those cuts?***

- For the majority of networks, bisection bandwidth and sparsest-cut do not predict throughput accurately, in the sense that worst-case estimated cut differs from the computed throughput by a large factor.
- Throughput under different traffic matrices on the same network consistently obeys $T_{A2A} \geq T_{RM(k)} \geq T_{RM(1)} \geq T_{LM} \geq T_{LB}$, i.e., all-to-all is consistently the easiest TM in this set, followed by random matchings, longest matching, and the theoretical lower bound.
- The heuristic for near-worst-case traffic, the longest matching TM, is a significantly more difficult TM than A2A and RM and often approaches the lower bound.

3.2.2.1 Do sparse cuts predict throughput?

We generated multiple networks from each of our topology families (with varying parameters such as size and node degree), computed throughput with the longest matching TM, and found sparse cuts using the heuristics of §3.2.1.1 with the same longest matching TM. Note that we will use the term **sparse cut** to refer to the sparsest cut that was found by any of the heuristics (as opposed to the true sparsest cut).

Figure 3.3 shows the results. Sparse cuts differ from throughput substantially, with up to a $3\times$ discrepancy. In only a small number of cases, the cut equals throughput. Table 3.1 shows this in more detail:

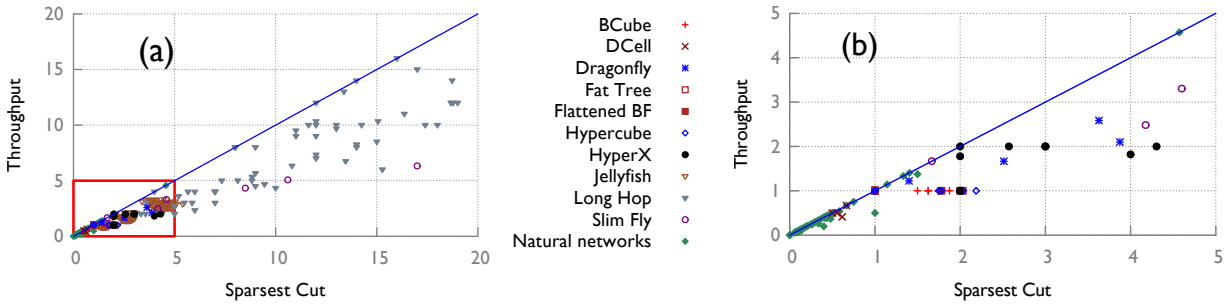

Figure 3.3 ***Throughput vs. cut for (a) all graphs, and (b) for the inset from (a). The comparisons are meaningful for individual networks, not*** **across** ***networks, since they have different numbers of nodes and degree distributions.***

comparing column 2 and the last column, we see that cuts accurately predicted throughput in less than 15% of the tested networks only. The majority of these were from our set of natural networks; the difference between cut and flow is more pronounced on computer networks. For example, Figure 3.3(b) shows that although HyperX networks of different sizes have approximately same flow value, they differ widely when sparse cuts are considered. This shows that estimation of worst-case throughput performance of networks using cut-based metrics can lead to erroneous results.

How well did our sparse cut heuristics perform? Table 3.1 shows how often each estimator found the sparse cut. More than one technique may find the sparse cut, hence the sum may not equal the total number of networks. Brute-force computation was helpful in finding 15% of the sparse cuts. Cuts involving one or two nodes and contiguous regions of the graph also found the sparse cut in a small fraction of networks (less than 10% each). The majority of such networks are the natural networks, which are often denser in the core and sparser in the edges. Sparse connectivity at the edges lead to bottlenecks at the edge which are revealed by cuts involving one or two nodes. Fat tree is another interesting case where every heuristic's cuts yield the accurate flow value. Overall, the eigenvector-based approximation found the largest number of sparse cuts (86%), but it is known not to be a tight approximation [26], and the full collection of heuristics did improve on it in a nontrivial fraction of cases.

Even with this suite of techniques, our calculation of sparse cuts is not guaranteed to find the *sparsest* cut, which could be closer to throughput. But even if that is the case, we can conclude that sparse cuts *that are feasible to compute in practice* are poor predictors of throughput (in addition to being computationally demanding). This complements our theoretical results (§3.1.5).

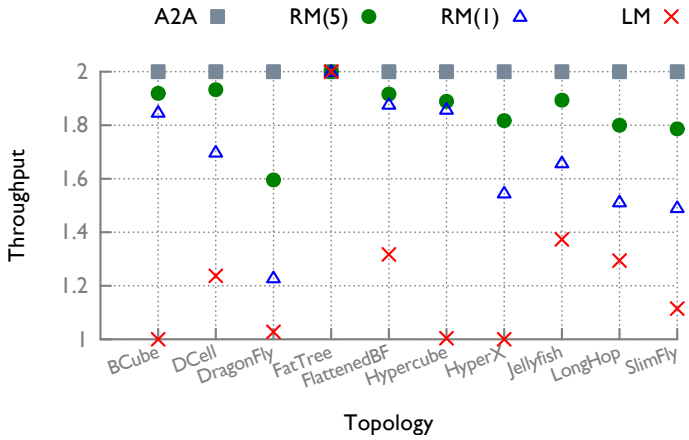

Figure 3.4 ***Comparison of throughput under different traffic matrices normalized with respect to the theoretical lower bound.***

3.2.2.2 Can we find near-worst-case traffic?

In this section, we evaluate our proposed throughput metric — in particular, how closely the TMs of §3.1.7 approach the worst case. We compare representative samples from each family of network under four types of TM: all to all (A2A), random matching with 5 servers per switch, random matching with 1 server per switch, and longest matching.

Figure 3.4 shows the throughput values normalized so that the theoretical lower bound on throughput is 1, and therefore A2A's throughput is 2. For all networks, $T_{A2A} \geq T_{RM(5)} \geq T_{RM(1)} \geq T_{LM} \geq 1$, matching the intuition discussed in §3.1.7. (As in Figure 3.3, throughput comparisons are valid across TMs for a particular network, not across networks. The networks used in this plot support approximately 250 servers each. However, the exact number of switches, links and servers varies across networks.)

Our longest matching TM is successful in matching the lower bound for BCube, Hypercube, HyperX, and (nearly) Dragonfly. In all other families except fat trees, the traffic under longest matching is significantly closer to the lower bound than with the other TMs. In fat trees, throughput under A2A and longest matching are equal. However, this is a characteristic of the network and not a shortcoming of the metric. In fat trees, it can be easily verified that the normalized traffic is the same under all TMs. In short, these results show that throughput measurement using longest matching is a more accurate estimate of worst-case throughput performance than cut-based approximations, in addition to being substantially easier to compute.

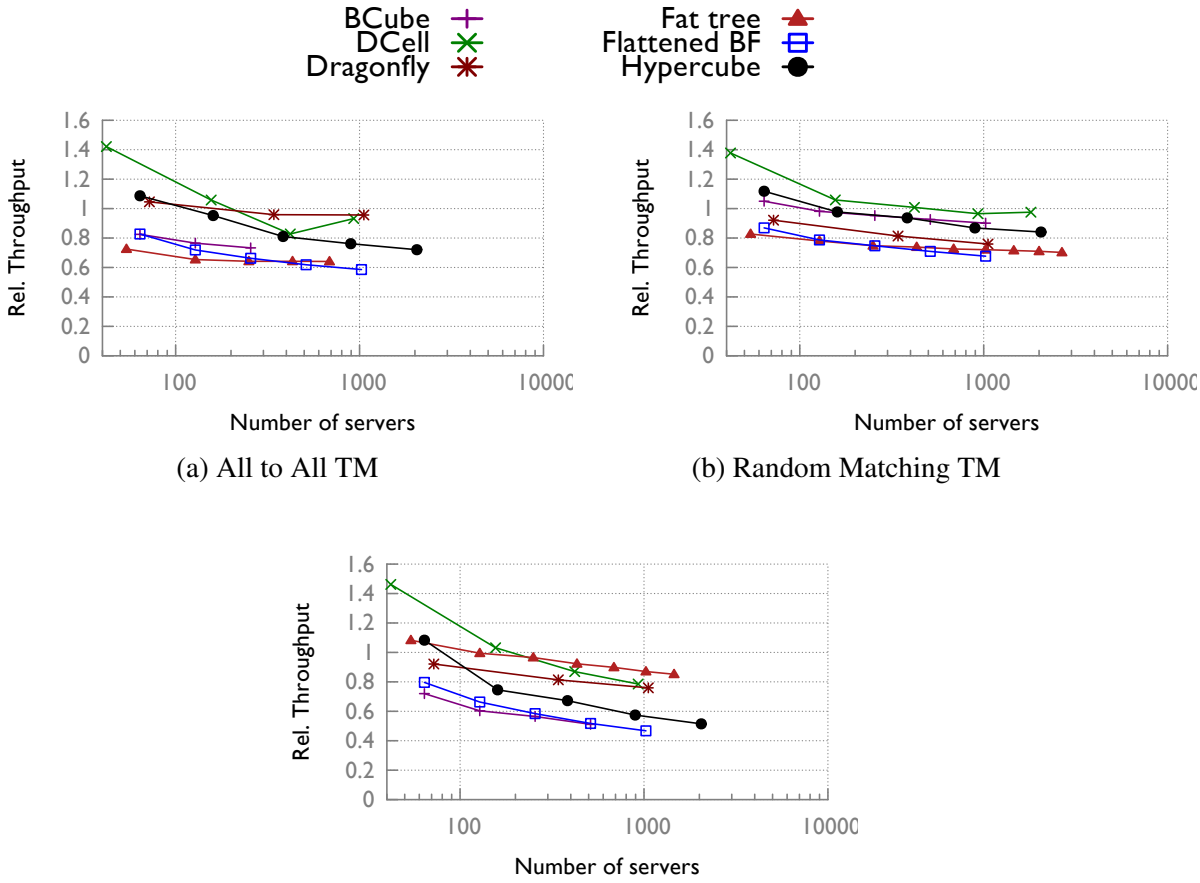

(a) All to All TM

(b) Random Matching TM

(c) Longest Matching TM

Figure 3.5 ***Comparison of TMs on topologies.***

3.2.3 Evaluation of topologies

Although the longest matching TM can give near worst-case performance results with limited computational effort, there is one more piece of the puzzle to allow comparison of networks. Networks may be built with different equipment – with a wide variation in number of switches and links. The raw throughput value does not account for this difference in network resources, and most proposed topologies can only be built with particular discrete numbers of servers, switches, and links, which inconveniently do not match.

Fortunately, uniform-random graphs like our Jellyfish design (Chapter 4) can be constructed for any size and specified degree distribution. Hence, random graphs serve as a convenient benchmark for easy comparison of network topologies. Our high-level approach to evaluating a network is to: (i) compute the network's throughput; (ii) build a random graph with precisely the same equipment, i.e., the same number of nodes each with the same number of links as the corresponding node in the original graph, (iii) compute

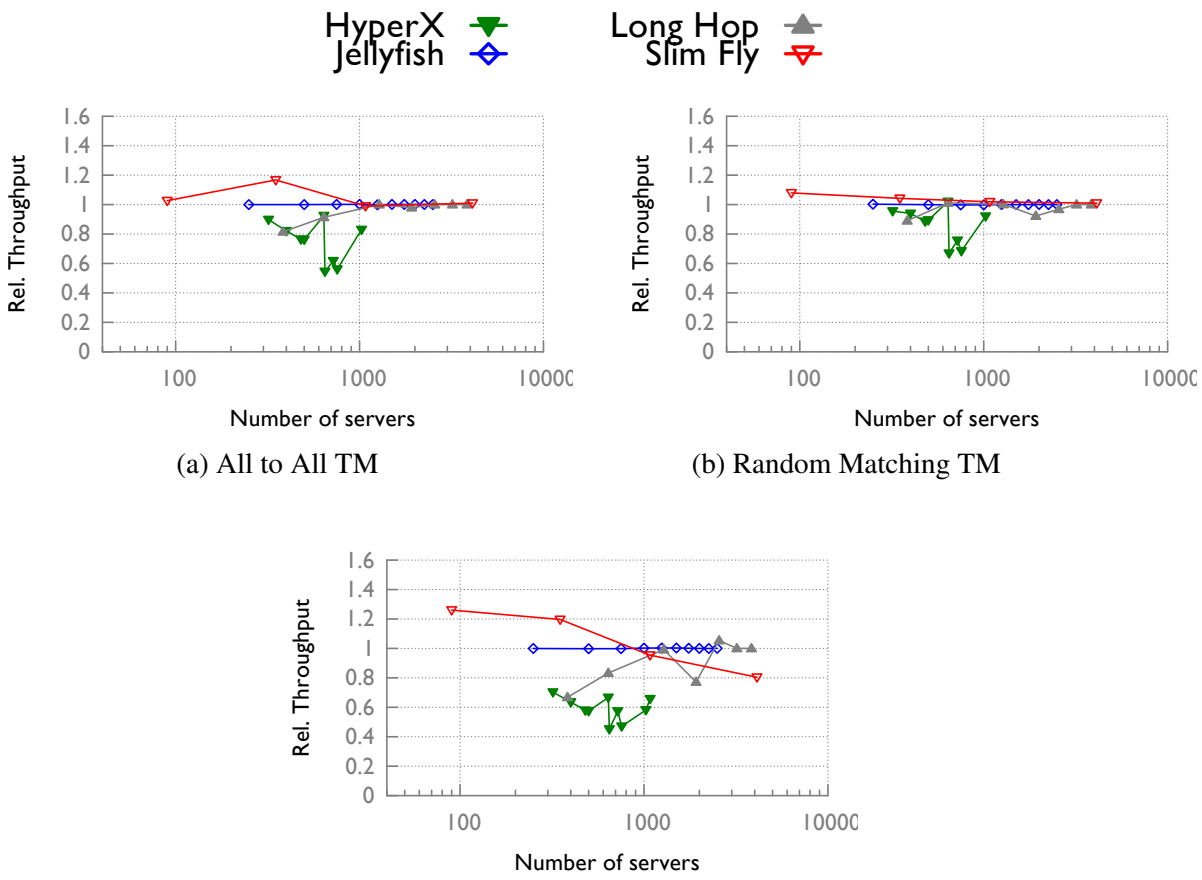

(a) All to All TM

(b) Random Matching TM

(c) Longest Matching TM

Figure 3.6 ***Comparison of TMs on more topologies.***

the throughput of this same-equipment random graph under the same TM; (iv) normalize the network's throughput with the random graph's throughput for comparison against other networks. This normalized value is referred to as **relative throughput**. Unless otherwise stated, each data-point is an average across 10 iterations, and all error bars are 95% two-sided confidence intervals. Minimal variations lead to narrow error bars in networks of size greater than 100.

We evaluate the performance of 10 types of computer networks under all three traffic matrices: all to all, random matching with one server, and longest matching. Figures 3.5 and 3.6 show the results, divided among two figures for visual clarity. Most topologies are in Figure 3.5, while Figure 3.6 shows Jellyfish, Slim Fly, Long Hop, and HyperX.

Overall, performance varies substantially, by around 1.6× with A2A traffic and more than 2× with longest matching. Furthermore, for the networks of Figure 3.5, which topology "wins" depends on the TM. For

example, Dragonfly has high relative throughput under A2A but under the longest matching TM, fat trees achieve the highest throughput at the largest scale. However, in all TMs, the Jellyfish random graph achieves consistently highest performance (relative throughput $= 1$ by definition), with Long Hop matching that performance at the largest scale. In comparison with random graphs, performance degrades for most networks with increasing size. We discuss each network's performance in detail below. Unless otherwise stated, reported metrics correspond to the largest network tested in each family.

BCube [42] The 2-ary BCube achieves 73% of the random graph's throughput under all to all traffic and 90% under random matching, but only 51% under longest matching.

DCell [43] 5-ary DCell achieves 93% of the random graph's throughput under all to all, 97% under random matching, and 79% under longest matching. The relative throughput performance degrades as the network size increases.

Dragonfly [53] networks constructed with low-radix switches of degrees varying from 4 to 8 have throughput performance under all-to-all traffic equal that of random graphs, i.e., a relative throughput approximately equal to 1. However, the performance degrades to 76% under random matching and further down to 72% under longest matching for the network constructed from switches of degree 8.

Fat Tree [7] constructed from switches of degree 14 can achieve only 65% of the throughput of random graphs under A2A. Interestingly, a fat tree achieves 73% of a random graph's throughput under random matching, and 89% with longest matching. While the fat-tree's non-blocking design is overkill for the random matching, compared to networks other than the random graph, it is advantageous for the longest matching. Note that the fat-tree's *absolute* performance does not improve when moving to the more difficult longest matching TM; instead, its *relative* throughput is higher because longest matching degrades performance more in the random graph than in the fat-tree.

Flattened butterfly [52] At the largest scale, the 2-ary flattened butterfly which can support 1024 servers achieves only 59% of the random graph's throughput under all-to-all traffic, but the performance improves to 71% under random matching. However, the worst-case performance under longest matching drops to 47% which is the worst performance across all topologies tested.

Hypercubes [47] achieve 72% of the random graph's throughput under all-to-all traffic, 84% under random matching, and 51% under longest matching.

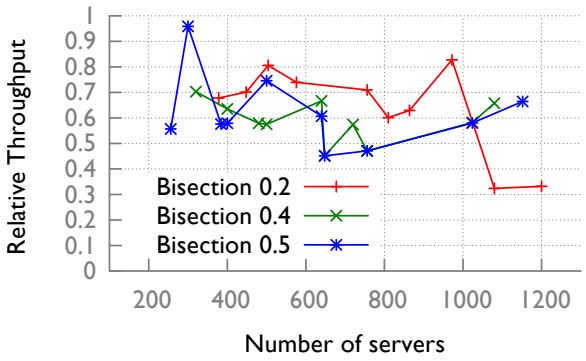

Figure 3.7 ***HyperX relative throughput under longest matching with different bisection bandwidths.***

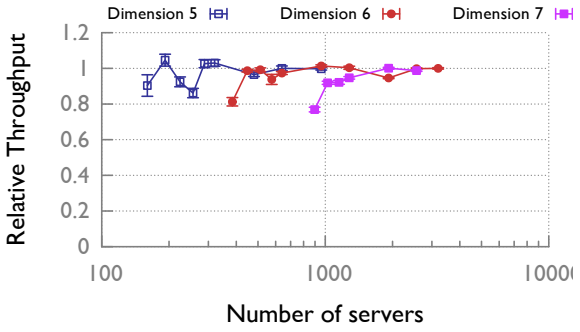

Figure 3.8 ***Long Hop relative throughput under longest matching TM.***

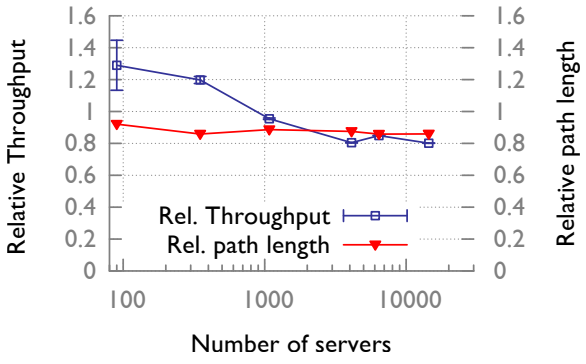

Figure 3.9 ***Slim Fly relative throughput under longest matching TM.***

HyperX [6] Unlike other topologies, the performance of HyperX is irregular. The variations arise from the choice of underlying topology: Given switch radix, number of servers and desired bisection bandwidth, HyperX attempts to find the least cost topology constructed from the building blocks – hypercube and flattened butterfly. Even a slight variation in one of the parameters can lead to a significant difference in HyperX construction and throughput.

We plot HyperX results for networks with bisection bandwidth of 0.4. In the worst case, the HyperX network that can support 648 hosts achieves a relative throughput of 55% under all-to-all traffic. For the same network, relative performance improves to 67% under random matching but further degrades to 45% under longest matching. We investigate the performance of HyperX networks with different bisection bandwidths under longest matching TM in Figure 3.7 and observe that the performance varies widely with network size under all values of bisection. More importantly, this further illustrates that *high bisection does not guarantee high performance*.

Jellyfish is our benchmark, and its (average) relative performance is 100% under all workloads by definition. Performance depends on randomness in the construction, but at larger sizes, performance differences between Jellyfish instances are minimal ($\approx 1\%$).

Long Hop networks [82] In Figure 3.8, we show that the relative throughput of Long Hop networks approaches 1 at large sizes under the longest matching TM. Similar trends are observed under both all-to-all and random matching workloads. The paper [82] claimed high performance (in terms of bisection bandwidth) with substantially less equipment than past designs, but we find that while Long Hop networks do have high performance, they are no better than random graphs, and sometimes worse.

Slim Fly [14] It was noted in [14] that Slim Fly's key advantage is path length. We observe in Figure 3.9 that the topology indeed has extremely short paths – about 85-90% relative to the random graph – but this does not translate to higher throughput. Slim Fly's performance is essentially identical to random graphs under all-to-all and random matching TMs with a relative performance of 101% using both. Relative throughput under the longest matching TM decreases with scale, dropping to 80% at the largest size tested. Hence, throughput performance cannot be predicted solely based on the average path length.

3.3 Comparison with related work

The literature on network topology design is large and growing, with a number of designs having been proposed in the past few years [7, 41, 42, 73, 43, 83, 36, 80, 29, 30]. However, each of these research proposals only makes a comparison with one or two other past proposals, with no standard benchmarks for the comparison. There has been no independent, rigorous evaluation of a large number of topologies.

Popa et. al. [76] assess 4 topologies to determine the one that incurs least expense while achieving a target level of performance under a specific workload (all-to-all traffic). Their attempts to equalize performance required careful calibration, and approximations still had to be made. Accounting for the different costs of building different topologies is an inexact process. We sidestep that issue by using the random graph as a normalizer: instead of attempting to match performance, for each topology, we build a random graph with *identical equipment*, and then compare throughput performance of the topology with that of the random graph. Thus the problem of massaging structured designs into roughly equivalent configurations is alleviated. This also makes it easy for others to use our tools, and to test arbitrary workloads. Apart from comparing topologies, our work also argues the superiority of flow-metrics to cuts.

Other work on comparing topologies is more focused on reliability and cuts in the topology [55]. Several researchers have also used sparsest cut and bisection bandwidth as proxies for throughput performance. Further, the usage of these two terms is not consistent across the literature. For instance, REWIRE [30] explicitly optimizes its topology designs for high sparsest cut, although it refers to the standard sparsest cut metric as bisection bandwidth. Tomic [82] builds topologies with the objective of maximizing bisection bandwidth (in a particular class of graphs). Webb et. al [85] use bisection bandwidth to pick virtual topologies over the physical topology. An interesting point of note is that they consider all-to-all traffic "a worst-case communication scenario", while our results (Figure 3.4) show that other traffic patterns can be significantly worse. PAST [81] tests 3 data center network proposals with the same sparsest cut (while referring to it as bisection bandwidth). Although it is not stated, the authors presumably used approximate methods because even approximating sparsest cut is believed to be NP-Hard [21]. While that does not imply that it could not be efficiently computed for these particular graphs, to the best of our knowledge, no sparsest-cut computation procedures are known for any of the networks tested in PAST. Further, PAST finds that the throughput performance of topologies with the same sparsest cut is different in packet-level simulations, raising questions about the usefulness of such a comparison; one must either build topologies of the

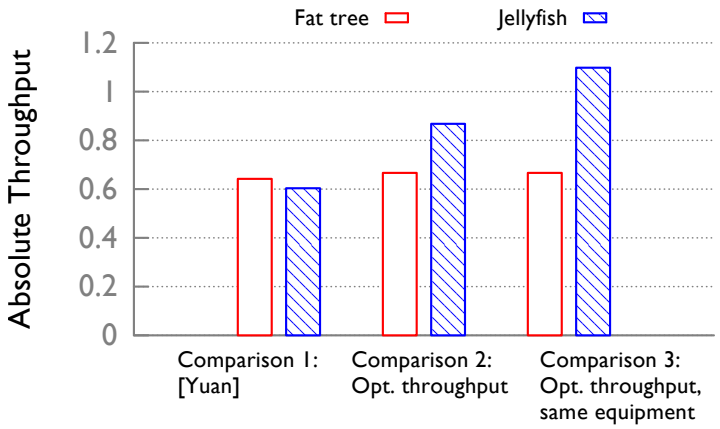

Figure 3.10 ***Throughput comparison of Fat-tree and Jellyfish based on [89], showing the effect of two methodological changes.***

same cost and compare them on throughput (as we do), or build topologies with the same performance and compare cost (as Popa et. al [76] do). These observations underscore the community's lack of clarity on the relationship between bisection bandwidth, sparsest cut, and throughput. A significant component of our work tackles this subject.

We note that throughput comparisons are a subtle exercise. Naive approaches can yield conclusions that are off by a sizable margin, for instance leading [89] to conclude that fat trees perform better than or similar to Jellyfish. We replicated the method of [89] using their LLSKR routing scheme, also finding similar throughput using the A2A TM (Fig. 3.10, Comparison 1). Roughly speaking, their method splits flows into sub-flows and routes them along certain paths according to LLSKR. It then estimates each subflow's throughput by counting and inverting the maximum number of intersecting subflows at a link along the path. When we move to the LP-based exact computation while still adhering to the same LLSKR path restrictions, we measure slightly higher throughput in fat trees and substantially higher in Jellyfish, now 30% greater than fat trees (Fig. 3.10, Comparison 2). This is even though we now maximize the *minimum* flow, while [89] measured the average! A second issue with the comparison in [89] is that more servers are added to Jellyfish than to fat tree — with 80 switches in each topology, their procedure would compare a fat tree with 128 servers to a Jellyfish topology with 160 servers. Equalizing all equipment, as in our standard comparison method, with 80 switches and 128 servers in both topologies, increases the performance gap to 65% (Comparison 3).

3.4 Conclusion

Although high throughput is a core goal of network design, measuring throughput is a subtle problem. We have shown that one common way of measuring throughput, via bisection and sparsest cut, produces inaccurate predictions of performance. We have put forward an improved benchmark for network capacity, including a near-worst-case traffic matrix, and have used this metric to compare a large number of network topologies, revealing new perspective on performance of several proposals. Particularly when designing networks for environments where traffic patterns may be unknown or variable and performance requirements are stringent, we believe evaluation under the near-worst-case longest matching TM will be useful.

Our findings also raise interesting directions for future work. First, our longest-matching traffic heuristically produces near-worst case performance, but does not always match the lower bound. Is there an efficient method to produce even-worse-case traffic for any given topology, or provably approximate it within less than $2\times$ Second, we observed that low average path length does not guarantee high throughput. How is throughput correlated with other fundamental graph properties? High correlations could suggest improvement in network design, while small correlation would further position throughput as an independent topological property of interest.

Our topology benchmarking tools and the topology datasets are all freely available [5].

CHAPTER 4

Homogeneous topology design

Having established our method of evaluating network throughput, we return to the problem of designing data center networks for high throughput. In this chapter, we look at the following formulation of the network design problem:

> Given N switches each with k ports, and S servers each with one port, with all ports having unit capacity, how should these ports be wired together in order to maximize network throughput?

In this setting, all the switches are homogeneous, *i.e.,* have the same line-speeds and number of ports. Nevertheless, this problem, like many other network topology design problems is hard because of the combinatorial explosion of the solution search space with the network size. Data center network designers have thus focused either on adapting known graph structures such as Clos networks [59] and hypercubes [47], or suggesting new ones based on intuitions about structure and symmetry (for instance, DCell [43] and BCube [42]). However, while numerous data center network architectures have recently been proposed [83, 36, 87, 42, 43, 41, 73, 59, 79, 52, 6] to achieve high throughput, none of these designs address two crucial problems:

- Incremental network expansion: how do we design high throughput networks that allow incremental addition of servers and switches?
- The optimality gap: how far are we from optimal topology design?

In the following, we discuss these two problems and our approach to addressing them.

This chapter includes previously published results from *Jellyfish: Networking Data Centers Randomly*. Ankit Singla, Chi-Yao Hong, Lucian Popa, P. Brighten Godfrey. USENIX NSDI, 2012. Section §4.3 also includes results from *High Throughput Data Center Topology Design*. Ankit Singla, P. Brighten Godfrey, and Alexandra Kolla. USENIX NSDI, 2014.

Incremental network expansion

Incremental network expansion may be necessitated by growth of the user base, which requires more servers, or by the deployment of more bandwidth-hungry applications. Expansion within a data center is possible through either planned overprovisioning of space and power, or by upgrading old servers to a larger number of more powerful but energy-efficient new servers. Planned expansion is a practical strategy to reduce up-front capital expenditure [60].

Industry experience indicates that incremental expansion is important. Consider the growth of Facebook's data center server population from roughly 30,000 in Nov. 2009 to >60,000 by June 2010 [69]. While Facebook has added entirely new data center facilities, much of this growth involves incrementally expanding existing facilities by "adding capacity on a daily basis" [68]. For instance, in 2012, Facebook announced that it would double the size of its facility at Prineville, Oregon [35]. A 2011 survey [31] of 300 enterprises that run data centers of a variety of sizes found that 84% of firms would probably or definitely expand their data centers in 2012. Several industry products advertise incremental expandability of the server pool, including SGI's IceCube (marketed as "The Expandable Modular Data Center" [4]; expands 4 racks at a time) and HP's EcoPod [49] (a "pay-as-you-grow" enabling technology [48]).

Do current high-bandwidth data center network proposals allow incremental growth? Consider the fat-tree interconnect, as proposed in [59], as an illustrative example. The entire structure is completely determined by the port-count of the switches available. This is limiting in at least two ways. First, it makes the design space very coarse: full bisection bandwidth fat-trees can only be built at sizes 3456, 8192, 27648, and 65536 corresponding to the commonly available port counts of 24, 32, 48, and 64[1]. Second, even if (for example) 50-port switches were available, the smallest "incremental" upgrade from the 48-port switch fat-tree would add 3,602 servers and would require replacing every switch.

There are, of course, some workarounds. One can replace a switch with one of larger port count or oversubscribe certain switches, but this makes capacity distribution constrained and uneven across the servers. One could leave free ports for future network connections [43, 29] but this wastes investment until actual expansion. Thus, without compromises on bandwidth or cost, such topologies are not amenable to incremental growth.

Since it seems that *structure* hinders incremental expansion, we propose the opposite: a random network

[1]Other topologies have similar problems: a hypercube [15] allows only power-of-2 sizes, a de Bruijn-like construction [76] allows only power-of-3 sizes, etc.

interconnect. The proposed interconnect, which we call **Jellyfish**, is a *degree-bounded*[2] *random graph* topology among top-of-rack (ToR) switches. The inherently sloppy nature of this design has the potential to be significantly more flexible than past designs. Additional components—racks of servers or switches to improve capacity—can be incorporated with a few random edge swaps. Jellyfish also allows construction of arbitrary-size networks, unlike topologies discussed above which limit the network to very coarse design points dictated by their structure.

Somewhat surprisingly, Jellyfish supports *more* servers than a fat-tree [59] built using the same network equipment while providing at least as high per-server bandwidth, measured either via bisection bandwidth or in throughput under a random-permutation traffic pattern. In addition, Jellyfish has lower mean path length, and is resilient to failures and miswirings.

The optimality gap

While all of the past literature makes claims of higher network capacity compared to a few preceding designs, there has been no notion of *optimality* in this work. The question of how far we may be from optimal topology design has been left completely unaddressed.

Towards answering this question, in this work, we prove a simple upper bound on the throughput achievable by any hypothetical network from the space of all possible solutions to the network design problem proposed above. Further, we show that our random graph based Jellyfish design achieves throughput within a few percent of optimal.

Key contributions

Our key contributions and conclusions are as follows:

- We propose Jellyfish, an incrementally-expandable, high-bandwidth data center interconnect based on random graphs.
- We show that Jellyfish provides quantitatively easier incremental expansion than prior work on incremental expansion in Clos networks [29], growing incrementally at only 40% of the expense of [29].

[2]Degree-bounded means that the number of connections per node is limited, in this case by switch port-counts.

- We show that Jellyfish can support 25% more servers than a fat-tree while using the same switch equipment and providing at least as high bandwidth. This advantage increases with network size and switch port-count.

- Further, we prove an upper bound on the throughput achievable by *any* topology with identical switches, and show that Jellyfish achieves throughput surprisingly close to this boundwithin a few percent at the scale of a few thousand servers for random permutation traffic.

- We also propose *degree-diameter optimal graphs* [28] as topologies which sit in the small optimality gap between Jellyfish and the upper bound. Although these not as flexible as Jellyfish, for settings such as modular containerized data centers, these may be a good topology choice.

We acknowledge that a data center network like Jellyfish, that lacks regular structure is a somewhat radical departure from traditional designs, and this presents several important challenges that must be addressed for Jellyfish to be viable. Among these are routing (schemes depending on a structured topology are not applicable), physical construction, and cabling layout. Our solutions to these problems are discussed in detail in Chapter 6, but we summarize the results here:

- Despite its lack of regular structure, packet-level simulations show that Jellyfish's bandwidth can be effectively utilized via existing forwarding technologies that provide high path diversity. The above listed '25% more servers' result accounts for the minor routing inefficiency in Jellyfish.

- We discuss effective techniques to realize physical layout and cabling of Jellyfish. Naively cabling Jellyfish may lead to higher cabling cost than other topologies, since its cables can be longer; but smart cabling schemes we propose make cabling Jellyfish cheaper than fat-trees while preserving most of its throughput advantage.

4.1 Jellyfish topology

Construction: The Jellyfish approach is to construct a random graph at the top-of-rack (ToR) switch layer. Each ToR switch i has some number k_i of ports, of which it uses r_i to connect to other ToR switches, and uses the remaining $k_i - r_i$ ports for servers. In the simplest case, which we consider by default throughout

this chapter, every switch has the same number of ports and servers: $\forall i$, $k = k_i$ and $r = r_i$. With N racks, the network supports $N(k - r)$ servers. In this case, the network is a *random regular graph*, which we denote as RRG(N, k, r). This is a well known construct in graph theory and has several desirable properties as we shall discuss later.

Formally, RRGs are sampled uniformly from the space of all r-regular graphs. This is a complex problem in graph theory [63]; however, a simple procedure produces "sufficiently uniform" random graphs which empirically have the desired performance properties. One can simply pick a random pair of switches with free ports (for the switch-pairs are not already neighbors), join them with a link, and repeat until no further links can be added. If a switch remains with ≥ 2 free ports (p_1, p_2) — which includes the case of incremental expansion by adding a new switch — these can be incorporated by removing a uniform-random existing link (x, y), and adding links (p_1, x) and (p_2, y). Thus only a single unmatched port might remain across the whole network.

Using the above idea, we generate a blueprint for the physical interconnection. (Allowing human operators to "wire at will" may result in poor topologies due to human biases – for instance, favoring shorter cables over longer ones.) We discuss cabling later in §6.5.

Intuition: Our two key goals are high bandwidth and flexibility. The intuition for the latter property is simple: lacking structure, the RRG's network capacity becomes "fluid", easily wiring up any number of switches, heterogeneous degree distributions, and newly added switches with a few random link swaps.

But why should random graphs have high bandwidth? We show quantitative results later, but here we present the intuition. The end-to-end throughput of a topology depends not only on the capacity of the network, but is also inversely proportional to the *amount of network capacity consumed to deliver each byte* — that is, the average path length. Therefore, assuming that the routing protocol is able to utilize the network's full capacity, and that there are no small cuts in the network (which is known from the good expansion properties of random graphs [19]), low average path length allows us to support more flows at high throughput. To see why Jellyfish has low path length, Fig. 4.1(a) and 4.1(b) visualize a fat-tree and a representative Jellyfish topology, respectively, with *identical* equipment. Both topologies have diameter 6, meaning that any server can reach all other servers in 6 hops. However, in the fat-tree, each server can only reach 3 others in ≤ 5 hops. In contrast, in the random graph, the typical origin server labeled o can reach 12 servers in ≤ 5 hops, and 6 servers in ≤ 4 hops. The reason for this is that many edges in the fat-tree are

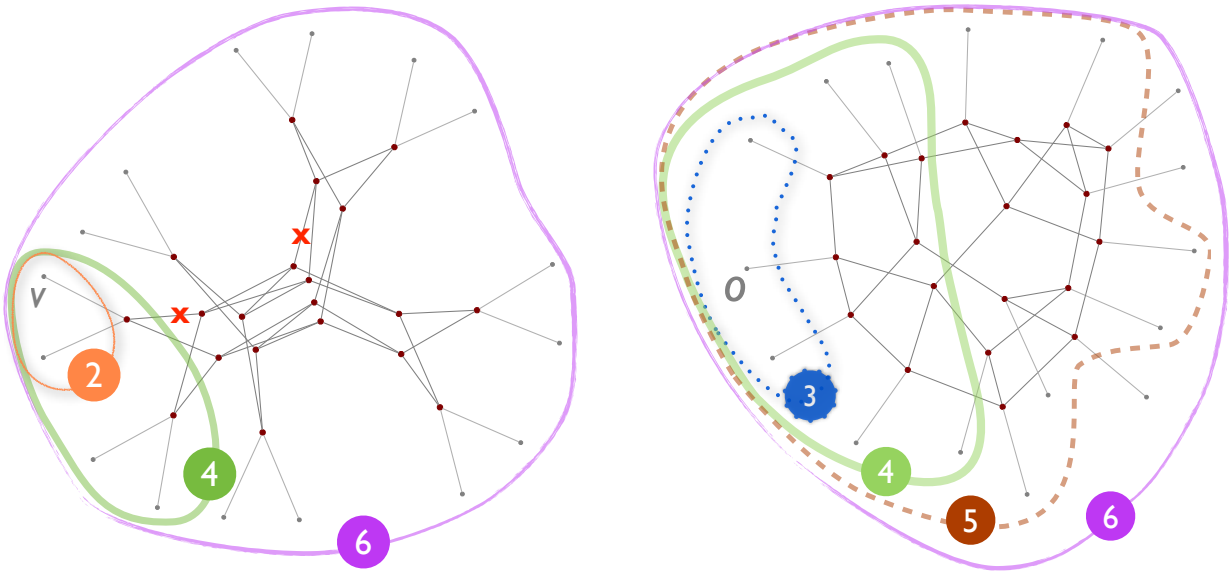

(a) (b)

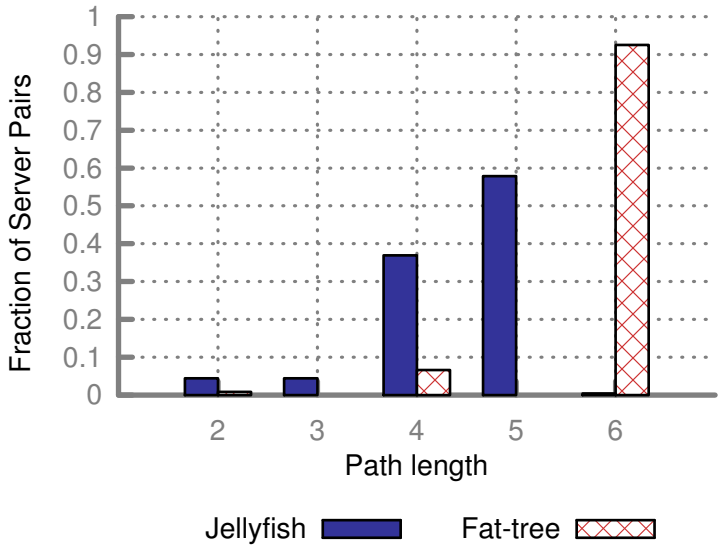

(c)

Figure 4.1 ***Random graphs have high throughput because they have low average path length, and therefore do less work to deliver each packet. (a): Fat-tree with*** 16 ***servers and*** 20 ***four-port switches. (b): Jellyfish with identical equipment. The servers are leaf nodes; switches are interior nodes. Each 'concentric' ring contains servers reachable from any server*** v ***in the fat-tree, and an arbitrary server*** o ***in Jellyfish, within the number of hops in the marked label. Jellyfish can reach many more servers in few hops because in the fat tree, many edges (like those marked "X") are redundant from a path-length perspective. (c): Path length distribution between servers for a*** 686***-server Jellyfish (drawn from*** 10 ***trials) and same-equipment fat-tree.***

not useful from the perspective of their effect on path length; for example, deleting the two edges marked X in Fig. 4.1(a) does not increase the path length between any pair of servers. In contrast, the RRG's diverse random connections lead to lower mean path length. Figure 4.1(c) demonstrates these effects at larger scale. With 686 servers, $>99.5\%$ of source-destination pairs in Jellyfish can be reached in fewer than 6 hops, while the corresponding number is only 7.5% in the fat-tree.

4.2 Jellyfish topology properties

This section evaluates the efficiency, flexibility and resilience of Jellyfish. Our goal is to measure the raw capabilities of the topology, were they to be coupled with optimal routing and congestion control. We study how to perform routing and congestion control separately, in Chapter 6. Further, while a comparison of 10 topologies is included in Chapter 3, we include herein detailed comparisons with the fat-tree, as well as a related proposal based on a different random-graph model. Our key findings are:

- Jellyfish can support 27% more servers at full capacity than a (same-switching-equipment) fat-tree at a scale of <900 servers. The trend is for this advantage to *improve* with scale.
- Jellyfish's network capacity is $>91\%$ of the best-known degree-diameter graphs [28], which we propose as benchmark bandwidth-efficient graphs.
- Paths are shorter on average in Jellyfish than in a fat-tree, and the *maximum* shortest path length (diameter) is the same or lower for all scales we tested.
- Incremental expansion of Jellyfish produces topologies identical in throughput and path length Jellyfish topologies generated from scratch.
- Jellyfish provides a significant cost-efficiency advantage over prior work (LEGUP [29]) on incremental network expansion in Clos networks. In a network expansion scenario that was made available for us to test, Jellyfish builds a slightly higher-capacity expanded network at only 40% of LEGUP's expense.
- Jellyfish is highly failure resilient, even more so than the fat-tree. Failing a random 15% of all links results in a capacity decrease of $<16\%$.

Evaluation methodology: Some of the results for network capacity in this section are based on explicit calculations of the theoretical bounds for bisection bandwidth for regular random graphs.

All throughput results presented in this section are based on calculations of throughput for a specific class of traffic demand matrices with optimal routing. While the details and rationale of our throughput metric are discussed in Chapter 3, we give a brief summary of methodology here.

The traffic matrices we use are *random permutation traffic*: each server sends at its full output link rate to a single other server, and receives from a single other server, and this permutation is chosen uniform-randomly. Intuitively, random permutation traffic represents the case of no locality in traffic, as might arise if VMs are placed without regard to what is convenient for the network[3]. Nevertheless, evaluating other traffic patterns is an important question that we leave for future work.

Given a traffic matrix, we characterize a topology's raw capacity with "ideal" load balancing by treating flows as splittable and fluid. This corresponds to solving a standard multi-commodity network flow problem, using a linear program solver.

For all throughput comparisons, we use the *same switching equipment* (in terms of both number of switches, and ports on each switch) for each set of topologies compared. Throughput results are always normalized to $[0, 1]$, and averaged over all flows.

For comparisons with the full bisection bandwidth fat-tree, we attempt to find, using a binary search procedure, the maximum number of servers Jellyfish can support using the same switching equipment as the fat-tree while satisfying the full traffic demands. Specifically, each step of the binary search checks a certain number of servers m by sampling three random permutation traffic matrices, and checking whether Jellyfish supports full capacity for *all* flows in *all* three matrices. If so, we say that Jellyfish supports m servers at full capacity. After our binary search terminates, we verify that the returned number of servers is able to get full capacity over each of 10 more samples of random permutation traffic matrices.

4.2.1 Efficiency

Bisection bandwidth vs. fat-tree: Bisection bandwidth, a common measure of network capacity, is the *worst-case* bandwidth spanning any two equal-size partitions of a network. Here, we compute the fat-tree's bisection bandwidth directly from its parameters; for Jellyfish, we model the network as a RRG and apply

[3] Supporting such flexible network-oblivious VM placement without a performance penalty is highly desirable [46].

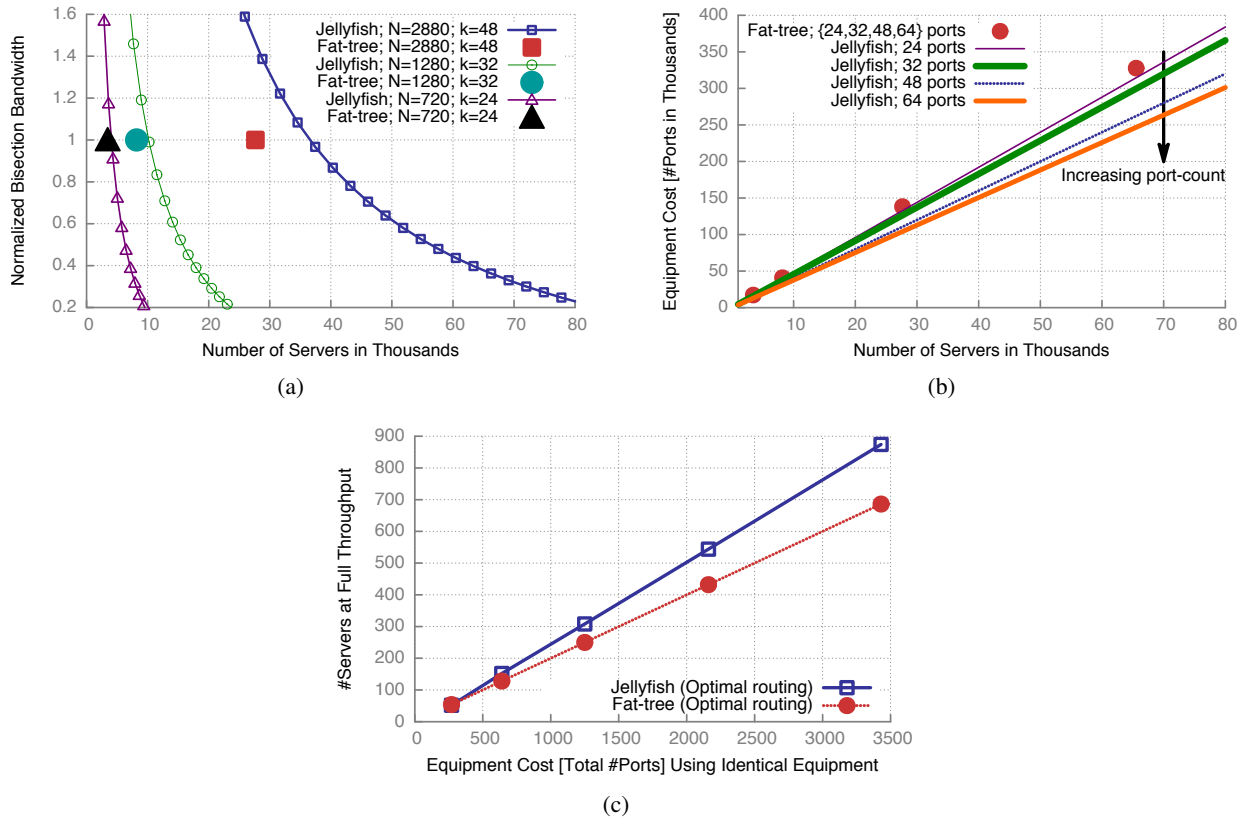

Figure 4.2 ***Jellyfish offers virtually continuous design space, and packs in more servers at high network capacity at the same expense as a fat-tree. From theoretical bounds: (a) Normalized bisection bandwidth versus the number of servers supported; equal-cost curves, and (b) Equipment cost versus the number of servers for commodity-switch port-counts*** (24, 32, 48) ***at full bisection bandwidth. Under optimal routing, with random-permutation traffic: (c) Servers supported at full capacity with the same switching equipment, for*** 6, 8, 10, 12 ***and*** 14***-port switches. Results for (c) are averaged over*** 8 ***runs.***

a lower bound of Bollobás [16]. We normalize bisection bandwidth by dividing it by the total line-rate bandwidth of the servers in one partition[4].

Fig. 4.2(a) shows that at the same cost, Jellyfish supports a larger number of servers (x axis) at full bisection bandwidth (y axis $= 1$). For instance, at the same cost as a fat-tree with 16,000 servers, Jellyfish can support >20,000 servers at full bisection bandwidth. Also, Jellyfish allows the freedom to accept lower bisection bandwidth in exchange for supporting more servers or cutting costs by using fewer switches.

Fig. 4.2(b) shows that the cost of building a full bisection-bandwidth network increases more slowly with the number of servers for Jellyfish than for the fat-tree, especially for high port-counts. Also, the design choices for Jellyfish are essentially continuous, while the fat-tree (following the design of [59]) allows only

[4]Values larger than 1 indicate overprovisioning.

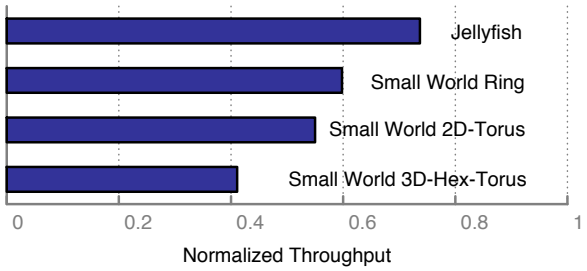

Figure 4.3 ***Jellyfish has higher capacity than the (same-equipment) small world data center topologies [79] built using a ring, a*** 2***D-Torus, and a*** 3***D-Hex-Torus as the underlying lattice. Results are averaged over*** 10 ***runs.***

certain discrete jumps in size which are further restricted by the port-counts of available switches. (Note that this observation would hold even for over-subscribed fat-trees.)

Jellyfish's advantage increases with port-count, approaching twice the fat-tree's bisection bandwidth. To see this, note that the fat-tree built using k-port switches has $k^3/4$ servers, and being a full-bisection interconnect, it has $k^3/8$ edges crossing each bisection. The fat-tree has $k^3/2$ switch-switch links, implying that its bisection bandwidth represents $\frac{1}{4}$ of its switch-switch links. For Jellyfish, in expectation, $\frac{1}{2}$ of its switch-switch links cross any given bisection of the switches, which is *twice* that of the fat-tree assuming they are built with the same number of switches and servers. Intuitively, Jellyfish's worst-case bisection should be slightly worse than this average bisection. The bound of [16] bears this out: in almost every r-regular graph with N nodes, every set of $N/2$ nodes is joined by at least $N(\frac{r}{4} - \frac{\sqrt{r \ln 2}}{2})$ edges to the rest of the graph. As the number of network ports $r \to \infty$ this quantity approaches $Nr/4$, i.e., $\frac{1}{2}$ of the $Nr/2$ links.

Throughput vs. fat-tree: Fig. 4.2(c) uses the random-permutation traffic model to find the number of servers Jellyfish can support at full capacity, matching the fat-tree in capacity and switching equipment. The improvement is as much as 27% more servers than the fat-tree at the largest size (874 servers) we are able to evaluate. As with results from Bollobás' theoretical lower bounds on bisection bandwidth (Fig. 4.2(a), 4.2(b)), the trend indicates that this improvement increases with scale.

Throughput vs. small world data centers (SWDC): SWDC [79] proposes a new topology for data centers inspired by a small-world distribution. We compare Jellyfish with SWDC using the same degree-6 topologies described in the SWDC paper. We emulate their 6-interface server-based design by using switches connected with 1 server and 6 network ports each. We build the three SWDC variants described in [79] at topology sizes as close to each other as possible (constrained by the lattice structure underlying these topolo-

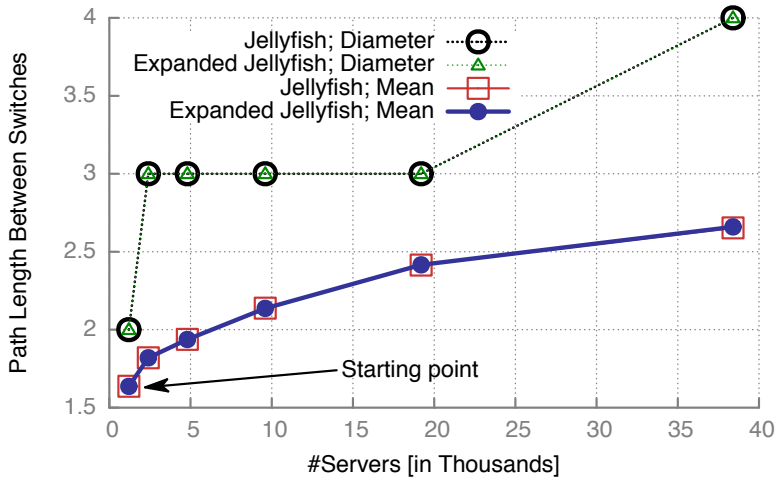

Figure 4.4 ***Jellyfish has short paths: Path length versus number of servers, with*** $k = 48$ ***port switches of which*** $r = 36$ ***connect to other switches and*** 12 ***connect to servers. Each data point is derived from*** 10 ***graphs. The diameter is*** ≤ 4 ***at these scales. This figure also shows that constructing Jellyfish from scratch, or using incremental growth yields topologies with very similar path length characteristics.***

gies) across sizes we can simulate. Thus, we use 484 switches for Jellyfish, the SWDC-Ring topology, and the SWDC-2D-Torus topology; for the SWDC-3D-Hex-Torus, we use 450 nodes. (Note that this gives the latter topology an advantage, because it uses the same degree, but a smaller number of nodes. However, this is the closest size where that topology is well-formed.) At these sizes, the first three topologies all yielded full throughput, so, to distinguish between their capacities, we oversubscribed each topology by connecting 2 servers at each switch instead of just one. The results are shown in Fig. 4.3. Jellyfish's throughput is $\sim 119\%$ of that of the closest competitor, the ring-based small world topology.

Path Length: Short path lengths are important to ensure low latency, and to minimize network utilization. In this context, we note that the theoretical *upper-bound* on the diameter of random regular graphs is fairly small: Bollobás and de la Vega [18] showed that in almost every r-regular graph with N nodes, the diameter is at most $1 + \lceil \log_{r-1}((2+\epsilon)rN\log N)\rceil$ for any $\epsilon > 0$. Thus, the server-to-server diameter is at most $3 + \lceil \log_{r-1}((2+\epsilon)rN\log N)\rceil$. Thus, the path length increases logarithmically (base r) with the number of nodes in the network. Given the availability of commodity servers with large port counts, this rate of increase is very small in practice.

We measured path lengths using an all-pairs shortest-paths algorithm. The average path length (Fig. 4.4) in Jellyfish is much smaller than in the fat-tree[5]. For example, for RRG(3200, 48, 36) with 38,400 servers,

[5]Note that the results in Fig. 4.4 use 48-port switches throughout, meaning that the only point of direct, fair comparison with a fat-tree is at the largest scale, where Jellyfish still compares favorably against a fat-tree built using 48-port switches and 27,648

the average path length between switches is <2.7 (Fig. 4.4), while the fat-tree's average is 3.71 at the smallest size, 3.96 at the size of $27{,}648$ servers. Even though Jellyfish's diameter is 4 at the largest scale, the 99.99^{th} percentile path-length across 10 runs did not exceed 3 for any size in Fig. 4.4.

4.2.2 Flexibility

Arbitrary-sized Networks: Several existing proposals admit only the construction of interconnects with very coarse parameters. For instance, a 3-level fat-tree allows only $k^3/4$ servers with k being restricted to the port-count of available switches, unless some ports are left unused. This is an arbitrary constraint, extraneous to operational requirements. In contrast, Jellyfish permits any number of racks to be networked efficiently.

Incremental Expandability: Jellyfish's construction makes it amenable to incremental expansion by adding either servers and/or network capacity (if not full-bisection bandwidth already), with increments as small as one rack or one switch. Jellyfish can be expanded such that rewiring is limited to the number of ports being added to the network; and the desirable properties are maintained: high bandwidth and short paths at low cost.

As an example, consider an expansion from an RRG(N, k, r) topology to RRG($N+1$, k, r). In other words, we are adding one rack of servers, with its ToR switch u, to the existing network. We pick a random link (v, w) such that this new ToR switch is not already connected with either v or w, remove it, and add the two links (u, v) and (u, w), thus using 2 ports on u. This process is repeated until all ports are filled (or a single odd port remains, which could be matched with another free port on an existing rack, used for a server, or left free). This completes incorporation of the rack, and can be repeated for as many new racks as desired.

A similar procedure can be used to expand network capacity for an under-provisioned Jellyfish network. In this case, instead of adding a rack with servers, we only add the switch, connecting all its ports to the network.

Jellyfish also allows for heterogeneous expansion: nothing in the procedure above requires that the new switches have the same number of ports as the existing switches. Thus, as new switches with higher port-counts become available, they can be readily used, either in racks or to augment the interconnect's

servers.

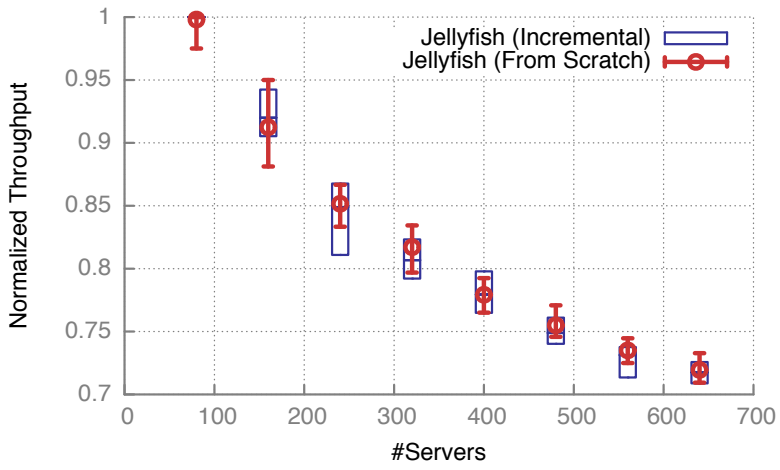

Figure 4.5 ***Incrementally constructed Jellyfish has the same capacity as Jellyfish built from scratch: We built a Jellyfish topology incrementally from*** 20 ***to*** 160 ***switches in increments of*** 20 ***switches, and compared the throughput per server of these incrementally grown topologies to Jellyfish topologies built from scratch using our construction routine. The plot shows the average, minimum and maximum throughput over*** 20 ***runs.***

bandwidth. There is, of course, the possibility of taking into account heterogeneity explicitly in the random graph construction and to improve upon what the vanilla random graph model yields. This (among other related problems) is addressed in Chapter 5.

We note that our expansion procedures (like our construction procedure) may not produce uniform-random RRGs. However, we demonstrate that the path length and capacity measurements of topologies we build incrementally match closely with ones constructed from scratch. Fig. 4.4 shows this comparison for the average path length and diameter where we start with an RRG with 1,200 servers and expand it incrementally. Fig. 4.5 compares the normalized throughput per server under a random permutation traffic model for topologies built incrementally against those built from scratch. The incremental topologies here are built by adding successive increments of 20 switches, and 80 servers to an initial topology also with 20 switches and 80 servers. (Throughout this experiment, each switch has 12 ports, 4 of which are attached to servers.) In each case, the results are close to identical.

Network capacity under expansion: Note that after normalizing by the number of servers $N(k-r)$, the lower bound on Jellyfish's normalized bisection bandwidth (§4.2.1) is independent of network size N. Of course, as N increases with fixed network degree r, average path length increases, and therefore, the demand for additional per-server capacity increases[6]. But since path length increases very slowly (as discussed

[6]This discussion also serves as a reminder that bisection-bandwidth, while a good metric of network capacity, is not the same as, say, capacity under worst-case traffic patterns.

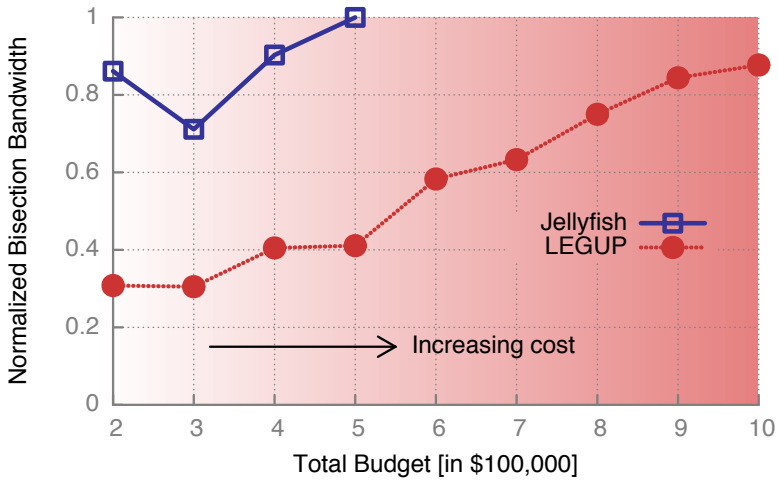

Figure 4.6 ***Jellyfish's incremental expansion is substantially more cost-effective than LEGUP's Clos network expansion. With the same budget for equipment and rewiring at each expansion stage (x-axis), Jellyfish obtains significantly higher bisection bandwidth (y-axis). Results are averaged over 10 runs. (The drop in Jellyfish's bisection bandwidth from stage 0 to 1 occurs because the number of servers increases in that step.)***

above), bandwidth per server remains high even for relatively large factors of growth. Thus, operators can keep the servers-per-switch ratio constant even under large expansion, with minor bandwidth loss. Adding only switches (without servers) is another avenue for expansion which can preserve or even increase network capacity. Our below comparison with LEGUP uses both forms of expansion.

Comparison with LEGUP [29]: While a LEGUP implementation is not publicly available, the authors were kind enough to supply a series of topologies produced by LEGUP. In this expansion arc, there is a budget constraint for the initial network, and for each successive expansion step; within the constraint, LEGUP attempts to maximize network bandwidth, and also may keep some ports free in order to ease expansion in future steps. The initial network is built with 480 servers and 34 switches; the first expansion adds 240 more servers and some switches; and each remaining expansion adds only switches. To build a comparable Jellyfish network, at each expansion step, under the same budget constraints, (using the same cost model for switches, *cabling, and rewiring*) we buy and randomly cable in as many new switches as we can. The number of servers supported is the same as LEGUP at each stage.

LEGUP optimizes for bisection bandwidth, so we compare both LEGUP and Jellyfish on that metric (using code provided by the LEGUP authors [29]) rather than on our previous random permutation throughput metric. The results are shown in Fig. 4.6. Jellyfish obtains substantially higher bisection bandwidth than LEGUP at each stage. In fact, by stage 2, Jellyfish has achieved higher bisection bandwidth than LEGUP in

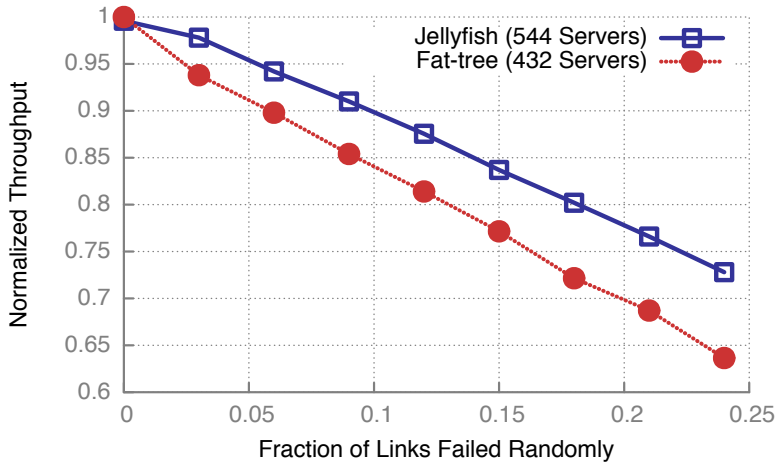

Figure 4.7 ***Jellyfish is highly resilient to failures: Normalized throughput per server decreases more gracefully for Jellyfish than for a same-equipment fat-tree as the percentage of failed links increases. Note that the y-axis starts at*** 60% ***throughput; both topologies are highly resilient to failures.***

stage 8, meaning (based on each stage's cost) that Jellyfish builds an equivalent network at cost 60% lower than LEGUP.

A minority of these savings is explained by the fact that Jellyfish is more bandwidth-efficient than Clos networks, as exhibited by our earlier comparison with fat-trees. But in addition, LEGUP appears to pay a significant cost to enable it to incrementally-expand a Clos topology; for example, it leaves some ports unused in order to ease expansion in later stages. We conjecture that to some extent, this greater incremental expansion cost is fundamental to Clos topologies.

4.2.3 Failure resilience

Jellyfish provides good path redundancy; in particular, an r-regular random graph is almost surely r-connected [17]. Also, the random topology maintains its (lack of) structure in the face of link or node failures – a random graph topology with a few failures is just another random graph topology of slightly smaller size, with a few unmatched ports on some switches.

Fig. 4.7 shows that the Jellyfish topology is even more resilient than the same-equipment fat-tree (which itself is no weakling). Note that the comparison features a fat-tree with fewer servers, but the same cost. This is to justify Jellyfish's claim of supporting a larger number of servers using the same equipment as the fat-tree, in terms of capacity, path length, and *resilience* simultaneously.

4.3 Near-optimality of Jellyfish

We refer the reader again to the network design problem which is the subject of this chapter:

> Given N switches each with k ports, and S servers each with one port, with all ports having unit capacity, how should these ports be wired together in order to maximize throughput?

Jellyfish, fat-trees, and other topologies are merely points in the combinatorically large design space of all graphs that address the above problem. While Jellyfish achieves higher throughput than the fat-tree, could some other topology achieve much higher throughput than Jellyfish itself?

We begin by noting that the symmetry of the problem suggests that each switch be connected to the same number of servers. Intuitively, spreading servers across switches in a manner that deviates from uniformity will create bottlenecks at the switches with larger numbers of servers. Thus, we assume that each switch uses out of its k ports, r ports to connect to other switches, and $k - r$ ports for servers. For simplicity, we also assume $S = N * (k - r)$. Now we can limit our focus to the switch-switch interconnect.

The design space for such networks is the set of all subgraphs H of the complete graph over N nodes K_N, such that H has degree r. For generic, application-oblivious design, we assume that the objective is to maximize throughput under a uniform traffic matrix such as all-to-all traffic or random permutation traffic among servers. To account for fairness, the network's throughput is defined as the maximum value of the minimum flow between source-destination pairs. We denote such a throughput measurement of an r-regular subgraph H of K_N under uniform traffic with f flows by $T_H(N, r, f)$. (For more details on the throughput metric, please refer back to Chapter 3.) The average path length of the network is denoted by $\langle D \rangle$.

For this scenario, we prove a simple upper bound on the throughput achievable by *any* hypothetical network.

Theorem 3. $T_H(N, r, f) \leq \frac{Nr}{\langle D \rangle f}$.

Proof. The network has a total of Nr edges (counting both directions) of unit capacity, for a total capacity of Nr. A flow i whose end points are a shortest path distance d_i apart, consumes at least $x_i d_i$ units of capacity in to obtain throughput x_i. Thus, the total capacity consumed by all flows is at least $\sum_i x_i d_i$. Given that we defined network throughput $T_H(N, r, f)$ as the minimum flow throughput, $\forall i, x_i \geq T_H(N, r, f)$. Total

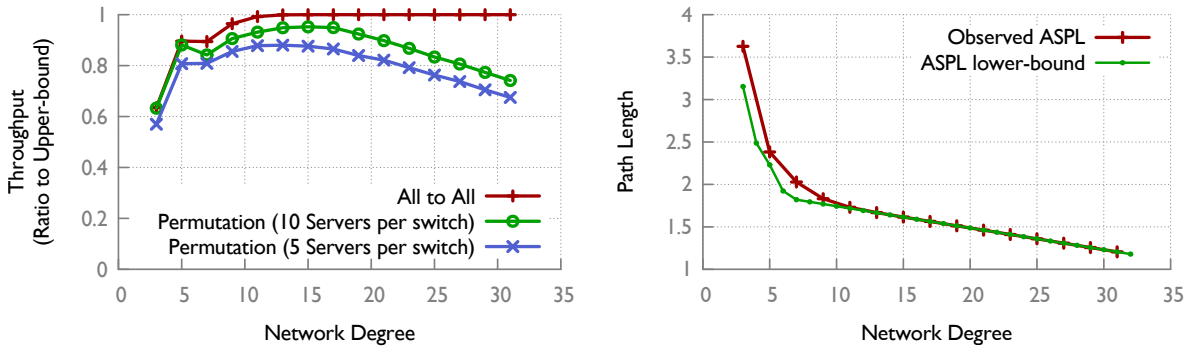

(a) (b)

Figure 4.8 ***Random graphs versus the bounds: (a) Throughput and (b) average shortest path length (ASPL) in random regular graphs compared to the respective upper and lower bounds for any graph of the same size and degree. The number of switches is fixed to*** 40 ***throughout. The network becomes denser rightward on the x-axis as the degree increases.***

capacity consumed is then at least $T_H(N, r, f) \sum_i d_i$. For uniform traffic patterns such as random permutations and all-to-all traffic, $\sum_i d_i = \langle D \rangle f$ because the average source-destination distance is the same as the graph's average shortest path distance. Also, total capacity consumed cannot exceed the network's capacity. Therefore, $\langle D \rangle f T_H(N, r, f) \leq Nr$, rearranging which yields the result. □

Further, [20] proves a lower bound on the average shortest path length of any r-regular network of size N:

$$\langle D \rangle \geq d^* = \frac{\sum_{j=1}^{k-1} jr(r-1)^{j-1} + kR}{N-1}$$
$$\text{where} \quad R = N - 1 - \sum_{j=1}^{k-1} r(r-1)^{j-1} \geq 0$$

and k is the largest integer such that the *inequality* holds.

This result, together with Theorem 3, yields an upper bound on throughput: $T_H(N, r, f) \leq \frac{Nr}{fd^*}$. Next, we show experimentally that random regular graphs achieve throughput close to this bound.

A *random regular graph*, denoted as RRG(N, k, r), is a graph sampled uniform-randomly from the space of all r-regular graphs of size N. This is a well-known construct in graph theory, on which Jellyfish is based.

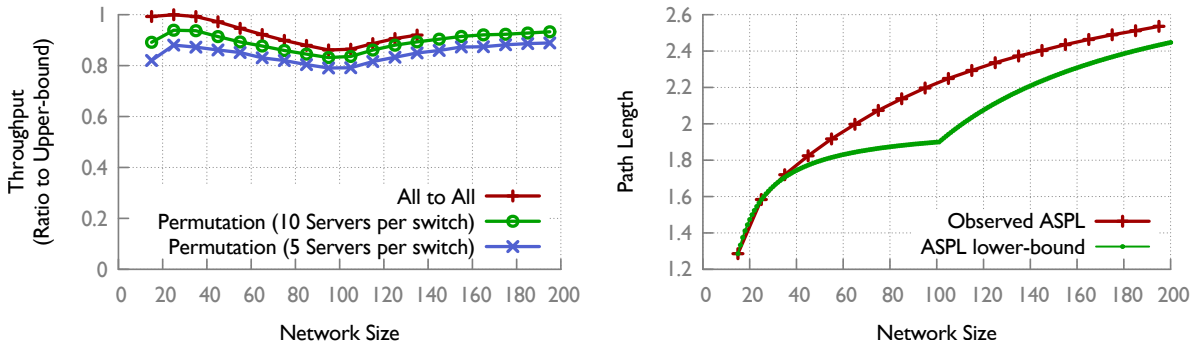

Figure 4.9 ***Random graphs versus the bounds: (a) Throughput and (b) average shortest path length (ASPL) in random regular graphs compared to the respective upper and lower bounds for any graph of the same size and degree. The degree is fixed to*** 10 ***throughout. The network becomes sparser rightward on the x-axis as the number of nodes increases.***

Fig. 4.8(a) and Fig. 4.9(a) compare throughput achieved by RRGs to the upper bound on throughput for any topology built with the same equipment. Fig. 4.8(a) shows this comparison for networks of increasing density (*i.e.,* the degree r increases, while the number of nodes N remains fixed at 40) for 3 uniform traffic matrices: a random permutation among servers with 5 servers at each switch, another with 10 servers at each switch, and an all-to-all traffic matrix. For the high-density traffic pattern, *i.e.,* all-to-all traffic, *exact optimal* throughput is achieved by the random graph for degree $r \geq 13$. Fig. 4.9(a) shows a similar comparison for increasing size N, with $r = 10$. Our simulator does not scale for all-to-all traffic because the number of commodities in the flow problem increases as the square of the network size for this pattern. Fig. 4.8(b) and 4.9(b) compare average shortest path length in RRGs to its lower bound. For both large network sizes, and very high network density, RRGs are surprisingly close to the bounds (right side of both figures).

The curve in Fig. 4.9(b) has two interesting features. First, there is a "curved step" behavior, with the first step at network size up to $N = 101$, and the second step beginning thereafter. To see why this occurs, observe that the bound uses a tree-view of distances from any node — for a network with degree d, d nodes are assumed to be at distance 1, $d(d-1)$ at distance 2, $d(d-1)^2$ at distance 3, etc. While this structure minimizes path lengths, it is optimistic — in general, not all edges from nodes at distance k can lead outward to unique new nodes[7]. As the number of nodes N increases, at some point the lowest level of this hypothetical tree becomes full, and a new level begins. These new nodes are more distant, so

[7]In fact, prior work shows that graphs with this structure do not exist for $d \geq 3$ and diameter $D \geq 3$ [67].

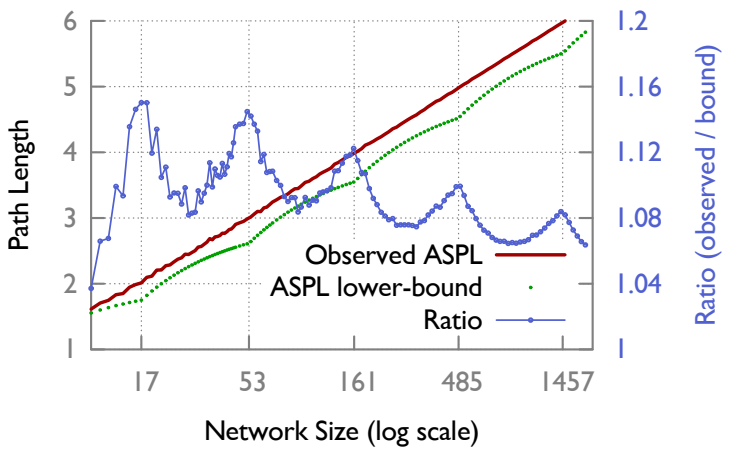

Figure 4.10 ***ASPL in random graphs compared to the lower bound. The degree is fixed to*** 4 ***throughout. The bound shows a "curved step" behavior. In addition, as the network size increases, the ratio of observed ASPL to the lower bound approaches*** 1***. The x-tics correspond to the points where the bound begins new distance levels.***

average path length suddenly increases more rapidly, corresponding to a new "step" in the bound. A second feature is that as $N \to \infty$, the ratio of observed ASPL to the lower bound approaches 1. This can be shown analytically by dividing an upper bound on the random regular graph's diameter [18] (which also upper-bounds its ASPL) by the lower bound of [20]. For greater clarity, we show in Fig. 4.10 similar behavior for degree $d = 4$, which makes it easier to show many "steps".

4.3.1 Topologies with higher throughput than Jellyfish?

As we show above, Jellyfish achieves throughput close to optimal. Even so, are there topologies that achieve throughput higher than Jellyfish, and closer still to the upper bound? Towards answering this question, we compare Jellyfish's capacity with that of the best known degree-diameter graphs. Below, we briefly explain what these graphs are, and why this comparison is interesting.

There is a fundamental trade-off between the degree and diameter of a graph of a fixed vertex-set (say of size N). At one extreme is a clique — maximum possible degree ($N - 1$), and minimum possible diameter (1). At the other extreme is a disconnected graph with degree 0 and diameter ∞. The problem of constructing a graph with maximum possible number N of nodes while preserving given diameter and degree bounds is known as the *degree-diameter problem* and has received significant attention in graph theory. The problem is quite difficult and the optimal graphs are only known for very small sizes: the largest degree-diameter graph known to be optimal has $N = 50$ nodes, with degree 7 and diameter 2 [28]. A

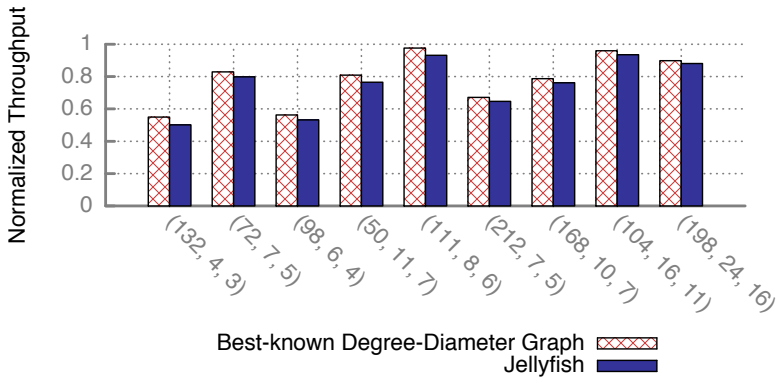

Figure 4.11 ***Jellyfish's network capacity is close to (i.e., $\sim 91\%$ or more in each case) that of the best-known degree-diameter graphs. The x-axis label (A, B, C) represents the number of switches (A), the switch port-count (B), and the network degree (C). Throughput is normalized against the non-blocking throughput. Results are averaged over*** 10 ***runs.***

collection of optimal and best known graphs for other degree-diameter combinations is maintained at [28].

The degree-diameter problem relates to our objective in that short average path lengths imply low resource usage and thus high network capacity. Intuitively, the best known degree-diameter topologies should support a large number of servers with high network bandwidth and low cost (small degree). While we note the distinction between average path length (which relates more closely to the network capacity) and diameter, degree-diameter graphs will have small average path lengths too.

Thus, we propose the best-known degree-diameter graphs as a benchmark for comparison. Note that such graphs do not meet our incremental expansion objectives; we merely use them as a capacity benchmark for Jellyfish topologies. But these graphs (and our measurements of them) may be of independent interest since they could be deployed as highly efficient topologies in a setting where incremental upgrades are unnecessary, such as a pre-fab container-based data center.

For our comparisons with the best-known degree-diameter graphs, the number of servers we attach to the switches was decided such that full-bisection bandwidth was not hit for the degree-diameter graphs (thus ensuring that we are measuring the full capacity of degree-diameter graphs.) Our results, in Fig. 4.11, show that the best-known degree-diameter graphs do achieve higher throughput than Jellyfish, and thus improve even more over fat-trees. But in the worst of these comparisons, Jellyfish still achieves $\sim 91\%$ of the degree-diameter graph's throughput.

4.4 Conclusion

We argue that Jellyfish is a highly flexible architecture for data center networks. It represents a novel approach to the significant problems of incremental expansion, while enabling high capacity, short paths, and resilience to failures and miswirings. Not only does Jellyfish achieve higher throughput than fat-trees and other topologies, it achieves throughput within a few percent of optimal.

CHAPTER 5

Heterogeneous topology design

As discussed in Chapter 4, while the network topology design problem is hard, for the homogeneous case, Jellyfish provides a flexible solution with nearly-optimal throughput. However, the case of *heterogeneous* networks, *i.e.,* networks composed of switches or servers with disparate capabilities, introduces even greater complexity. Heterogeneous network equipment is, in fact, the common case in the typical data center: servers connect to top-of-rack (ToR) switches, which connect to aggregation switches, which connect to core switches, with each type of switch possibly having a different number of ports as well some variations in line-speed. For instance, the ToRs may have both 1 Gbps and 10 Gbps connections while the rest of the network may have only 10 Gbps links. Further, as the network expands over the years and new, more powerful equipment is added to the data center, one can expect more heterogeneity — each year the number of ports supported by non-blocking commodity Ethernet switches increases. While line-speed changes are slower, the move to 10 Gbps and even 40 Gbps is happening now, and higher line-speeds are expected in the near future.

In spite of heterogeneity being commonplace in data center networks, very little is known about heterogeneous network design. For instance, there is no clarity on whether the traditional ToR-aggregation-core organization is superior to a "flatter" network without such a switch hierarchy; or on whether powerful core switches should be connected densely together, or spread more evenly throughout the network.

To attack this problem, we use random graphs as building blocks for heterogeneous network design by first optimizing the volume of connectivity between groups of nodes, and then forming connections randomly within these volume constraints. Using this approach we obtain the following results:

- We show empirically that in this framework, for a set of switches with different port counts but uni-

This chapter includes previously published results from *High Throughput Data Center Topology Design*. Ankit Singla, P. Brighten Godfrey, and Alexandra Kolla. USENIX NSDI, 2014.

form line-speed, attaching servers to switches in proportion to the switch port count is optimal.

- In our investigation of networks built with two switch types (with different port-counts, but the same line-speeds), somewhat surprisingly, we find that a wide range of connectivity arrangements provides nearly identical throughput. A useful consequence of this result is that there is significant opportunity for clustering switches to achieve shorter cable lengths on average, without compromising on throughput. This is a result we will employ in developing our cabling scheme in Chapter 6.

- In the case of multiple line-speeds, we show that complex bottleneck behavior may appear and there may be multiple configurations of equally high capacity.

- We apply the above insights to improving a real-world heterogeneous design. The topology proposed in VL2 [41] incorporates heterogeneous line-speeds and port-counts, and has been deployed in Microsoft's cloud data centers[1]. Using our approach, VL2's throughput can be improved by as much as 43% at the scale of a few thousand servers simply by rewiring existing equipment, with gains increasing with network size.

While our results in Chapter 4 show that random graphs achieve close to the best possible throughput in the homogeneous network design setting, we are unable, at present, to make a similar claim for heterogeneous networks, where node degrees and line-speeds may be different. However, in this chapter, we present for this setting, interesting experimental results which challenge traditional topology design assumptions.

5.1 Simulation methodology

While the details of our throughput evaluation method have been discussed in Chapter 3, we summarize the approach briefly here.

Our experiments measure the capacity of network topologies. For this chapter, our goal is to study topologies explicitly independent of systems-level issues such as routing and congestion control. Thus, we model network traffic using fluid splittable flows which are routed optimally. Throughput is then the solution to the standard maximum concurrent multi-commodity flow problem [58]. Note that by maximizing

[1]Based on personal exchange, and mentioned at `http://research.microsoft.com/en-us/um/people/sudipta/`.

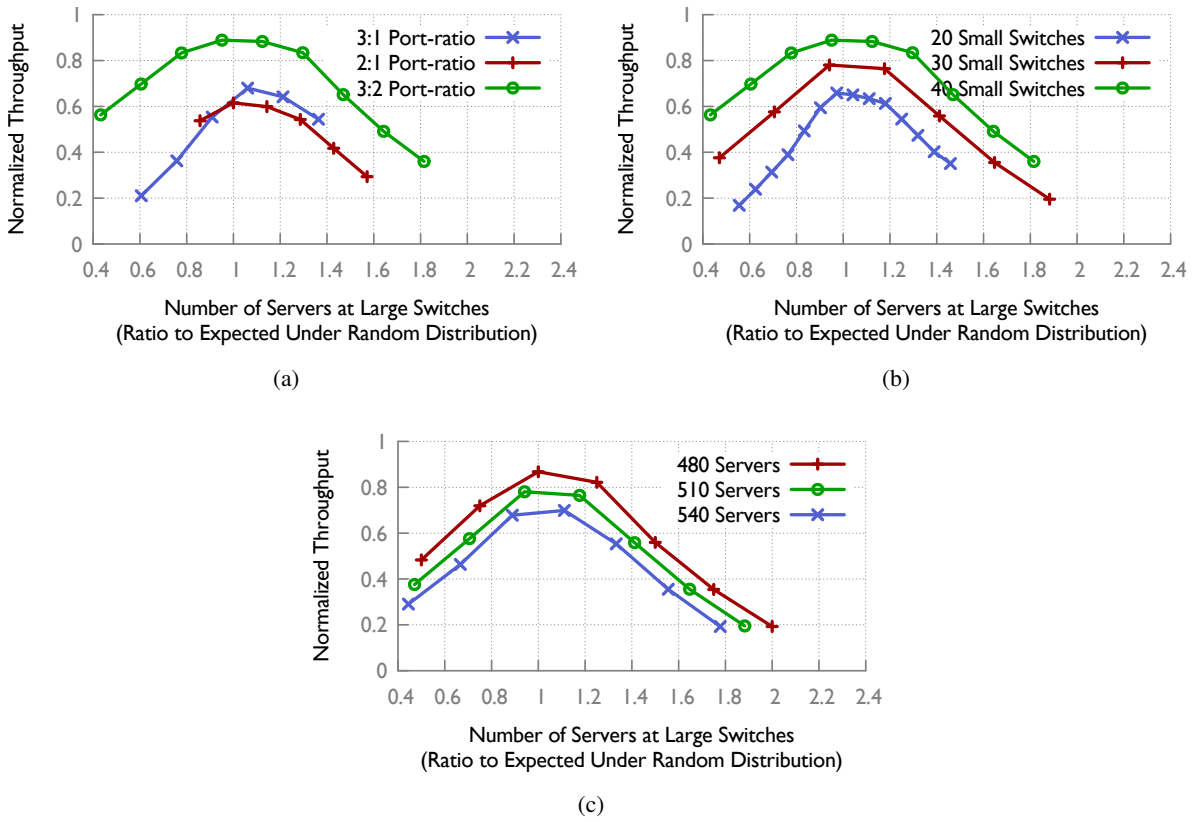

Figure 5.1 ***Distributing servers across switches: Peak throughput is achieved when servers are distributed proportionally to port counts*** *i.e.,* ***x-axis=1, regardless of (a) the absolute port counts of switches; (b) the absolute counts of switches of each type; and (c) oversubscription in the network.***

the minimum flow throughput, this model incorporates a strict definition of fairness. We use a linear program solver to obtain the maximum flow. Unless otherwise specified, the workload we use is a random permutation traffic matrix, where each server sends traffic to (and receives traffic from) exactly one other server.

Any comparisons between networks are made using identical switching equipment, unless noted otherwise. Across all experiments, we test a wide range of parameters, varying the network size, node degree, and oversubscription. A representative sample of results is included here. Most experiments average results across 20 runs, with standard deviations in throughput being $\sim 1\%$ of the mean except at small values of throughput in the uninteresting cases. Exceptions are noted in the text.

5.2 Heterogeneous port counts

We consider a simple scenario where the network is composed of two types of switches with different port counts (line-speeds being uniform throughout). Two natural questions arise that we shall explore here: (a) How should we distribute servers across the two switch types to maximize throughput? (b) Does biasing the topology in favor of more connectivity between larger switches increase throughput?

First, we shall assume that the interconnection is an unbiased random graph built over the remaining connectivity at the switches after we distribute the servers. Later, we shall fix the server distribution but bias the random graph's construction. Finally we will examine the combined effect of varying both parameters at once.

Distributing servers across switches: We vary the numbers of servers apportioned to large and small switches, while keeping the total number of servers and switches the same[2]. We then build a random graph over the ports that remain unused after attaching the servers. We repeat this exercise for several parameter settings, varying the numbers of switches, ports, and servers. A representative sample of results is shown in Fig. 5.1. The particular configuration in Fig. 5.1(a) uses 20 larger and 40 smaller switches, with the port counts for the three curves in the figure being 30 and 10 (3:1), 30 and 15 (2:1), and 30 and 20 (3:2) respectively. Fig. 5.1(b) uses 20 larger switches (30 ports) and 20, 30 and 40 smaller switches (20 ports) respectively for its three curves. Fig. 5.1(c) uses the same switching equipment throughout: 20 larger switches (30 ports) and 30 smaller switches (20 ports), with 480, 510, and 540 servers attached to the network. Along the x-axis in each figure, the number of servers apportioned to the larger switches increases. The x-axis label normalizes this number to the *expected* number of servers that would be apportioned to large switches if servers were spread randomly across all the ports in the network. As the results show, distributing servers in proportion to switch degrees (*i.e.,* x-axis$= 1$) is optimal.

This result, while simple, is remarkable in the light of current topology design practices, where top-of-rack switches are the only ones connected directly to servers.

Next, we conduct an experiment with a diverse set of switch types, rather than just two. We use a set of switches such that their port-counts k_i follow a power law distribution. We attach servers at each switch i in proportion to k_i^β, using the remaining ports for the network. The total number of servers is kept constant as we test various values of β. (Appropriate distribution of servers is applied by rounding where necessary to

[2]Clearly, across the same type of switches, a non-uniform server-distribution will cause bottlenecks and sub-optimal throughput.

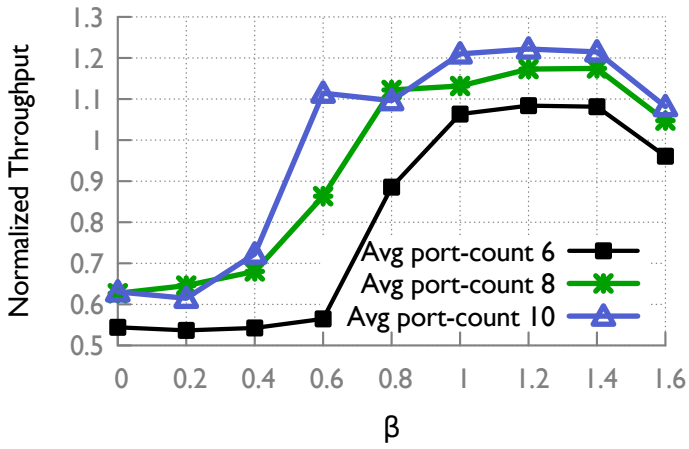

Figure 5.2 ***Distributing servers across switches: Switches have port-counts distributed in a power-law distribution. Servers are distributed in proportion to the β^{th} power of switch port-count. Distributing servers in proportion to degree ($\beta = 1$) is still among the optimal configurations.***

achieve this.) $\beta = 0$ implies that each switch gets the same number of servers regardless of port count, while $\beta = 1$ is the same as port-count-proportional distribution, which was optimal in the previous experiment. The results are shown in Fig. 5.2. $\beta = 1$ is optimal (within the variance in our data), but so are other values of β such as 1.2 and 1.4. The variation in throughput is large at both extremes of the plot, with the standard deviation being as much as 10% of the mean, while for $\beta \in \{1, 1.2, 1.4\}$ it is $< 4\%$.

Switch interconnection: We repeat experiments similar to the above, but instead of using a uniform random network construction, we vary the number of connections across the two clusters of (large and small) switches[3]. The distribution of servers is fixed throughout to be in proportion to the port counts of the switches.

As Fig. 5.3 shows, throughput is surprisingly stable across a wide range of volumes of cross-cluster connectivity. x-axis $= 1$ represents the topology with no bias in construction, *i.e.,* vanilla randomness; $x < 1$ means the topology is built with fewer cross-cluster connections than expected with vanilla randomness, etc. Regardless of the absolute values of the parameters, when the interconnect has too few connections across the two clusters, throughput drops significantly. This is perhaps unsurprising – as our experiments in §5.4.1 will confirm, the cut across the two clusters is the limiting factor for throughput in this regime. What *is* surprising, however, is that across a wide range of cross-cluster connectivity, throughput remains stable at its peak value. Our theoretical analysis in §5.4.2 will address this behavior.

[3]Note that specifying connectivity across the clusters automatically restricts the remaining connectivity to be within each cluster.

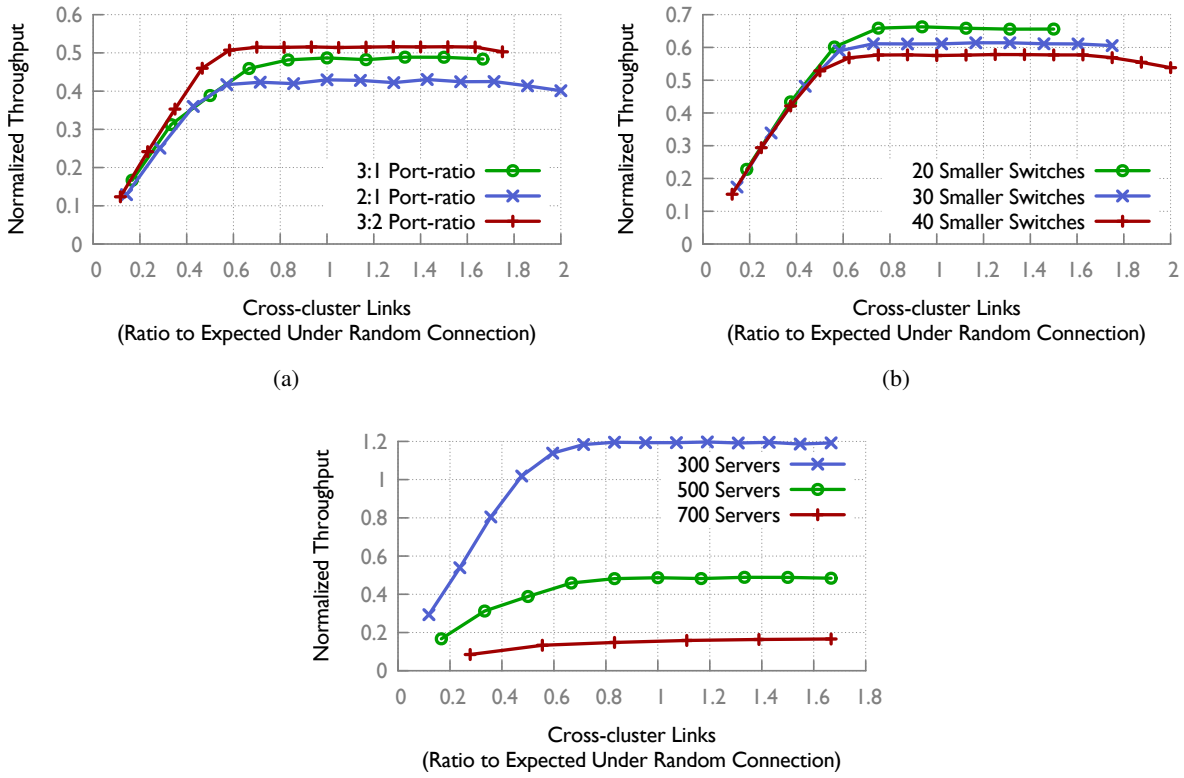

Figure 5.3 ***Interconnecting switches: Peak throughput is stable to a wide range of cross-cluster connectivity, regardless of (a) the absolute port counts of switches; (b) the absolute counts of switches of each type; and (c) oversubscription in the network.***

Combined effect: The above results leave open the possibility that joint optimization across the two parameters (server placement and switch connectivity pattern) can yield better results. Thus, we experimented with varying both parameters simultaneously as well. Two representative results from such experiments are included here. All the data points in Fig. 5.4(a) use the same switching equipment and the same number of servers. Fig. 5.4(b), likewise, uses a different set of equipment. Each curve in these figures represents a particular distribution of servers. For instance, '16H, 2L' has 16 servers attached to each larger switch and 2 to each of the smaller ones. On the x-axis, we again vary the cross-cluster connectivity (as in Fig. 5.3(a)). As the results show, while there are indeed multiple parameter values which achieve peak throughput, a combination of distributing servers proportionally (corresponding to '12H, 4L' and '14H, 7L' respectively in the two figures) and using a vanilla random interconnect is among the optimal solutions. Large deviations from these parameter settings lead to lower throughput.

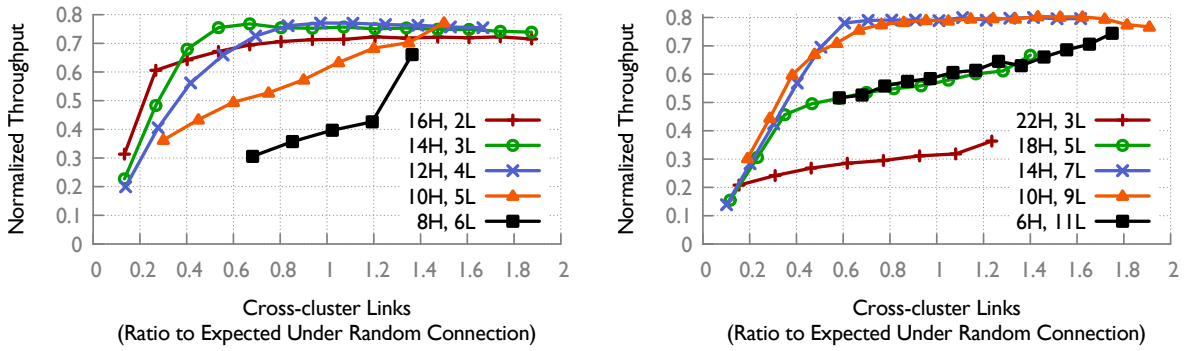

Figure 5.4 ***Combined effect of server distribution and cross-cluster connectivity: Multiple configurations are optimal, but proportional server distribution with a vanilla random interconnect is among them. (a)*** 20 ***large,*** 40 ***small switches, with*** 30 ***and*** 10 ***ports respectively. (b)*** 20 ***large,*** 40 ***small switches, with*** 30 ***and*** 20 ***ports respectively. Results from*** 10 ***runs.***

5.3 Heterogeneous line-speeds

Data center switches often have ports of different line-speeds, *e.g.*, tens of 1GbE ports, with a few 10GbE ports. How does this change the above analysis change?

To answer this question, we modify our scenario such that the small switches still have only low line-speed ports, while the larger switches have both low line-speed ports and high line-speed ports. The high line-speed ports are assumed to connect only to other high line-speed ports. We vary both the server distribution and the cross-cluster connectivity and evaluate these configurations for throughput. As the results in Fig. 5.5(a) indicate, the picture is not as clear as before, with multiple configurations having nearly the same throughput. Each curve corresponds to one particular distribution of servers across switches. For instance, '36H, 7L' has 36 servers attached to each large switch, and 7 servers attached to each small switch. The total number of servers across all curves is constant. While we are unable to make clear qualitative claims of the nature we made for scenarios with uniform line-speed, our simulation tool can be used to determine the optimal configuration for such scenarios.

We also investigate the impact of the number and the line-speed of the high line-speed ports on the large switches. For these tests, we fix the server distribution, and vary cross-cluster connectivity. We measure throughput for various 'high' line-speeds (Fig. 5.5(b)) and numbers of high line-speed links (Fig. 5.5(c)). While higher number or line-speed does increase throughput, its impact diminishes when cross-cluster connectivity is too small. This is expected: as the bottlenecks move to the cross-cluster edges, having high

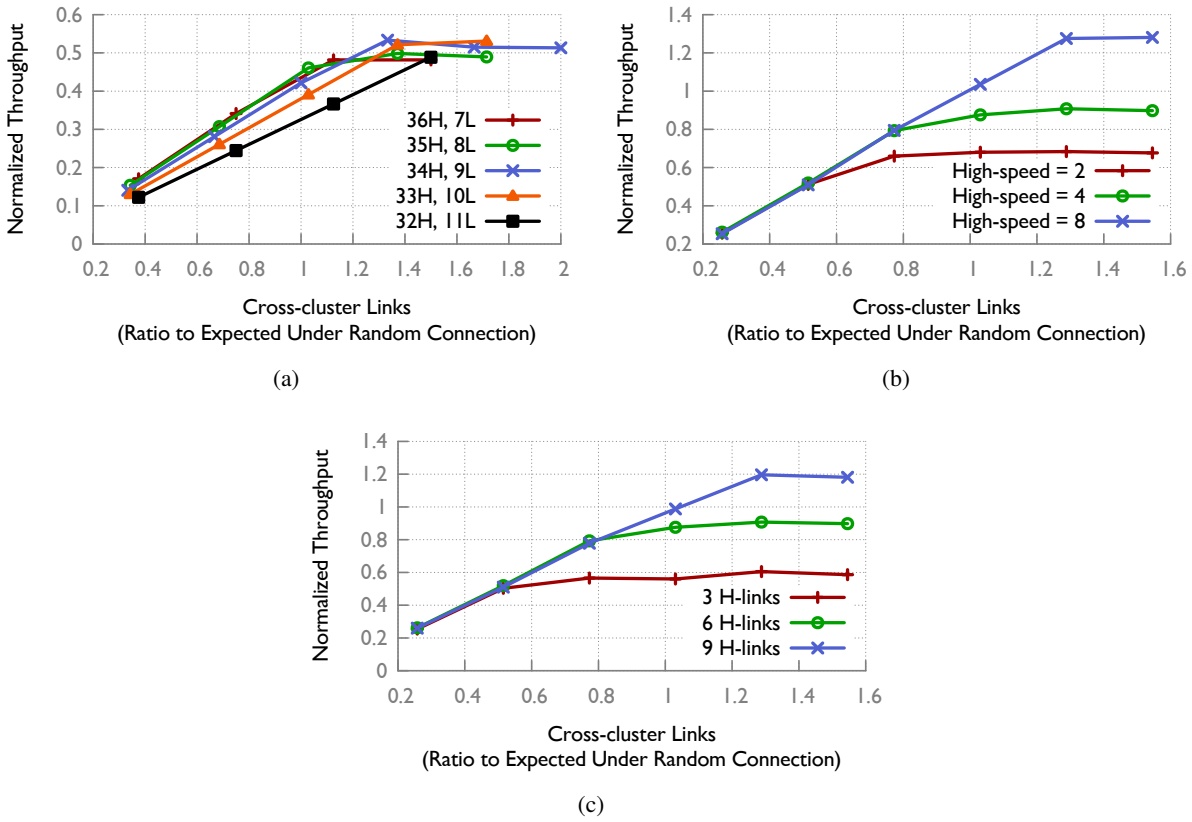

Figure 5.5 ***Throughput variations with the amount of cross-cluster connectivity: (a) various server distributions for a network with*** 20 ***large and*** 20 ***small switches, with*** 40 ***and*** 15 ***low line-speed ports respectively, with the large switches having*** 3 ***additional*** 10× ***capacity connections; (b) with different line-speeds for the high-speed links keeping their count fixed at*** 6 ***per large switch; and (c) with different numbers of the high-speed links at the big switches, keeping their line-speed fixed at*** 4 ***units.***

capacity between the large switches does not increase the *minimum* flow.

In the following, we attempt to add more than just the intuition for our results. We seek to explain throughput behavior by analyzing factors such as bottlenecks, total network utilization, shortest path lengths between nodes, and the path lengths actually used by the network flows.

5.4 Explaining throughput results

We investigate the cause of several of the throughput effects we observed in the previous section. First, in §5.4.1, we break down throughput into component factors — network utilization, shortest path length, and "stretch" in paths — and show that the majority of the throughput changes are a result of changes in utilization, though for the case of varying server placement, path lengths are a contributing factor. Note that

a decrease in utilization corresponds to a saturated bottleneck in the network.

Second, in §5.4.2, we explain in detail the surprisingly stable throughput observed over a wide range of amounts of connectivity between low- and high-degree switches. We give an upper bound on throughput, show that it is empirically quite accurate in the case of uniform line-speeds, and give a lower bound that matches within a constant factor for a restricted class of graphs. We show that throughput in this setting is well-described by two regimes: (1) one where throughput is limited by a sparse cut, and (2) a "plateau" where throughput depends on two topological properties: total volume of connectivity and average path length $\langle D \rangle$. The transition between the regimes occurs when the sparsest cut has a fraction $\Theta(1/\langle D \rangle)$ of the network's total connectivity.

Note that bisection bandwidth, a commonly-used measure of network capacity which is equivalent to the sparsest cut in this case, begins falling as soon as the cut between two equal-sized groups of switches has less than $\frac{1}{2}$ the network connectivity. This result demonstrates (among other things) that bisection bandwidth is not a good measure of performance, as we have also discussed in detail in Chapter 3.

5.4.1 Experiments

Throughput can be exactly decomposed as the product of four factors:

$$T = \frac{C \cdot U}{\langle D \rangle \cdot AS} = C \cdot U \cdot \frac{1}{\langle D \rangle} \cdot \frac{1}{AS}$$

where C is the total network capacity, U is the average link utilization, $\langle D \rangle$ is the average shortest path length, and AS is the average stretch, i.e., the ratio between average length of routed flow paths[4] and $\langle D \rangle$. Throughput may change due to any one of these factors. For example, even if utilization is 100%, throughput could improve if rewiring links reduces path length (this explained the random graph's improvement over the fat-tree in §4.3). On the other hand, even with very low $\langle D \rangle$, utilization and therefore throughput will fall if there is a bottleneck in the network.

We investigate how each of these factors influences throughput (excluding C which is fixed). Fig. 5.6 shows throughput (T), utilization (U), inverse shortest path length ($1/\langle D \rangle$), and inverse stretch ($1/AS$). An increase in any of these quantities increases throughput. To ease visualization, for each metric, we normalize its value with respect to its value when the throughput is highest so that quantities are unitless and easy to

[4]This average is weighted by amount of flow along each route.

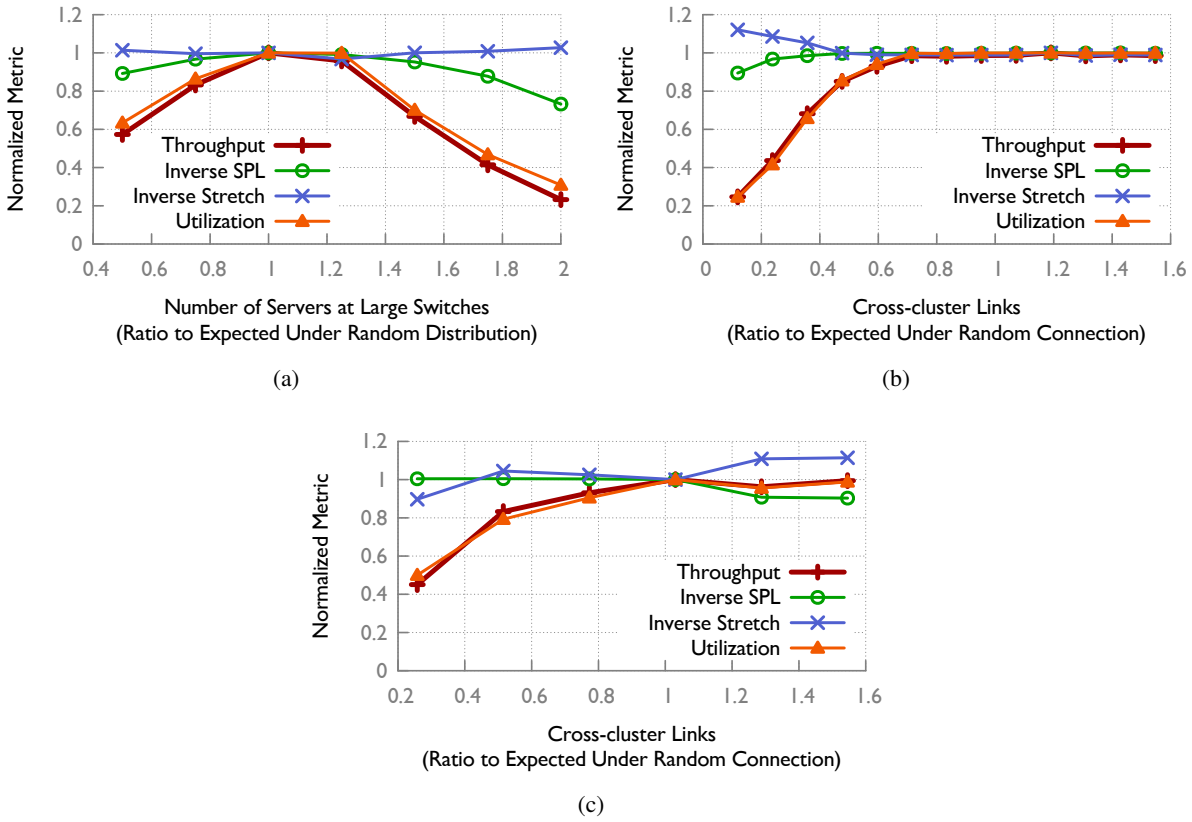

Figure 5.6 ***The dependence of throughput on all three relevant factors: inverse path length, inverse stretch, and utilization. Across experiments, total utilization best explains throughput, indicating that bottlenecks govern throughput.***

compare.

Across experiments, our results (Fig. 5.6) show that high utilization best explains high throughput. Fig. 5.6(a) analyzes the throughput results for '480 Servers' from Fig. 5.1(c), Fig. 5.6(b) corresponds to '500 Servers' in Fig. 5.3(c), and Fig. 5.6(c) to '3 H-links' in Fig. 5.5(c). Note that it is not obvious that this should be the case: Network utilization would also be high if the flows took long paths and used capacity wastefully. At the same time, one could reasonably expect 'Inverse Stretch' to also correlate with throughput well — if the paths used are close to shortest, then the flows are not wasting capacity. Path lengths do play a role — for example, the right end of Fig. 5.6(a) shows an increase in path lengths, explaining why throughput falls about 25% more than utilization falls — but the role is less prominent than utilization.

Given the above result on utilization, we examined where in the network the corresponding bottlenecks occur. From our linear program solver, we are able to obtain the link utilization for each network link. We averaged link utilization for each link type in a given network and flow scenario *i.e.,* computing average

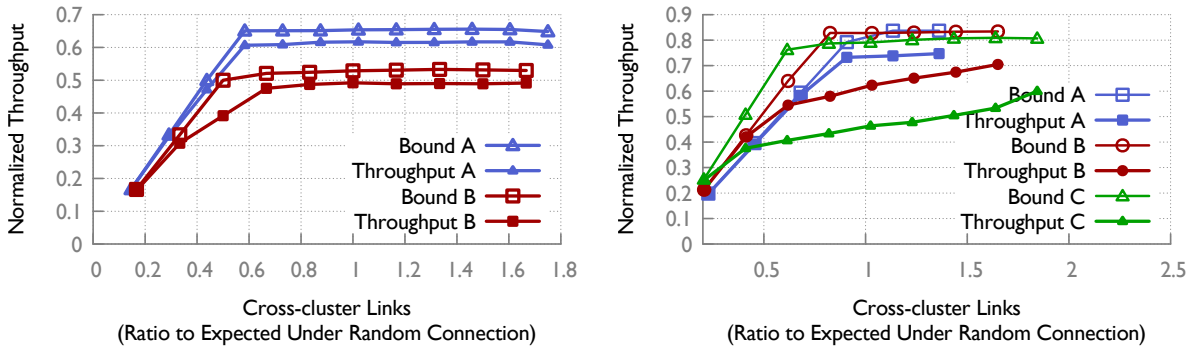

Figure 5.7 ***Our analytical throughput bound from Eqn. 5.1 is close to the observed throughput for the uniform line-speed scenario (a) for which the bound and the corresponding throughput are shown for two representative configurations A and B, but can be quite loose with non-uniform line-speeds (b).***

utilization across links between small and large switches, links between small switches only, etc. The movement of under-utilized links and bottlenecks shows clear correspondence to our throughput results. For instance, for Fig. 5.3(c), as we move leftward along the x-axis, the number of links across the clusters decreases, and we can expect bottlenecks to manifest at these links. This is exactly what the results show. For example, for the leftmost point ($x = 1.67$, $y = 1.67$) on the '500 Servers' curve in Fig. 5.3(c), links inside the large switch cluster are on average $< 20\%$ utilized while the links between across clusters are close to fully utilized ($> 90\%$ on average). On the other hand, for the points with higher throughput, like ($x = 1$, $y = 0.49$), all network links show uniformly high utilization ($\sim 100\%$). Similar observations hold across all our experiments.

5.4.2 Analysis

Fig. 5.3 shows a surprising result: network throughput is stable at its peak value for a wide range of cross-cluster connectivity. In this section, we provide upper and lower bounds on throughput to explain the result. Our upper bound is empirically quite close to the observed throughput in the case of networks with uniform line-speed. Our lower bound applies to a simplified network model and matches the upper bound within a constant factor. This analysis allows us to identify the point (*i.e.,* amount of cross-cluster connectivity) where throughput begins to drop, so that our topologies can avoid this regime, while allowing flexibility in the interconnect.

Upper-bounding throughput. We will assume the network is composed of two "clusters", which are simply

arbitrary sets of switches, with n_1 and n_2 attached servers respectively. Let C be the sum of the capacities of all links in the network (counting each direction separately), and let $\bar{C}$ be that of the links crossing the clusters. To simplify this exposition, we will assume the number of flows crossing between clusters is exactly the expected number for random permutation traffic: $n_1 \frac{n_2}{n_1+n_2} + n_2 \frac{n_1}{n_1+n_2} = \frac{2n_1n_2}{n_1+n_2}$. Without this assumption, the bounds hold for random permutation traffic with an asymptotically insignificant additive error.

Our upper bound has two components. First, recall our path-length-based bound from §4.3 shows the throughput of the minimal-throughput flow is $T \leq \frac{C}{\langle D \rangle f}$ where $\langle D \rangle$ is the average shortest path length and f is the number of flows. For random permutation traffic, $f = n_1 + n_2$.

Second, we employ a cut-based bound. The cross-cluster flow is $\geq T \frac{2n_1n_2}{n_1+n_2}$. This flow is bounded above by the capacity $\bar{C}$ of the cut that separates the clusters, so we must have $T \leq \bar{C} \frac{n_1+n_2}{2n_1n_2}$.

Combining the above two upper bounds, we have

$$T \leq min \left\{ \frac{C}{\langle D \rangle (n_1 + n_2)}, \frac{\bar{C}(n_1 + n_2)}{2n_1n_2} \right\} \tag{5.1}$$

Fig. 5.7 compares this bound to the actual observed throughput for two cases with uniform line-speed (Fig. 5.7(a)) and a few cases with mixed line-speeds (Fig. 5.7(b)). The bound is quite close for the uniform line-speed setting, both for the cases presented here and several other experiments we conducted, but can be looser for mixed line-speeds.

The above throughput bound begins to drop when the cut-bound begins to dominate. In the special case that the two clusters have equal size, this point occurs when

$$\bar{C} \leq \frac{C}{2\langle D \rangle}. \tag{5.2}$$

A drop in throughput when the cut capacity is inversely proportional to average shortest path length has an intuitive explanation. In a random graph, most flows have many shortest or nearly-shortest paths. Some flows might cross the cluster boundary once, others might cross back and forth many times. In a uniform-random graph with large $\bar{C}$, near-optimal flow routing is possible with any of these route choices. As $\bar{C}$ diminishes, this flexibility means we can place some restriction on the choice of routes without impacting the flow. However, the flows which cross clusters must still utilize at least one cross-cluster hop, which is on

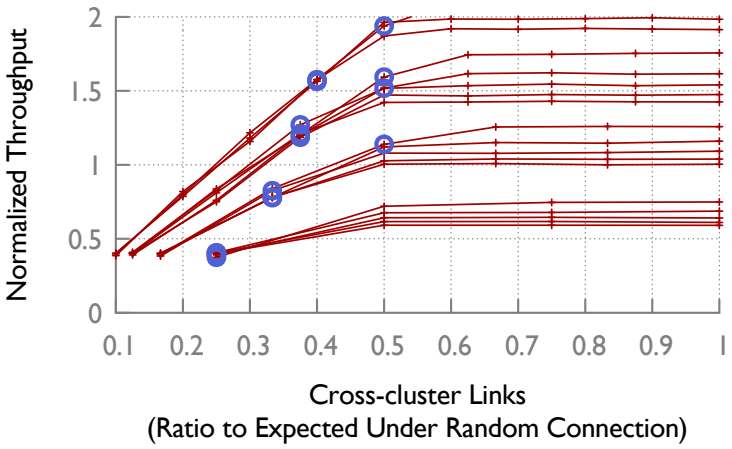

Figure 5.8 ***Throughput shows a characteristics profile with respect to varying levels of cross-cluster connectivity. The one point marked on each curve indicates our analyticallly determined threshold of cross-cluster connectivity below which throughput must be smaller than its peak value.***

average a fraction $1/\langle D\rangle$ of their hops. Therefore in expectation, since $\frac{1}{2}$ of all (random-permutation) flows cross clusters, at least a fraction $\frac{1}{2\langle D\rangle}$ of the total traffic volume will be cross-cluster. We should therefore expect throughout to diminish once less than this fraction of the total capacity is available across the cut, which recovers the bound of Equation 5.2.

However, while Equation 5.2 determines when the *upper bound* on throughput drops, it does not bound the point at which *observed* throughput drops: since the upper bound might be loose, throughput may drop earlier or later. However, given a peak throughput value, we can construct a bound based on it. Say the peak throughput in a configuration is T^*. $T^* \leq \bar{C}\frac{n_1+n_2}{2n_1n_2}$ implies throughput must drop below T^* when $\bar{C}$ is less than $C^* := T^*\frac{2n_1n_2}{n_1+n_2}$. If we are able to empirically estimate T^* (which is not unreasonable, given its stability), we can determine the value of $\bar{C}^*$ below which throughput *must* drop.

Fig. 5.8 has 18 different configurations with two clusters with increasing cross-cluster connectivity (equivalently, $\bar{C}$). The one point marked on each curve corresponds to the $\bar{C}^*$ threshold calculated above. As predicted, below $\bar{C}^*$, throughput is less than its peak value.

Lower-bounding throughput. For a restricted class of random graphs, we can lower-bound throughput as well, and thus show that our throughput bound (Eqn. 5.1), and the drop point of Eqn. 5.2, are tight within constant factors.

We restrict this analysis to networks $G = (V, E)$ with n nodes each with constant degree d. All links have unit capacity in each direction. The vertices V are grouped into two equal size clusters V_1, V_2, i.e.,

$|V_1| = |V_2| = \frac{1}{2}n$. Let p, n be such that each node has pn neighbors within its cluster and qn neighbors in the other cluster, so that $p + q = d/n = \Theta(1/n)$. Under this constraint, we choose the remaining graph from the uniform distribution on all d-regular graphs. Thus, for each of the graphs under consideration, the total inter-cluster connectivity is $\bar{C} = 2q \cdot |V_1| \cdot |V_2| = q \cdot \frac{n^2}{2}$. Decreasing q corresponds to decreasing the cross-cluster connectivity and increasing the connectivity within each cluster. Our result below holds with high probability (w.h.p.) over the random choice of the graph. Let $T(q)$ be the throughput with the given value of q, and let T^* be the throughput when $p = q$ (which will also be the maximum throughput).

Our main result is the following theorem, which explains the throughput results by proving that while $q \geq q^*$, for some value q^* that we determine, the throughput $T(q)$ is within a constant factor of T^*. Further, when $q < q^*$, $T(q)$ decreases roughly linearly with q. The proof can be found in Appendix C.

Theorem 4. *There exist constants c_1, c_2 such that if $q^* = c_1 \frac{1}{\langle D \rangle} p$, then for $q \geq q^*$ w.h.p. $T(q) \geq c_2 T^*$. For $q < q^*$, $T(q) = \Theta(q)$.*

One interesting implication of this result is that a significant fraction of the connections may be 'localized' to within each cluster, without incurring much reduction in the topology's throughput. This immediately implies a possible cabling optimization for such networks, which we explore in Chapter 6.

5.5 Improving VL2

In this section, we apply the lessons learned from our experiments and analysis to improve upon a real world topology. Our case study uses the VL2 [41] topology deployed in Microsoft's data centers. VL2 incorporates heterogeneous line-speeds and port-counts and thus provides a good opportunity for us to test our design ideas.

VL2 background: VL2 [41] uses three types of switches: top-of-racks (ToRs), aggregation switches, and core switches. Each ToR is connected to 20 1GbE servers, and has 2 10GbE uplinks to different aggregation switches. The rest of the topology is a full bipartite interconnection between the core and aggregation switches. If aggregation switches have DA ports each, and core switches have DI ports each, then such a topology supports $\frac{DA.DI}{4}$ ToRs at full throughput.

Rewiring VL2: As results in §5.2 indicate, connecting ToRs to only aggregation switches, instead of distributing their connectivity across all switches is sub-optimal. Further, the results on the near-optimality of

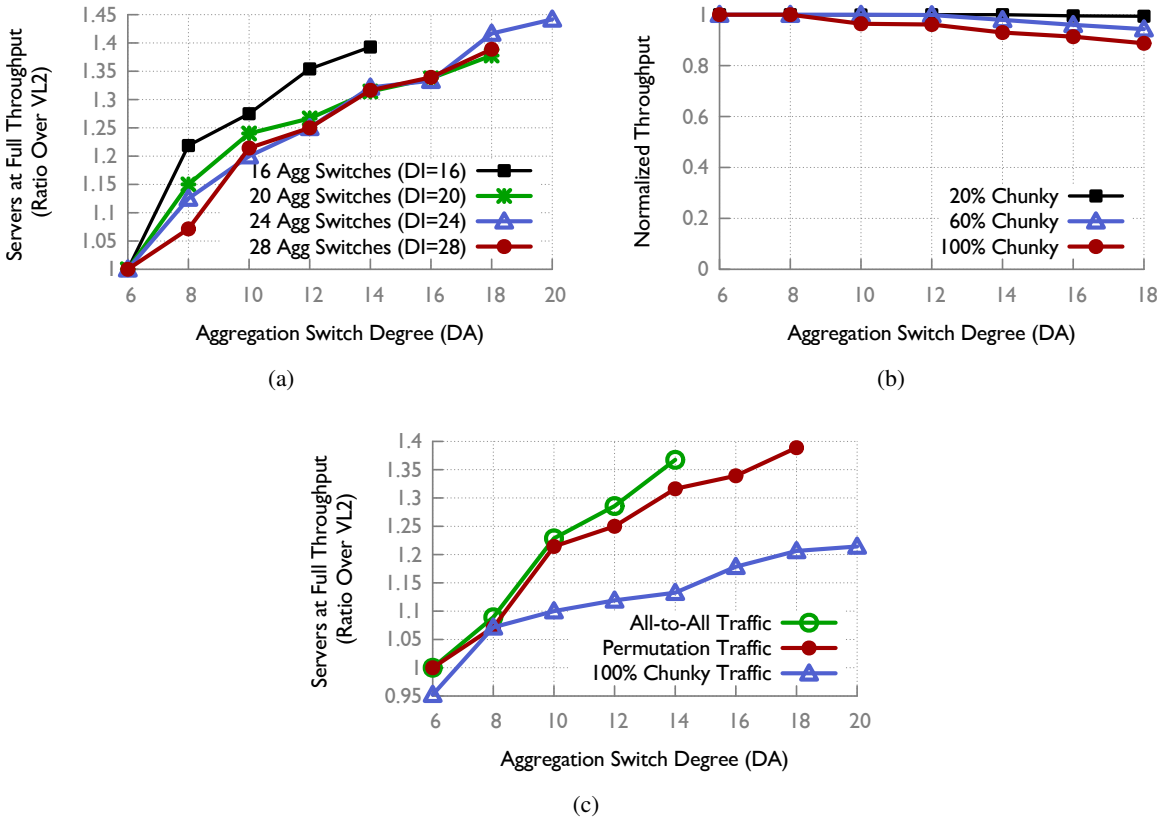

Figure 5.9 ***Improving VL2: (a) The number of servers our topology supports in comparison to VL2 by rewiring the same equipment; (b) Throughput under various chunky traffic patterns; and (c) The number of servers our topology can support in comparison to VL2 when we require it to achieve full throughput for all-to-all traffic, permutation traffic, and chunky traffic.***

random graphs in Chapter 4 imply further gains from using randomness in the interconnect as opposed to VL2's complete bipartite interconnect. In line with these observations, our experiments show significant gains obtained by modifying VL2.

In modifying VL2, we distribute the ToRs over aggregation and core switches in proportion to their degrees. We connect the remaining ports uniform randomly. To measure our improvement, we calculate the number of ToRs our topology can support at full throughput compared to VL2. By 'supporting at full throughput', we mean observing full 1 Gbps throughput for each flow in random permutation traffic across each of 20 runs. We obtain the largest number of ToRs supported at full throughput by doing a binary search. As Fig. 5.9(a) shows, we gain as much as a 43% improvement in the number of ToRs (equivalently, servers) supported at full throughput at the largest size. Note that the largest size we evaluated is fairly small – 2,400 servers for VL2 – and our improvement increases with the network's size.

5.6 Other traffic matrices

We evaluate the throughput of our VL2-like topology under other traffic matrices besides random permutations. For these experiments, we use the topologies corresponding to the '28 Agg Switches (DI=28)' curve in Fig. 5.9(a). (Thus, by design, the throughput for random permutations is expected, and verified, to be 1.) In addition to the random permutation, we test the following other traffic matrices: (a) All-to-all: where each server communicates with every other server; and (b) $x\%$ Chunky: where each of $x\%$ of the network's ToRs sends all of its traffic to *one* other ToR in this set (*i.e.,* a ToR-level permutation), while the remaining $(100 - x)\%$ ToRs are engaged in a server-level random permutation workload among themselves.

Our experiments showed that using the network to interconnect the same number of servers as in our earlier tests with random permutation traffic, full throughput is still achieved for all but the chunky traffic pattern. In Fig. 5.9(b), we present results for 5 chunky patterns. Except when a majority of the network is engaged in the chunky pattern, throughput is within a few percent of full throughput. We note that 100% Chunky is a hard to route traffic pattern which is easy to avoid. Even assigning applications to servers randomly will ensure that the probability of such a pattern is near-zero.

Even so, we repeat the experiment from Fig. 5.9(a) where we had measured the number of servers our modified topology supports at full throughput under random permutations. In this instance, we require our topology to support full throughput under the 100% Chunky traffic pattern. The results in Fig. 5.9(c) show that the gains are smaller, but still significant, 22% at the largest size, and increasing with size. It is also noteworthy that all-to-all traffic is easier to route than both the other workloads.

5.7 Conclusion

Our work presents the first systematic approach to the design of heterogeneous networks, allowing us to improve upon a deployed data center topology by as much as 43% even at the scale of just a few thousand servers, with this improvement increasing with size. In addition, we further the understanding of network throughput by showing how cut-size, path length, and utilization affect throughput.

While significant work remains in the space of designing and analyzing topologies, this work takes the first steps away from the myriad point solutions and towards a theoretically grounded approach to the problem.

CHAPTER 6

Systems challenges: routing and cabling

In the preceding chapters, we establish that Jellyfish topologies have high capacity, but it remains unclear whether this potential can be realized in real networks. There are two layers which can affect performance in real deployments: routing and congestion control. In our experiments with various combinations of routing and congestion control for Jellyfish (§6.1), we find that standard ECMP does not provide enough path diversity for Jellyfish, and to utilize the entire capacity we need to also use longer paths. We then provide in-depth results for Jellyfish's throughput and fairness using the best setting found earlier—k-shortest paths and multipath TCP (§6.2). Finally, we discuss practical strategies for deploying k-shortest-path routing (§6.3).

6.1 ECMP is not enough

Evaluation methodology: We use the simulator developed by the MPTCP authors for both Jellyfish and fat-tree. For routing, we test: (a) ECMP (equal cost multipath routing; We used 8-way ECMP, but 64-way ECMP does not perform much better, see Fig. 6.1), a standard strategy to distribute flows over shortest paths; and (b) k-shortest paths routing, which could be useful for Jellyfish because it can utilize longer-than-shortest paths. For k-shortest paths, we use Yen's Loopless-Path Ranking algorithm [88, 1] with $k = 8$ paths. For congestion control, we test standard TCP (1 or 8 flows per server pair) and the recently proposed multipath TCP (MPTCP) [86], using the recommended value of 8 MPTCP subflows. The traffic model continues to be a random permutation at the server-level, and as before, for the fat-tree comparisons, we build Jellyfish using the same switching equipment as the fat-tree.

This chapter includes previously published results from *Jellyfish: Networking Data Centers Randomly*. Ankit Singla, Chi-Yao Hong, Lucian Popa, P. Brighten Godfrey. USENIX NSDI, 2012.

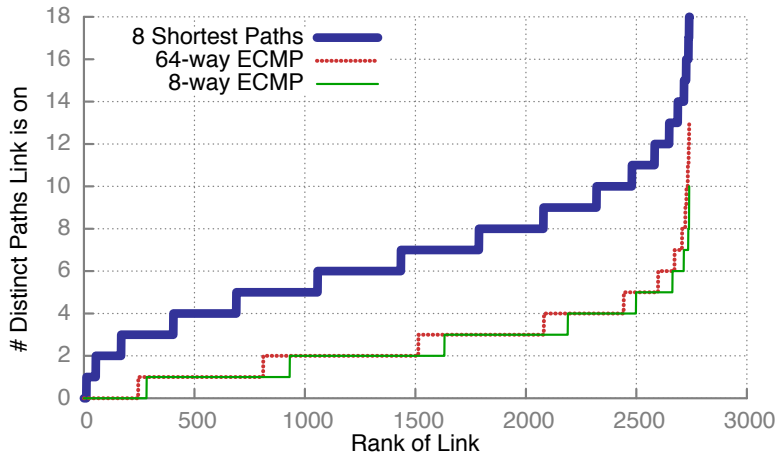

Figure 6.1 ***ECMP does not provide path diversity for Jellyfish: Inter-switch link's path count in ECMP and k-shortest-path routing for random permutation traffic at the server-level on a typical Jellyfish of 686 servers (built using the same equipment as a fat-tree supports 686 servers). For each link, we count the number of distinct paths it is on. Each network cable is considered as two links, one for each direction.***

Summary of results: Table 6.1 shows the average per server throughput as a percentage of the servers' NIC rate for two sample Jellyfish and fat-tree topologies under different routing and load balancing schemes. We make two observations: (1) ECMP performs poorly for Jellyfish, not providing enough path diversity. For random permutation traffic, Fig. 6.1 shows that about 55% of links are used by no more than 2 paths under ECMP; while for 8-shortest path routing, the number is 6%. Thus we need to make use of k-shortest paths. (2) Once we use k-shortest paths, each congestion control protocol works as least as well for Jellyfish as for the fat-tree.

The results of Table 6.1 depend on the oversubscription level of the network. In this context, we attempt to match fat-tree's performance given the routing and congestion control inefficiencies. We found that Jellyfish's advantage slightly reduces in this context compared to using idealized routing as before: In comparison to the same-equipment fat-tree (686 servers), now we can support, at same or higher performance, 780 servers (*i.e.*, 13.7% more that the fat-tree) with TCP, and 805 servers (17.3% more) with MPTCP. With ideal routing and congestion control, Jellyfish could support 874 servers (27.4% more). However, as we show quantitatively in §6.2, Jellyfish's advantage improves significantly with scale. At the largest scale we could simulate, Jellyfish supports 3,330 servers to the fat-tree's 2,662 — a $> 25\%$ improvement (after accounting for routing and congestion control inefficiencies).

Congestion control	Fat-tree (686 svrs) ECMP	Jellyfish (780 svrs) ECMP	Jellyfish (780 svrs) 8-shortest paths
TCP 1 flow	48.0%	57.9%	48.3%
TCP 8 flows	92.2%	73.9%	92.3%
MPTCP 8 subflows	93.6%	76.4%	95.1%

Table 6.1 ***Packet simulation results for different routing and congestion control protocols for Jellyfish (780 servers) and a same-equipment fat-tree (686 servers). Results show the normalized per server average throughput as a percentage of servers' NIC rate over 5 runs. We did not simulate the fat-tree with 8-shortest paths because ECMP is strictly better, and easier to implement in practice for the fat-tree.***

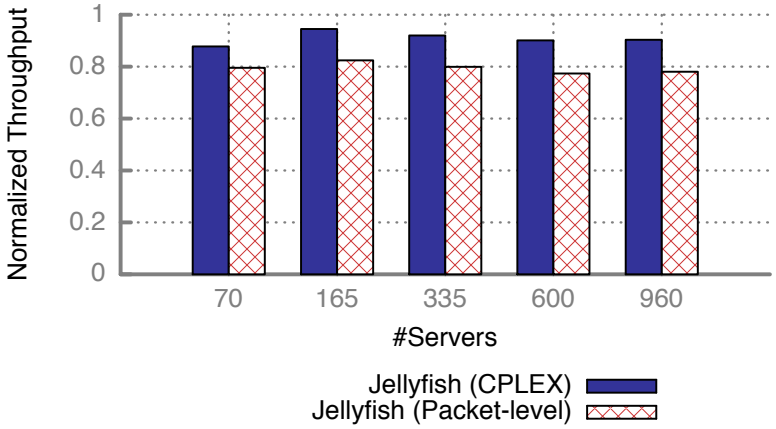

Figure 6.2 ***Simple k-shortest path forwarding with MPTCP exploits Jellyfish's high capacity well: We compare the throughput using the same Jellyfish topology with both optimal routing, and our simple routing mechanism using MPTCP, which results in throughput between $86\% - 90\%$ of the optimal routing in each case. Results are averaged over 10 runs.***

6.2 k-Shortest-Paths with MPTCP

The above results demonstrate using one representative set of topologies that using k-shortest paths with MPTCP yields higher performance than ECMP/TCP. In this section we measure the efficiency of k-shortest path routing with MPTCP congestion control against the optimal performance (presented in §4.2), and later make comparisons against fat-trees at various sizes.

Routing and Congestion Control Efficiency: The result in Fig. 6.2 shows the gap between the optimum performance, and the performance realized with routing and congestion control inefficiencies. At each size, we use the same slightly oversubscribed[1] Jellyfish topology for both setups. In the worst of these comparisons, Jellyfish's packet-level throughput is at $\sim 86\%$ of the CPLEX optimal throughput. (In comparison, the fat-tree's throughput under MPTCP/ECMP is 93-95% of its optimum.) There is a possibility that this gap

[1] An undersubscribed network may simply show 100% throughput, masking some of the routing and transport inefficiency.

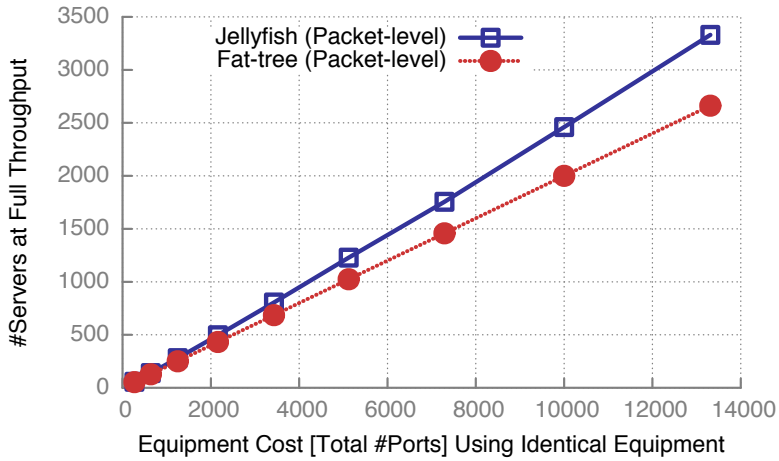

Figure 6.3 ***Jellyfish supports a larger number of servers (*** $>25\%$ ***at the largest scale shown, with an increasing trend) than the same-equipment fat-tree at the same (or higher) throughput, even with inefficiencies of routing and congestion control accounted for. Results are averages over*** 20 ***runs for topologies smaller than*** $1{,}400$ ***servers, and averages over*** 10 ***runs for larger topologies.***

can be closed using smarter routing schemes, but nevertheless, as we discuss below, Jellyfish maintains most of its advantage over the fat-tree in terms of the number of servers supported at the the same throughput.

Fat-tree Throughput Comparison: To compare Jellyfish's performance against the fat-tree, we first find the average per-server throughput a fat-tree yields in the packet simulation. We then find (using binary search) the number of servers for which the average per-server throughput for the comparable Jellyfish topology is either the same, or higher than the fat-tree; this is the same methodology applied for Table 6.1. We repeat this exercise for several fat-tree sizes. The results (Fig. 6.3) are similar to those in Fig. 4.2(c), although the gains of Jellyfish are reduced marginally due to routing and congestion control inefficiencies. Even so, at the maximum scale of our experiment, Jellyfish supports 25% more servers than the fat-tree (3,330 in Jellyfish, versus 2,662 for the fat-tree). We note however, that even at smaller scale (for instance, 496 servers in Jellyfish, to 432 servers in the fat-tree) the improvement can be as large as $\sim 15\%$.

We show in Fig. 6.4, the stability of our experiments by plotting the average, minimum and maximum throughput for both Jellyfish and the fat-tree at each size, over 20 runs (varying both topologies and traffic) for small sizes and 10 runs for sizes $>1{,}400$ servers.

Fairness: We evaluate how flow-fair the routing and congestion control is in Jellyfish. We use the packet simulator to measure each flow's throughput in both topologies and show in Fig. 6.5, the normalized throughput per flow in increasing order. Note that Jellyfish has a larger number of flows because we make all com-

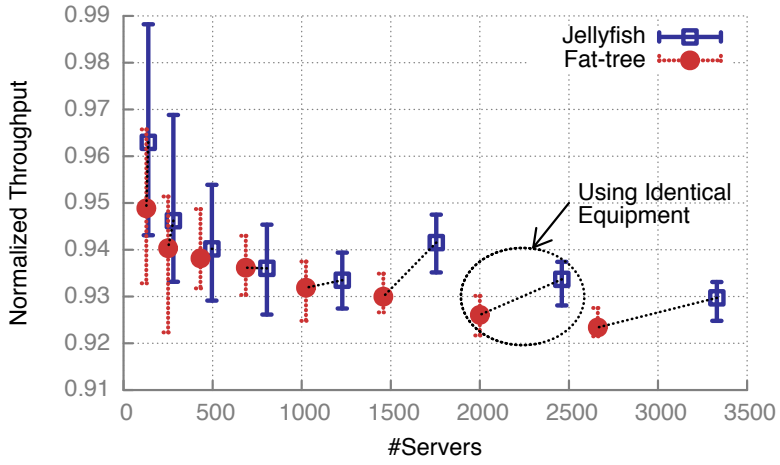

Figure 6.4 ***The packet simulation's throughput results for Jellyfish show similar stability as the fat-tree. (Note that the y-axis starts at*** 91% ***throughput.) Average, minimum and maximum throughput-per-server values are shown. The data plotted is from the same experiment as Fig. 6.3. Jellyfish has the same or higher average throughput as the fat-tree while supporting a larger number of servers. Each Jellyfish data-point uses equipment identical to the closest fat-tree data-point to its left (as highlighted in one example).***

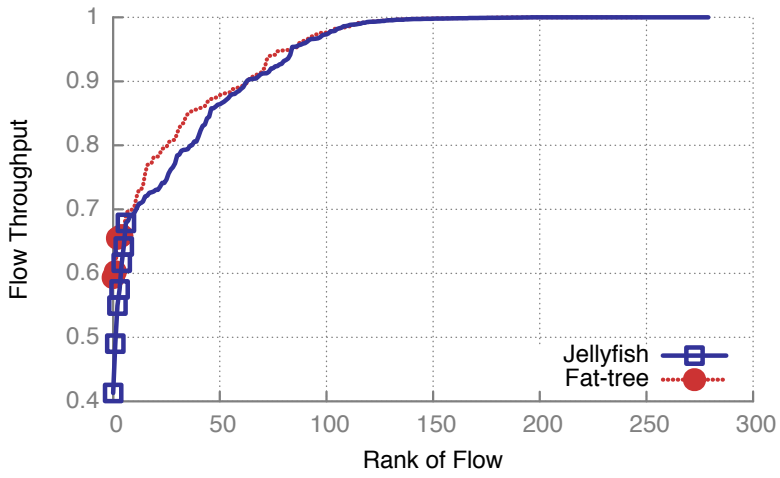

Figure 6.5 ***Both Jellyfish and the fat-tree show good flow-fairness: The distribution of normalized flow throughputs in Jellyfish and fat-tree is shown for one typical run. After the few outliers (shown with points), the plot is virtually continuous (the line). Note that Jellyfish has more flows because it supports a higher number of servers (at same or higher*** **per-server** ***throughput). Jain's fairness index for both topologies is*** $\sim 99\%$.

parisons using the same network equipment and the larger number of servers supported by Jellyfish. Both the topologies have similarly good fairness; Jain's fairness index [51] over these flow throughput values for both topologies: 0.991 for the fat-tree and 0.988 for Jellyfish.

6.3 Implementing k-Shortest-Path routing

In this section, we discuss practical possibilities for implementing k-shortest-paths routing. For this, each switch needs to maintain a routing table containing for each other switch, k shortest paths.

OpenFlow [64]: OpenFlow switches can match end-to-end connections to routing rules, and can be used for routing flows along pre-computed k-shortest paths. Recently, Devoflow [70] showed that OpenFlow rules can be augmented with a small set of local routing actions for randomly distributing load over allowed paths, without invoking the OpenFlow controller.

SPAIN [72]: SPAIN allows multipath routing by using VLAN support in commodity off-the-shelf switches. Given a set of pre-computed paths, SPAIN merges these paths into multiple trees, each of which is mapped to a separate VLAN. SPAIN supports arbitrary topologies, and can enable use of k-shortest path routing in Jellyfish.

MPLS [77]: One could set up MPLS tunnels between switches such that all the pre-computed k-shortest paths between a switch pair are configured to have the same cost. This would allow switches to perform standard equal-cost load balancing across paths.

6.4 Related work

There is a vast literature on routing, addressing various goals like QoS-aware routing [23, 62, 84]; routing under system constraints like deadlock-free routing [74]; routing under economic constraints, such as that with BGP in the Internet; etc. We focus here on building a routing scheme that achieves high throughput over various traffic patterns for our random graph-based data center topologies. The data center setting affords unique freedom with regards to routing design: topologies with large numbers of links and paths, relatively new equipment with tens of thousands of forwarding entries, and the data center operator exercising full control over the entire network. While various routing schemes have been proposed for various networks,

including those in data centers, we show here that we can indeed exploit this design freedom to build efficient routing solutions for *unstructured* networks.

6.5 Physical construction and cabling

Key considerations in data center wiring include:

- **Number of cables:** Each cable represents both a material and a labor cost.
- **Length of cables:** The cable price/meter is \$5-6 for both electrical and optical cables, but the cost of an optical transceiver can be close to \$200 [71]. We limit our interest in cable length to whether or not a cable is short enough, i.e., $<$10 meters in length [53, 36], for use of an electrical cable.
- **Cabling complexity:** Will Jellyfish awaken the dread spaghetti monster? Complex and irregular cabling layouts may be hard to wire and thus susceptible to more wiring errors. We will consider whether this is a significant factor. In addition, we attempt to design layouts that result in aggregation of cables in bundles, in order to reduce manual effort (and hence, expense) for wiring.

In the rest of this section, we first address a common concern across data center deployments: handling wiring errors (§6.5.1). We then investigate cabling Jellyfish in two deployment scenarios, using the above metrics (number, length and complexity of cabling) to compare against cabling a fat-tree network. The first deployment scenario is represented by small clusters ($\sim$1,000 servers); in this category we also include the intra-container clusters for 'Container Data Centers' (CDC)[2] (§6.5.2). The second deployment scenario is represented by massive-scale data centers (§6.5.3). In this work we only analyze massive data centers built using containers, leaving more traditional data center layouts to future work.[3]

6.5.1 Handling wiring errors

We envision Jellyfish cabling being performed using a blueprint automatically generated based on the topology and the physical data center layout. The blueprint is then handed to workers to connect cables manually.

[2] As early as 2006, The Sun Blackbox [2] promoted the idea of using shipping containers for data centers. There are also new products in the market exploiting similar physical design ideas [3, 4, 49].

[3] The use of container-based data centers seems to be an industry trend, with several players, Google and Microsoft included, already having container-based deployments [36].

While some human errors are inevitable in cabling, these are easy to detect and fix. Given Jellyfish's sloppy topology, a small number of miswirings may not even require fixing in many cases. Nevertheless, we argue that fixing miswirings is relatively inexpensive. For example, the labor cost of cabling is estimated at $\sim 10\%$ of total cabling cost [71]. With a pessimistic estimate where the total cabling cost is 50% of the network cost, the cost of fixing (for example) 10% miswirings would thus be just 0.5% of the network cost. We note that wiring errors can be detected using a link-layer discovery protocol [66].

6.5.2 Small clusters and CDCs

Small clusters and CDCs form a significant section of the market for data centers, and thus merit separate consideration. In a 2011 survey [31] of 300 US enterprises (with revenues ranging from \$1B-\$40B) which operate data centers, 57% of data centers occupy between $5{,}000$ and $15{,}000$ square feet; and 75% have a power load $<$2MW, implying that these data centers house a few thousand servers [30]. As our results in §4.2.1 show, even at a few hundred servers, cost-efficiency gains from Jellyfish can be significant ($\sim 20\%$ at $1{,}000$ servers). Thus, it is useful to deploy Jellyfish in these scenarios.

We propose a cabling optimization (along similar lines as the one proposed in [59]). The key observation is that in a high-capacity Jellyfish topology, there are more than twice as many cables running between switches than from servers to switches. Thus, placing all the switches in close proximity to each other reduces cable length, as well as manual labor. This also simplifies the small amounts of rewiring necessary for incremental expansion, or for fixing wiring errors.

Number of cables: Requiring fewer network switches for the same server pool also implies requiring fewer cables ($15-20\%$ depending on scale) than a fat-tree. This also implies that there is more room (and budget) for packing more servers in the same floor space.

Length of cables: For small clusters, and inside CDC containers using the above optimization, cable lengths are short enough for electrical cables without repeaters.

Complexity: For a few thousand servers, space equivalent to 3-5 standard racks can accommodate the switches needed for a full bisection bandwidth network (using available 64-port switches). These racks can be placed at the physical center of the data center, with aggregate cable bundles running between them. From this 'switch-cluster', aggregate cables can be run to each server-rack. With this plan, manual cabling

is fairly simple. Thus, the nightmare cable-mess image a random graph network may bring to mind is, at best, alarmist.

A unique possibility allowed by the assembly-line nature of CDCs, is that of fabricating a random-connect *patch panel* such that workers only plug cables from the switches into the panel in a regular easy-to-wire pattern, and the panel's internal design encodes the random interconnect. This could greatly accelerate manual cabling.

Whether or not a patch panel is used, the problems of layout and wiring need to be solved only *once* at design time for CDCs. With a standard layout and construction, building automated tools for verifying and detecting miswirings is also a one-time exercise. Thus, the cost of any additional complexity introduced by Jellyfish would be amortized over the production of many containers.

Cabling under expansion: Small Jellyfish clusters can be expanded by leaving enough space near the 'switch-cluster' for adding switches as servers are added at the periphery of the network. In case no existing switch-cluster has room for additional switches, a new cluster can be started. Cable aggregates run from this new switch-cluster to all new server-racks and to all other switch-clusters. We note that for this to work with only electrical cabling, the switch-clusters need to be placed within 10 meters of each other as well as the servers. Given the constraints the support infrastructure already places on such facilities, we do not expect this to be a significant issue.

As discussed before, the Jellyfish expansion procedure requires a small amount of rewiring. The addition of every two network ports requires two cables to be moved (or equivalently, one old cable to be disconnected and two new cables to be added), since each new port will be connected to an existing port. The cables that need to be disconnected and the new cables that need to be attached can be automatically identified. Note that in the 'switch-cluster' configuration, all this activity happens at one location (or with multiple clusters, only between these clusters). The only cables not at the switch-cluster are the ones between the new switch and the servers attached to it (if any). This is just *one* cable aggregate.

We note that the CDC usage may or may not be geared towards incremental expansion. Here the chief utility of Jellyfish is its efficiency and reliability.

6.5.3 Jellyfish in massive-scale data centers

We now consider massive scale data centers built by connecting together multiple containers of the type described above. In this setting, as the number of containers grows, most Jellyfish cables are likely to be between containers. Therefore, inter-container cables in turn require expensive optical connectors, and Jellyfish can result in excessive cabling costs compared to a fat-tree.

However, we argue that Jellyfish can be adapted to wire massive data centers with lower cabling cost than a fat-tree, while still achieving higher capacity and accommodating a larger number of servers. For cabling the fat-tree in this setting, we apply the layout optimization suggested in [59], *i.e.,* make each fat-tree 'pod' a container, and divide the core-switches among these pods equally. With this physical structure, we can calculate the number of intra-container cables (from here on referred to as 'local') and inter-container cables ('global') used by the fat-tree. We then build a Jellyfish network placing the same number of switches as a fat-tree pod in a container, and using the same number of containers. Now, in this setting, where we are looking at containers (or clusters) connected to each other, we are in position to exploit the intuition from Theorem 4 (Chapter 5) – we can have a much smaller number of cables running between containers than dictated by uniform randomness, without losing much throughput. The resulting Jellyfish network can be seen as a 2-layered random graph—a random graph within each container, and a random graph between containers. We vary the number of local and global connections to see how this affects performance in relation to the unrestricted Jellyfish network.

Note that with the same switching equipment as the fat-tree, Jellyfish networks would be overprovisioned if we used the same numbers of servers. To make sure that any loss of throughput due to our cable-optimization is clearly visible, we add a larger number of servers per switch to make Jellyfish oversubscribed.

Fig. 6.6 plots the capacity (average server throughput) achieved for 4 sizes[4] of 2-layer Jellyfish, as we vary the number of local and global connections, while keeping the total number of connections constant for a topology. Throughput is normalized to the corresponding unrestricted Jellyfish. The throughput drops by $<6\%$ when 60% of the network connections per switch are 'localized'. The percentage of local links for the equivalent fat-tree is 53.6%. Thus, Jellyfish can achieve a higher degree of localization, while still having a higher capacity network; recall that Jellyfish is 27% more efficient than the fat-tree at the largest

[4]These are very far from massive scale, but these simulations are directed towards observing general trends. Much larger simulations are beyond our simulator's capabilities.

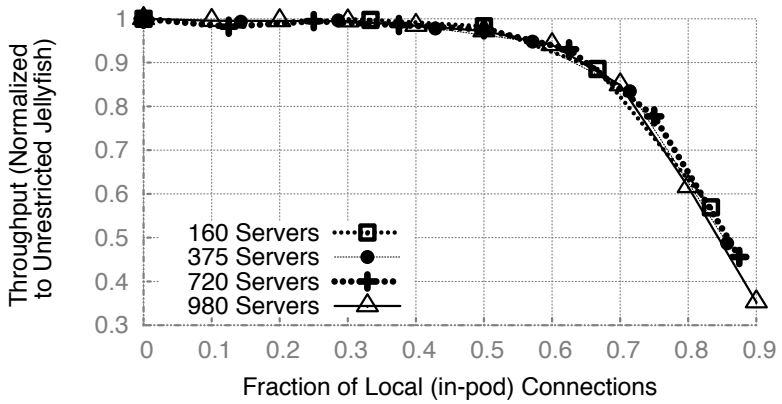

Figure 6.6 ***Localization of Jellyfish random links is a promising approach to tackle cabling for massive scale data centers: As links are restricted to be more and more local, the network capacity decreases (as expected). However, when*** 50% ***of the random links for each switch are constrained to remain inside the pod, there is*** $<3\%$ ***loss of throughput.***

scale (§4.2.1). The effect of cable localization on throughput was similar across the sizes we tested. For the fat-tree, the fraction of local links (conveniently given by $0.5(1 + 1/k)$ for a fat-tree built with k-port switches) *decreases* marginally with size.

Complexity: Building Jellyfish over switches distributed uniformly across containers will, with high probability, result in cable assemblies between every pair of containers. A $100{,}000$ server data center can be built with ~ 40 containers. Even if *all* ports (except those attached to servers) from each switch in each container were connected to other containers, we could aggregate cables between each container-pair leaving us with ~ 800 such cable assemblies, each with fewer than 200 cables. With the external diameter of a 10GBASE-SR cable being only $245um$, each such assembly could be packed within a pipe of radius $<1cm$. Of course, with higher over-subscription at the inter-container layer, these numbers could decrease substantially.

Cabling under expansion: In massive-scale data centers, expansion can occur through addition of new containers, or expansion of containers (if permissible). Laying out spare cables together with the aggregates between containers is helpful in scenarios where a container is expanded. When a new container is added, new cable aggregates must be laid out to every other container. Patch panels can again make this process easier by exposing the ports that should be connected to the other containers.

6.6 Other practical concerns

What about non-uniform traffic matrices? In line with the design objective of hosting arbitrary applications at high throughput, the approach we have taken is to study *difficult* traffic matrices, rather than TMs specific to particular environments. We show in Chapter 3 that an all-to-all workload bounds performance under any workload within a factor of 2. As such, testing this TM is more useful than any other specific, arbitrary choice. In addition, we evaluate other traffic matrices which are even harder to route, including the random permutation TM, the Chunky TM (§5.6), and the longest matching TM (§3.2.3). Further, our code is available [5], and is easy to augment with arbitrary traffic patterns to test.

What about latency? We include a rigorous analysis of latency in terms of path length (Fig. 4.8(b), 4.9(b)), showing that average shortest path lengths are close to optimal in random graphs. Further, we show that even worst-case path length (diameter) in random graphs is smaller than or similar to that in fat-trees (Fig. 4.4). Beyond path length, latency depends on the transport protocol's ability to keep queues small. In this regard, we note that techniques being developed for low latency transport (such as DCTCP [9], HULL [8], pFabric [10]) are topology agnostic.

But randomness?! 'Random' $\not\Rightarrow$ 'inconsistent performance': the standard deviations in throughput are $\sim 1\%$ of the mean (and even smaller for path length). Also, by 'maximizing the minimum flow' to measure throughput, we impose a strict definition of fairness, eliminating the possibility of randomness skewing results across flows. Further, we show that random graphs achieve flow-fairness comparable to fat-trees under a practical routing scheme (§6.2).

CHAPTER 7

Future work and open problems

While we have presented here foundational results on the design of both homogeneous and heterogeneous topologies, many interesting problems remain unresolved:

- Throughput bounds for heterogeneous networks: While we have been able to prove a bound on the throughput of any topology built with *identical* switches (§4.3), a similar result in the heterogeneous network setting eludes us. So far, our results rely on the use of near-optimal homogeneous networks as building blocks. While this approach is intuitive, it leaves open the possibility of designs that achieve higher throughput in the heterogeneous settings.

- Generalizing our results to multiple switch types: Most of our results in the heterogeneous network setting (Chapter 5) are limited to two types of switches. This is because as one increases the number of switches, the parameter space grows immensely – one could have different volumes of connectivity between all pairs of types of switches, etc. For a small number of switch types (such as 3), our analysis method can still be used, even though it is a bit cumbersome. However, for general settings, what we would ideally want is some *predictive* method (as opposed to the empirical measurement-based approach we took here.

- Theoretical proof for our result on distributing servers across switches in proportion to their port-counts: While our empirical analysis (§5.2) bears out this result across a vast set of parameter choices, we have so far not been able to prove this analytically.

- Routing independent of MPTCP: While our approach to routing, using k-shortest paths together with multipath TCP, yields good results (§6.2), it may not be a good choice in certain settings. For instance, in a public cloud environment, where the operator may host customer virtual machines, these virtual

machines may not necessarily be equipped to use MPTCP. It would thus be desirable to build a simple scheme that works entirely at the routing layer (as opposed to involving the transport layer, as we do).

- Geometric topology design: In this work, we took the approach of decomposing the topology design and physical cabling problems, whereby, we first used a model where each connection (or edge) has the same cost regardless of length, and later, restricted a certain fraction of edges to be short, thus simplifying cabling (§6.5.3). This approach nevertheless leaves open the possibility, that using a more sophisticated model, where the dependence of edge-cost on length is captured in the topology design itself, even cheaper networks can be designed.

- Application-layer evaluation: Our approach to evaluating topologies is based on application-oblivious techniques, but nevertheless, we believe it is valuable to test the performance of high-value, large applications on different network topologies. Results from one such comparison show higher application performance over Jellyfish in comparison to the fat-tree [11], even at the small scale of 30 hosts. Larger and more diverse evaluations of a similar nature would be very useful.

APPENDIX A

Proof of Theorem 1

We revisit the *maximum concurrent flow* problem, based on which we defined throughput in §3.1: Given a network $G = (V, E_G)$ with capacities $c(u, v)$ for every edge $(u, v) \in E_G$, and a collection (not necessarily disjoint) of pairs $(s_i, t_i), i = 1, \ldots, k$ each having a unit flow demand, we are interested in maximizing the minimum flow. Instead of the traffic matrix (TM) formulation of §3.1, for the following discussion, it will be convenient to think of the pairs of vertices that require flow between them as defining a demand graph, $H = (V, E_H)$. Thus, given G and H, we want the maximum throughput. As we noted in §3.1, this problem can be formulated as a standard linear program, and is thus computable in polynomial time.

We are interested in comparing our suggested throughput metric with sparsest cut. We first prove the following theorem.

Theorem 5. *The dual of the linear program for computing throughput is a linear programming relaxation for sparsest cut.*

Proof. We shall use a formulation of the throughput linear program that involves an exponential number of variables but for which is easier to derive the dual. We denote by $P_{s,t}$ the set of all paths from s to t in G and we introduce a variable x_p for each path $p \in P_{s,t}$, for each $(s, t) \in E_H$, corresponding to how many units of flow from s to t are routed through path p.

$$
\begin{aligned}
&\text{max} && y && \\
&\text{subject to} && \sum_{p \in P_{s,t}} x_p \geq y && \forall (s,t) \in E_H, \\
& && \sum_{p:(u,v)\in p} x_p \leq c(u,v) && \forall (u,v) \in E_G \\
& && x_p \geq 0 && \forall p \\
& && y \geq 0. &&
\end{aligned}
$$

The dual of the above linear program will have one variable $w(s,t)$ for each $(s,t) \in E_H$ and one variable $z(u,v)$ for each $(u,v) \in E_G$.

$$
\begin{aligned}
&\text{min} && \sum_{u,v} z(u,v)c(u,v) && \\
&\text{subject to} && \sum_{(s,t)\in E_H} w(s,t) \geq 1 && \\
& && \sum_{(u,v)\in p} z(u,v) \geq w(s,t) && \forall (s,t) \in E_H, p \in P_{s,t} \\
& && w(s,t) \geq 0 && \forall (s,t) \in E_H \\
& && z(u,v) \geq 0 && \forall (u,v) \in E_G.
\end{aligned}
$$

It is not hard to realize that in an optimal solution, without loss of generality, $w(s,t)$ is the length of the shortest path from s to t in the graph weighted by the $z(u,v)$. We can also observe that in an optimal solution we have $\sum w(s,t) = 1$. These remarks imply that the above dual is equivalent to the following program, where we introduce a variable $l(x,y)$ for every pair or vertices in $E_G \cup E_H$.

$$
\begin{aligned}
\text{min} \quad & \sum_{u,v} l(u,v)c(u,v) \\
\text{subject to} \quad & \sum_{(s,t)\in E_H} l(s,t) = 1 \\
& \sum_{(u,v)\in p} l(u,v) \geq l(s,t) && \forall (s,t) \in E_H, p \in P_{s,t} \\
& l(u,v) \geq 0 && \forall (u,v) \in E_G \cup E_H
\end{aligned}
$$

The constraints $\sum_{(u,v)\in p} l(u,v) \geq l(s,t)$ can be equivalently restated as triangle inequalities. This means that we require $l(u,v)$ to be a metric over V. These observations give us one more alternative formulation:

$$\text{min}_{l(\cdot,\cdot) \text{ metric}} \frac{\sum_{(u,v)\in E_G} c(u,v) \cdot l(u,v)}{\sum_{(s,t)\in E_H} l(s,t)} \tag{A.1}$$

We can finally see that the above formulation is a linear programming relaxation for a cut problem. More specifically, the sparsest cut problem is asking to find a cut S that minimizes the ratio

$$\frac{\sum_{(u,v)\in E_G \text{ cut by S}} c(u,v)}{|\text{ edges} \in E_H \text{ cut by S}|} \tag{A.2}$$

This is equivalent to minimizing ratio (A.1) over ℓ_1 metrics only.

If we take E_H to be the complete graph (corresponding to all-to-all demands), we get the standard sparsest cut definition:

$$\frac{\sum_{(u,v)\in E_G \text{ cut by S}} c(u,v)}{|S||\bar{S}|} \tag{A.3}$$

□

Before we prove Theorem 1 from §3.1, we shall demonstrate the following claim.

Claim 6. *If G is a d-regular expander graph on N nodes and H is the complete graph, the value of the linear program for throughput is $O(\frac{d \log d}{N \log N})$. The value of the sparsest cut is $\Omega(\frac{d}{N})$.*

Proof. Let us denote by T the optimal value of expression (A.1). Note that this is the optimal value of the dual for the linear program for throughput, therefore equal to the optimal throughput. By taking $l(\cdot, cdot)$ to be the shortest path metric on G, we calculate:

$$T \leq \frac{\sum_{(i,j)\in E_G} l(i,j)}{\sum_{i,j\in V} l(i,j)} \leq \frac{d/2.|V|}{\Theta(N^2 \frac{\log N}{\log d})} \leq O(\frac{d \log d}{N^2 \log N}) \tag{A.4}$$

Here, the first inequality follows from the fact that for d-regular graphs, each node can reach no more than d^i nodes in i hops. This means that given a vertex v, there exist $\Theta(N)$ nodes with distance at least $\frac{\log N}{\log d}$ from it, which means that the total distance between all pairs of nodes is $\Theta(N^2 \frac{\log N}{\log d})$.

Let Φ denote the minimum value of ratio (A.3) for G. Since G is an expander, this ratio is

$$\Phi \geq \Omega(\frac{d \cdot |S|}{|S||V-S|}) = \Omega(\frac{d}{N}) \tag{A.5}$$

□

Theorem 1. *Let graph G be any $2d$-regular expander on $N = \frac{n}{dp}$ nodes, where d is a constant and p is a free parameter. Let graph B be constructed by replacing each edge of G with a path of length p. Then, B has throughput $T_B = O(\frac{1}{np \log n})$ and sparsest cut $\Phi_B = \Omega(\frac{1}{np})$.*

Proof. Let (S_1, S_2) be the sparsest cut in B. Let $(S_1{}', S_2{}')$ be the corresponding cut in G. Namely, if an edge was cut in B by (S_1, S_2) that belonged to a path p_e then $(S_1{}', S_2{}')$ cuts e. Let Φ_B be the value of the cut (S_1, S_2) in A and Φ_G the value of $(S_1{}', S_2{}')$ in G. Then

$$\Phi_B = \frac{E(S_1, S_2)}{|S_1||S_2|} = \frac{E(S_1{}', S_2{}')}{|S_1||S_2|} \geq \frac{E(S_1{}', S_2{}')}{p \cdot |S_1'| p \cdot |S_2'|} \geq \frac{\Phi_G}{p^2}$$

by equation (A.5) we have $\Phi_G \geq \Omega(\frac{1}{N}) = \Omega(\frac{p}{n})$ which gives us

$$\Phi_B \geq \Omega(\frac{1}{np})$$

On the other hand, let T_B be the value of the throughput of B. We follow a similar reasoning as we did

in equation (A.4).

$$T_B \leq \frac{\sum_{(i,j)\in E_G} l(i,j)}{\sum_{i,j\in V} l(i,j)} \leq \frac{Ndp}{\Theta((Np)^2 p \log N)} \leq O(\frac{1}{Np^2 \log N}) = O(\frac{1}{np \log n}) \tag{A.6}$$

□

APPENDIX B

Proof of Theorem 2

Proof. T_{A2A} has demand $\frac{1}{n}$ on each flow, so the largest feasible multicommodity flow routing of T_{A2A} in G has capacity $\frac{t}{n}$ allocated to each flow. Let C be a graph representing this routing, i.e., a complete digraph with capacity $\frac{t}{n}$ on each link. Systems-oriented readers may find it useful to think of C as an overlay network implemented with reserved bandwidth in G. In other words, to prove the theorem, it is sufficient to show that taking T to be any hose-model traffic matrix, $T \cdot t/2$ is feasible in C.

For this, we use a two-hop routing scheme analogous to Valiant load balancing [13]. Consider any traffic demand $v \rightsquigarrow w$. In the first step, we split this demand flow into n equal parts, routing flow $\frac{1}{n} \cdot T(v, w) \cdot t/2$ from v to every node in the network, along the direct links (or the zero-hop path when the target is v itself). In the second step, the traffic arriving at each node is sent along at most one link to its final destination.

We now have to show that this routing is feasible in C. Consider any link $i \rightarrow j$. This link will carry a fraction $\frac{1}{n}$ of all the traffic originated by i, and a fraction $\frac{1}{n}$ of all the traffic destined to j. Because T is a hose model TM, each node originates and sinks a total of ≤ 1 unit of traffic; and since we are actually attempting to route the scaled traffic matrix $T \cdot t/2$, each node originates and sinks a total of $\leq t/2$ units of traffic. Therefore, link i carries a total of

$$\frac{t}{2} \cdot \frac{1}{n} + \frac{t}{2} \cdot \frac{1}{n} = \frac{t}{n},$$

which is the available capacity on each link of C and is hence feasible. □

APPENDIX C

Proof of Theorem 4

Our proof consists of four parts. First, in Lemma 1, we compute the peak value of throughput (within constant factors) T^*. In Lemma 2, we show that the sparsest cut value (defined below) is linear in q for a bipartite demand graph across the clusters[1]. In Lemma 3, we show that for $q \leq q^*$, throughput is within a constant factor of the sparsest cut value and thus reduces linearly with q. Finally, we show that for $q > q^*$, throughput is within a constant factor of its peak value.

We will use a celebrated result that can be found in [61] as Theorem 4.1. We paraphrase it here to suit our needs:

Theorem 7 (Linial, London, Rabinovich)**.** *We are given a network $G = (V, E, C)$ with vertices V, edges E, and their capacities C. We are also given a demand graph $H = (V, E')$ with $k = |E'|$ source-sink pairs. For a set $S \subseteq V$, let $\mathsf{Cap}(S)$ be the sum of the capacities of edges connecting S and S' and $\mathsf{Dem}(S)$ be the number of source-sink pairs separated by S. Let $T(G, H)$ be the throughput for given G and H. Then there exists a set $S \subseteq V$ such that*

$$\frac{\mathsf{Cap}(S)}{\mathsf{Dem}(S)} \leq O(\log k) \cdot T(G, H)$$

The minimum of the ratios $\frac{\mathsf{Cap}(S)}{\mathsf{Dem}(S)}$, *i.e.,* $\min_{S \subseteq V} \frac{|E_G(S,S')|}{|E_H(S,S')|}$ is referred to as the non-uniform sparsest cut of graph G with a demand graph H [61]. Then, the above theorem immediately implies the following relationship between the sparsest cut ϕ and throughput T for a graph G and demand graph H:

$$\phi(G, H) \leq O(\log k) \cdot T(G, H) \tag{C.1}$$

In the below, K_{V_1,V_2} refers to the *complete bipartite* demand graph where each node communicates with

[1] In general, the sparsest cut is NP-Hard to compute. It is the specific setting that makes this possible.

(and only with) all nodes in the opposite cluster. We shall use this demand graph to prove our results, and then show later that throughput under this demand graph is within a constant factor of throughput under random permutations.

Lemma 1. *When $p = q = q_0$, for demand graph $H = K_{V_1,V_2}$, $T(q = q_0) = T^* = \Theta(\frac{1}{n \log n})$.*

Proof. For $q = p$, it is well known [34] that G is an almost optimal expander with high probability, and all the balanced cuts have about the same number of edges being cut, which is $O(d \cdot n)$. Thus the (non-uniform) sparsest cut value is:

$$\phi(q_0) = \Theta\left(\frac{d \cdot n}{n^2}\right) = \Theta\left(\frac{d}{n}\right) \tag{C.2}$$

From equation C.1, we obtain that for some constant c,

$$T(q_0) \geq c\frac{1}{\log k}\phi(q_0) \geq \Omega\left(\frac{1}{\log n}\right)\left(\frac{d}{n}\right) \tag{C.3}$$

For constant d, we obtain:

$$T(q_0) \geq \Omega\left(\frac{1}{n \log n}\right) \tag{C.4}$$

Next, we invoke our path-length based bound: $T \leq \frac{|E|}{\langle D \rangle f}$, which, in this setting implies $T \leq O(\frac{nd}{\langle D \rangle n^2})$. Under our graph model (and trivially for d-regular graphs), the following result holds [24, 25] for average shortest path length $\langle D \rangle$:

$$\langle D \rangle \geq \Omega\left(\frac{\log n}{\log d}\right) \tag{C.5}$$

Using this result, for constant d, we obtain $T \leq O(\frac{1}{n \log n})$, which, together with equation C.4, yields the lemma's result. □

Lemma 2. *For $H = K_{V_1,V_2}$, $\phi(G, H) = \Theta(q)$.*

Proof. In the most general case, a cut in G can be described by the vertex sets $S = (k_1 \in V_1) \cup (k_2 \in V_2)$ and $S' = V \setminus S$, so that arbitrary subsets k_1 and k_2 of V_1 and V_2 respectively, are separated from the rest of the graph by the cut. Then:

$$E_G(S, S') \;=\; E_G(k_1, V_1 \setminus k_1) + E_G(k_2, V_2 \setminus k_2) + E_G(k_1, V_2 \setminus k_2) + E_G(k_2, V_1 \setminus k_1) \tag{C.6}$$

Note that k_1 and k_2 are both subgraphs of random regular graphs V_1 and V_2 of degree pn (using only the internal edges of each cluster). Also, across the clusters V_1 and V_2, we have a bipartite expander graph of degree qn. According to the expander mixing lemma [33], the number of cut-edges across subgraphs of each of these expanders is within a constant factor of the expected number of edges. Thus, for some constants c_l, c_m, and c_n:

$$E_G(k_1, V_1 \setminus k_1) \geq c_l pnk_1 \frac{n/2 - k_1}{n/2} = c_l k_1 pn(1 - 2k_1/n) \tag{C.7}$$

$$E_G(k_2, V_2 \setminus k_2) \geq c_m k_2 pn(1 - 2k_2/n) \tag{C.8}$$

$$E_G(k_1, V_2 \setminus k_2) + E_G(k_2, V_1 \setminus k_1) \geq c_n(k_1 qn(1 - 2k_2/n) + k_2 qn(1 - 2k_1/n)) \tag{C.9}$$

Using $c_{min} = min\{c_l, c_m, c_n\}$, $k = k_1 + k_2$, and degree $d = pn + qn$, we obtain (after simplification) from the above equations:

$$E_G(S, S') \geq c_{min}(kd + 2pk^2 + 4k_1 k_2 d/n) \tag{C.10}$$

For $H = K_{V_1,V_2}$, $E_H(S, S') = kn/2 - 2k_1 k_2$. With a fixed k, it is easy to show that $E_G(S, S')/E_H(S, S')$ is minimized when $(k_1, k_2) = (0, k)$ or $(k, 0)$; the minimum value being $c_{min}\frac{2d-4kp}{n}$. For $k \in (0, n/2]$, the minimum value of this expression is $c_{min}\frac{2d-2pn}{n} = 2qc_{min}$. Thus $E_G(S, S')/E_H(S, S') \geq 2qc_{min}$, and further, $\phi(G, H) = \min_{S \subseteq V} \frac{|E_G(S,S')|}{|E_H(S,S')|} \geq 2qc_{min}$. To conclude the lemma's proof, we note that $\frac{|E_G(V_1,V_2)|}{|E_H(V_1,V_2)|} = 2q$ implies that $\phi(G, H) \leq 2q$. □

Lemma 3. *For any constant c_1, if $q^* = c_1 \frac{1}{\langle D \rangle} p$, then for $q < q^*$, $T(G, H) \leq \phi(G, H) = \Theta(q)$. Further, there is a constant c_2 (that depends on c_1) such that $T(G, H) \geq c_2 \phi(G, H) = c_2 q$. Thus, for $q < q^*$, $T(G, H) = \Theta(q)$.*

Proof. In Lemma 2, we have shown that $\phi(G, H) = \phi(q) = \Theta(q)$. This allows us to conclude that $T(G, H) \leq \phi(G, H) = \Theta(q)$, since the flow cannot be greater than the sparsest cut.

To show that $T(G,H) \geq c_2\phi(G,H)$ for $q < q^*$, it suffices to show that a flow of value $\Theta(q)$ can be supported on our network. In the following, we show the existence of such a flow, sending $\Theta(q)$ units between every pair of nodes $(u,v) \in V_1 \times V_2$.

With each node $u \in V_1$ having qn edges to V_2, we have qn^2 edges across the V_1-V_2 cut. We route flow $\Theta(q)$ between each (u,v) as follows: u splits the flow equally to all nodes in V_1 sending each $\Theta(q/n)$. Each receiving node $l \in V_1$ further splits the flow equally across all its qn cross-cluster edges, sending $\Theta(1/n^2)$ of the (u,v)-flow over each edge. Thus, each cross cluster edge carries $\Theta(n^2 \times 1/n^2) = \Theta(1)$ flow, and the constant can be adjusted such that the unit capacity constraint is satisfied. Further note that the flow between each pair of nodes $(u,w) \in V_1 \times V_1$ is $\Theta(n \times q/n) = \Theta(q)$. In our regime, $q < p/\log n < \frac{d}{n \log n}$. As we already showed in Lemma 1, for a random regular graph, throughput (even for the complete demand graph) is $\Theta(\frac{d}{n \log n})$, and hence this flow is feasible. The same argument applies to internal flow in V_2 where flow from each cross-cluster edge is split again to the destinations.

Lastly, note that $T(q = q^*) = \Theta(q^*) = c_1 \cdot p\frac{\log d}{\log n} = c_3 \cdot d\frac{\log d}{n \log n} = \Theta(T^*)$ □

Thus far, we have shown that for $q < q^*$, throughput $T(q) = \Theta(q)$ and $T(q = q^*) = \Theta(T^*)$, *i.e.,* within constant factor of the peak throughput. The following lemma will establish that $T(q > q^*) = \Theta(T^*)$ and thus prove our result.

Lemma 4. *For $q > q^*$, $T(q)$ is within a constant factor of the peak throughput T^*.*

Proof. First, we note than when $q > p$, the graph is an optimal bipartite expander and thus throughput is within a constant factor of $T(p = q) = \Theta(T^*)$ [34]. When $q^* < q < p$, as we increase q, p does not change by more than a factor of 2. Thus, we can apply the same argument as Lemma 3 to route $\Theta(T^*)$ flow: clearly, increasing q does not decrease flow, and p changing by a constant factor only reduces it by a constant factor at most. □

Proof of Theorem 4. The above three lemmata directly imply the theorem for the demand graph $H = K_{V_1,V_2}$. Note further that random permutation traffic demands P can be routed within H at a constant factor lower flow throughput. Specifically, for each flow $v \to w$ between two nodes in the same cluster V_1 in P, we can split the flow $v \to w$ into $n/2$ subflows, from v to each node in V_2 and from there to w. After handling the other types of traffic (within cluster V_2 and across clusters) similarly, this produces a bipartite demand graph with a constant factor larger demands than H. Hence, the theorem is concluded. □

APPENDIX D

Measuring cuts

We employ several heuristics for estimating sparsest cut.

Brute-force computation Brute force computation of sparsest cut is computationally intensive since it considers all possible cuts in the network (2^{n-1} cuts in a network with n nodes). In addition to bandwidth, the number of flows traversing each cut has to be estimated which adds further overhead in the computation of sparsest cut.

Due to the computational complexity, brute force evaluation of sparsest cut is possible only for networks of size less than 20. However, we perform limited brute-force computation on all networks by capping the computation at $10,000$ cuts.

One-node cuts Designed computer networks as well as naturally occurring networks tend to be denser at the core and sparse at the edges. When the core has high capacity, it is likely that the worst-case cut occurs at the edges. Hence, this heuristic considers all cuts with only a single node in a subset formed by the cut. There exists n cuts with a single node. This is a very small fraction of the total 2^{n-1} cuts.

Two-node cuts $\frac{n*(n-1)}{2}$ cuts with two nodes in a subset also reveal the limited connectivity at the edges of the network.

Expanding cuts It is likely that the network is clustered,i.e., it contains two or more highly connected components connected by a few links. Subsets of all possible combinations of contiguous nodes in the network can be very large. We optimize our search to a subspace of this category of cuts. Starting from each node, we consider cuts which include nodes within a distance k from the node. When $k = 0$, the cut involves only the originating node and is equivalent to the single node case discussed before. When $k = 1$, all nodes within distance 1 from the node are considered – the node and its neighbors. k is incremented until

the entire graph is covered. If d is the diameter of the network, the number of cuts considered is less than or equal to $n * d$.

Eigenvector based optimizations Eigenvector corresponding to the second smallest eigenvalue of the normalized Laplacian of a graph can give a set of n cuts, the worst of which is within a constant factor from the actual cut [26]. The nodes of the graph are sorted in the ascending order corresponding to their value in the second eigenvector [26]. We sweep this vector of sorted nodes to obtain the n cuts.

REFERENCES

[1] An implementation of k-shortest path algorithm. http://code.google.com/p/k-shortest-paths/.

[2] Project blackbox. http://www.sun.com/emrkt/blackbox/story.jsp.

[3] Rackable systems. ICE Cube modular data center. http://www.rackable.com/products/icecube.aspx.

[4] SGI ICE Cube Air expandable line of modular data centers. http://sgi.com/products/data_center/ice_cube_air.

[5] Topobench - topology evalutaion tool. github.com/ankitsingla/topobench, 2013.

[6] Jung Ho Ahn, Nathan Binkert, Al Davis, Moray McLaren, and Robert S. Schreiber. HyperX: Topology, Routing, and Packaging of Efficient Large-scale Networks. In *Proceedings of the Conference on High Performance Computing Networking, Storage and Analysis*, SC '09, 2009.

[7] Mohammad Al-Fares, Alexander Loukissas, and Amin Vahdat. A scalable, commodity data center network architecture. In *SIGCOMM*, 2008.

[8] M. Alizadeh, A. Kabbani, T. Edsall, B. Prabhakar, A. Vahdat, and M. Yasuda. Less is More: Trading a little Bandwidth for Ultra-Low Latency in the Data Center. *NSDI*, 2012.

[9] Mohammad Alizadeh, Albert Greenberg, David A. Maltz, Jitu Padhye, Parveen Patel, Balaji Prabhakar, Sudipta Sengupta, and Murari Sridharan. DCTCP: Efficient packet transport for the commoditized data center. In *SIGCOMM*, 2010.

[10] Mohammad Alizadeh, Shuang Yang, Sachin Katti, Nick McKeown, Balaji Prabhakar, and Scott Shenker. Deconstructing datacenter packet transport. *HotNets*, 2012.

[11] Hilfi Alkaff and Indranil Gupta. Cross-layer scheduling in cloud computing systems (research paper). *International Conference on Cloud Engineering*, 2015.

[12] Konstantin Andreev and Harald Racke. Balanced graph partitioning. *Theory of Computing Systems*, 39(6):929–939, 2006.

[13] Moshe Babaioff and John Chuang. On the optimality and interconnection of valiant load-balancing networks. In *INFOCOM*, 2007.

[14] M. Besta and T. Hoefler. Slim Fly: A Cost Effective Low-Diameter Network Topology. In *IEEE/ACM International Conference on High Performance Computing, Networking, Storage and Analysis (SC14)*, Nov. 2014.

[15] L. N. Bhuyan and Agrawal D. P. Generalized hypercube and hyperbus structures for a computer network. *IEEE Transactions on Computers*, 1984.

[16] Béla Bollobás. The isoperimetric number of random regular graphs. *Eur. J. Comb.*, 1988.

[17] Béla Bollobás. Random graphs, 2nd edition. 2001.

[18] Béla Bollobás and W. Fernandez de la Vega. The diameter of random regular graphs. In *Combinatorica 2*, 1981.

[19] Andrei Broder and Eli Shamir. On the second eigenvalue of random regular graphs. In *FOCS*, 1987.

[20] V. G. Cerf, D. D. Cowan, R. C. Mullin, and R. G. Stanton. A lower bound on the average shortest path length in regular graphs. *Networks*, 1974.

[21] Shuchi Chawla, Robert Krauthgamer, Ravi Kumar, Yuval Rabani, and D Sivakumar. On the hardness of approximating multicut and sparsest-cut. *Computational Complexity*, 2006.

[22] Chandra Chekuri. Routing and network design with robustness to changing or uncertain traffic demands. *SIGACT News*, 38(3):106–129, September 2007.

[23] Shigang Chen and Klara Nahrsted. An overview of quality of service routing for next-generation high-speed networks: problems and solutions. *Network, IEEE*, 12(6):64–79, 1998.

[24] Fan Chung and Linyan Lu. The diameter of sparse random graphs. *Advances in Applied Mthematics*, 26:257–279, 2001.

[25] Fan Chung and Linyan Lu. The average distance in random graphs with given expected degree. *PNAS*, 2002.

[26] F.R.K. Chung. Laplacians of graphs and cheeger's inequalities. In *Combinatorics, Paul Erds is Eighty, Vol. 2*, pages 157–172. Janos Bolyai Mathematical Society, Budapest, 1996.

[27] Charles Clos. A study of non-blocking switching networks. *Bell System Technical Journal*, 32(2):406–424, 1953.

[28] Francesc Comellas and Charles Delorme. The (degree, diameter) problem for graphs. `http://maite71.upc.es/grup_de_grafs/table_g.html/`.

[29] Andrew R. Curtis, S. Keshav, and Alejandro Lopez-Ortiz. LEGUP: using heterogeneity to reduce the cost of data center network upgrades. In *CoNEXT*, 2010.

[30] A.R. Curtis, T. Carpenter, M. Elsheikh, A. Lopez-Ortiz, and S. Keshav. Rewire: An optimization-based framework for unstructured data center network design. In *INFOCOM, 2012 Proceedings IEEE*, pages 1116–1124, March 2012.

[31] Digital Reality Trust. What is Driving the US Market? `http://goo.gl/qiaRY`, 2001.

[32] P. Elias, A. Feinstein, and C. Shannon. A note on the maximum flow through a network. *Information Theory, IEEE Transactions on*, 2(4):117–119, Dec 1956.

[33] David Ellis. Eigenvalues, random walks and Ramanujan graphs. `https://www.dpmms.cam.ac.uk/~dce27/Eigenvalues2.pdf`.

[34] David Ellis. The expansion of random regular graphs. https://www.dpmms.cam.ac.uk/~dce27/randomreggraphs3.pdf.

[35] Facebook. Facebook to expand Prineville data center. http://goo.gl/fJAoU.

[36] Nathan Farrington, George Porter, Sivasankar Radhakrishnan, Hamid Hajabdolali Bazzaz, Vikram Subramanya, Yeshaiahu Fainman, George Papen, and Amin Vahdat. Helios: A hybrid electrical/optical switch architecture for modular data centers. In *SIGCOMM*, 2010.

[37] Uriel Feige and Robert Krauthgamer. A polylogarithmic approximation of the minimum bisection. *SIAM Journal on Computing*, 31(4):1090–1118, 2002.

[38] Sonja Filiposka and Carlos Juiz. Community-based complex cloud data center. *Physica A: Statistical Mechanics and its Applications*, 419(0):356 – 372, 2015.

[39] L. R. Ford and D. R. Fulkerson. Maximal flow through a network. *Canadian Journal of Mathematics*, 8:399 –404, 1956.

[40] Michael R. Garey and David S. Johnson. *Computers and Intractability: A Guide to the Theory of NP-Completeness*. 1979.

[41] Albert Greenberg, James R. Hamilton, Navendu Jain, Srikanth Kandula, Changhoon Kim, Parantap Lahiri, David A. Maltz, Parveen Patel, and Sudipta Sengupta. Vl2: A scalable and flexible data center network. In *SIGCOMM*, 2009.

[42] C. Guo, G. Lu, D. Li, H. Wu, X. Zhang, Y. Shi, C. Tian, Y. Zhang, and S. Lu. BCube: a high performance, server-centric network architecture for modular data centers. *SIGCOMM Computer Communication Review*, 39(4):63–74, August 2009.

[43] Chuanxiong Guo, Haitao Wu, Kun Tan, Lei Shi, Yongguang Zhang, and Songwu Lu. Dcell: A scalable and fault-tolerant network structure for data centers. In *SIGCOMM*, 2008.

[44] Gurobi Optimization Inc. Gurobi optimizer reference manual. http://www.gurobi.com, 2013.

[45] László Gyarmati and Tuan Anh Trinh. Scafida: A scale-free network inspired data center architecture. In *SIGCOMM Computer Communication Review*, 2010.

[46] James Hamilton. Datacenter networks are in my way. http://goo.gl/Ho6mA.

[47] Frank Harary, John P Hayes, and Horng-Jyh Wu. A survey of the theory of hypercube graphs. *Computers & Mathematics with Applications*, 15(4):277–289, 1988.

[48] HP. HP EcoPOD. http://goo.gl/8A0Ad.

[49] HP. Pod 240a data sheet. http://goo.gl/axHPp.

[50] T. C. Hu. Multicommodity network flows. *Oper. Res.*, 11(3):344 – 360, 1963.

[51] Rajendra K. Jain, Dah-Ming W. Chiu, and William R. Hawe. A quantitative measure of fairness and discrimination for resource allocation in shared computer systems. Technical report, Digital Equipment Corporation, 1984.

[52] John Kim, William J. Dally, and Dennis Abts. Flattened butterfly: a cost-efficient topology for high-radix networks. *SIGARCH Comput. Archit. News*, 35(2):126–137, June 2007.

[53] John Kim, William J. Dally, Steve Scott, and Dennis Abts. Technology-Driven, Highly-Scalable Dragonfly Topology. In *Proceedings of the 35th Annual International Symposium on Computer Architecture*, ISCA '08, pages 77–88, 2008.

[54] Murali Kodialam, T. V. Lakshman, and Sudipta Sengupta. Traffic-oblivious routing in the hose model. *IEEE/ACM Trans. Netw.*, 19(3):774–787, 2011.

[55] David S. Lee and Jeffrey L. Kalb. Network topology analysis. Technical report, 2008.

[56] Frank T. Leighton. Introduction to parallel algorithms and architectures: Arrays, trees, hypercubes. 1991.

[57] Tom Leighton and Satish Rao. Multicommodity max-flow min-cut theorems and their use in designing approximation algorithms. *J. ACM*, 46(6):787–832, November 1999.

[58] Tom Leighton and Satish Rao. Multicommodity max-flow min-cut theorems and their use in designing approximation algorithms. *Journal of the ACM*, 1999.

[59] Charles E. Leiserson. Fat-trees: universal networks for hardware-efficient supercomputing. *IEEE Trans. Comput.*, 34(10):892–901, October 1985.

[60] Alda Licis. Data center planning, design and optimization: A global perspective. `http://goo.gl/Sfydq`.

[61] Nathan Linial, Eran London, and Yuri Rabinovich. The geometry of graphs and some of its algorithmic applications. *Combinatorica*, 15:577–591, 1995.

[62] King-Shan Lui, Klara Nahrstedt, and Shigang Chen. Routing with topology aggregation in delay-bandwidth sensitive networks. *Networking, IEEE/ACM Transactions on*, 12(1):17–29, 2004.

[63] Brendan D. McKay and Nicholas C. Wormald. Uniform generation of random regular graphs of moderate degree. *J. Algorithms*, 1990.

[64] Nick McKeown, Tom Anderson, Hari Balakrishnan, Guru Parulkar, Larry Peterson, Jennifer Rexford, Scott Shenker, and Jonathan Turner. OpenFlow: enabling innovation in campus networks. *SIGCOMM CCR*, 2008.

[65] Andreas Bieniek Michael, Michael Nolle, and Gerald Schreiber. A message passing model for communication on random regular graphs. In *International Parallel Processing Symposium (IPPS)*, 1996.

[66] Microsoft. Link layer topology discovery protocol. `http://goo.gl/bAcZ5`.

[67] Mirka Miller and Jozef Siran. Moore graphs and beyond: A survey of the degree/diameter problem. *ELECTRONIC JOURNAL OF COMBINATORICS*, 2005.

[68] Rich Miller. Facebook now has 30,000 servers. `http://goo.gl/EGD2D`.

[69] Rich Miller. Facebook server count: 60,000 or more. `http://goo.gl/79J4`.

[70] Jeffrey C. Mogul, Jean Tourrilhes, Praveen Yalagandula, Puneet Sharma, Andrew R. Curtis, and Sujata Banerjee. Devoflow: cost-effective flow management for high performance enterprise networks. In *Hotnets*, 2010.

[71] J. Mudigonda, P. Yalagandula, and J.C. Mogul. Taming the flying cable monster: A topology design and optimization framework for data-center networks. *USENIX ATC*, 2011.

[72] Jayaram Mudigonda, Praveen Yalagandula, Mohammad Al-Fares, and Jeffrey C. Mogul. SPAIN: COTS data-center ethernet for multipathing over arbitrary topologies. In *NSDI*, 2010.

[73] Radhika Niranjan Mysore, Andreas Pamboris, Nathan Farrington, Nelson Huang, Pardis Miri, Sivasankar Radhakrishnan, Vikram Subramanya, and Amin Vahdat. Portland: A scalable fault-tolerant layer 2 data center network fabric. In *SIGCOMM*, 2009.

[74] Lionel M Ni and Philip K McKinley. A survey of wormhole routing techniques in direct networks. *Computer*, 26(2):62–76, 1993.

[75] D. Padua. *Encyclopedia of Parallel Computing*. Number v. 4 in Springer reference. Springer, 2011.

[76] Lucian Popa, Sylvia Ratnasamy, Gianluca Iannaccone, Arvind Krishnamurthy, and Ion Stoica. A cost comparison of datacenter network architectures. In *CoNEXT*, 2010.

[77] E. Rosen, A. Viswanathan, and R. Callon. Multiprotocol Label Switching Architecture. RFC 3031, 2001.

[78] F. Shahrokhi and D.W. Matula. The maximum concurrent flow problem. *Journal of the ACM*, 37(2):318–334, 1990.

[79] Ji-Yong Shin, Bernard Wong, and Emin Gn Sirer. Small-world datacenters. *ACM SOCC*, 2011.

[80] Ankit Singla, Atul Singh, Kishore Ramachandran, Lei Xu, and Yueping Zhang. Proteus: a topology malleable data center network. In *HotNets*, 2010.

[81] Brent Stephens, Alan Cox, Wes Felter, Colin Dixon, and John Carter. Past: Scalable ethernet for data centers. In *CoNEXT*, 2012.

[82] Ratko V. Tomic. Optimal networks from error correcting codes. In *ACM/IEEE Symposium on Architectures for Networking and Communications Systems (ANCS)*, 2013.

[83] Guohui Wang, David G. Andersen, Michael Kaminsky, Konstantina Papagiannaki, T. S. Eugene Ng, Michael Kozuch, and Michael Ryan. c-through: Part-time optics in data centers. In *SIGCOMM*, 2010.

[84] Jun Wang, Li Xiao, King-Shan Lui, and Klara Nahrstedt. Bandwidth sensitive routing in diffserv networks with heterogeneous bandwidth requirements. In *Communications, 2003. ICC'03. IEEE International Conference on*, volume 1, pages 188–192. IEEE, 2003.

[85] Kevin C Webb, Alex C Snoeren, and Kenneth Yocum. Topology switching for data center networks. In *HotICE*, 2011.

[86] Damon Wischik, Costin Raiciu, Adam Greenhalgh, and Mark Handley. Design, Implementation and Evaluation of Congestion Control for Multipath TCP. In *NSDI*, 2011.

[87] Haitao Wu, Guohan Lu, Dan Li, Chuanxiong Guo, and Yongguang Zhang. MDCube: A High Performance Network Structure for Modular Data Center Interconnection. In *CoNext*, 2009.

[88] J.Y. Yen. Finding the K Shortest Loopless Paths in a Network. *Management Science*, 1971.

[89] Xin Yuan, Santosh Mahapatra, Wickus Nienaber, Scott Pakin, and Michael Lang. A New Routing Scheme for Jellyfish and Its Performance with HPC Workloads. In *Proceedings of the International Conference on High Performance Computing, Networking, Storage and Analysis*, SC '13, pages 36:1–36:11, 2013.